Flow of water through coarse granular materials. December 1964.

Author:
Dudgeon, C. R.

Publication details:
Report No. UNSW Water Research Laboratory Report No. 76

Publication Date:
1964

DOI:
https://doi.org/10.4225/53/5796b5b7a7783

THE UNIVERSITY OF NEW SOUTH WALES

WATER RESEARCH LABORATORY

Manly Vale, N.S.W., Australia

REPORT No. 76

Flow of Water through Coarse Granular Materials

by

C. R. Dudgeon

https://doi.org/10.4225/53/5796b5b7a7783

DECEMBER, 1964

TABLE 3.

Summary of Permeability Test Data.

Test Series No.	Material	Median Diameter mm	Median Diameter ft.	Porosity pc By weighing Solids	Porosity pc By draining Voids
1	BM3-2.3/4" B. Metal	16	5.2×10^{-2}	45.5	42.6
2	M123 Marble mixture	24.9	8.2×10^{-2}	37.9	35.8
4	G1 Nepean R. sand	0.53	1.74×10^{-3}	38.7	27.2
5	G3 3/8" R. Gravel	5.8	1.9×10^{-2}	39.2	36.9
6	G2 –1/4" R. Gravel	2.3	7.5×10^{-3}	41.8	37.1
8	BM1 3/16" B. Metal	3.2	1.05×10^{-2}	47.7	45.9
9	BM2 3/8" Blue Metal	6.4	2.10×10^{-2}	45.8	41.6
10	G6 3" R. gravel	55	1.80×10^{-1}	36.9	37.3
11	BM5 3" Blue Metal	37	1.21×10^{-1}	48.3	46.3
12	G5 $1\frac{1}{2}$" R. gravel	26	8.5×10^{-2}	37.2	34.9
13	G4 3/4" R. gravel	16	5.2×10^{-2}	36.7	33.9
14	BM4 $1\frac{1}{2}$" Blue Metal	25	8.2×10^{-2}	43.8	41.8
15	BM3-1. 3/4" Blue Metal	14	4.6×10^{-2}	42.8	39.5
16	M1 16 mm Marbles	16.0	5.24×10^{-2}	36.9	36.9
17	M2 25 mm Marbles	24.9	8.16×10^{-2}	36.9	38.0
18	G7 6" R. Gravel	110	3.60×10^{-1}	40.6	40.4
19	M1 16 mm Marbles	16.0	5.24×10^{-2}	41.5	41.3
20	M1 16 mm Marbles	16.0	5.24×10^{-2}	37.2	37.8
21	BM3-1. 3/4" B. metal	14	4.6×10^{-2}	51.5	48.5
22	M3 29 mm Marbles	29.0	9.5×10^{-2}	38.5	38.0

Note: (a) Porosities shown on Figures 4 to 10 are those obtained by weighing solids.

(b) Marble mixture M123 consists of 16, 25 and 29 mm marbles in the proportions 1.23: 1.05: 1.00 by weight.

Contents

Contents (cont'd.)

Contents (cont'd.)

List of Tables.

- ---------

List of Figures.

List of Figures (cont'd.)

List of Photographs

List of Appendices.

List of Symbols.

A	gross cross-sectional area of flow	ft^2
K	permeability	ft^2
P	porosity	-
Q	discharge	$ft^3/sec.$
R	hydraulic radius	ft
$\mathbb{R} = \frac{Vd\rho}{\mu}$	Reynolds number	-
$S = \frac{\Delta h}{\Delta l}$	Hydraulic gradient	-
$S_p = \gamma S = \frac{\Delta p}{\Delta l}$	pressure loss gradient	$lb/ft^2/ft$
T	tortuosity factor	
$V = \frac{Q}{A}$	velocity or "flow velocity" or "discharge velocity" or "filter velocity"	ft/sec.
V_f	particle fall velocity	ft/sec.
$V_v = \frac{V}{P}$	"voids velocity"	ft/sec
a	permeability factor in the equation $S = aV^n$	indeterminate
c	Kozeny constant	-
d	particle "characteristic length" or diameter	ft.
f	Darcy friction factor	-
$f' = \frac{f}{2}$	Fanning friction factor	-
g	gravitational acceleration	ft^2/sec

List of Symbols (cont'd.)

$k = \frac{K\gamma}{\mu}$	coefficient of permeability in the Darcy equation $V = kS$	ft/ sec.
n	exponent in the equation $S = aV^n$	-
Δh	increment of head loss	ft.
$\Delta l, \Delta x$	increment of distance in the direction of flow	ft.
Δp	increment of pressure loss	lb/ft^2
γ	specific weight	lb/ft^3
μ	viscosity	$lb.sec/ft^2$
$\nu = \frac{\mu}{\rho}$	kinematic viscosity	ft^2/sec
ρ	density	$slugs/ft^3$
ϕ	function sign	-

SUMMARY.

The permeability characteristics of a variety of coarse, non-cohesive granular materials were determined from tests in a 22 inch diameter permeameter. The materials included sand, broken stone and river gravel up to 6 inches in size and three sizes of glass spheres. Provision was made for the determination and exclusion of wall effects by measurement of flow through the full cross-section and also through a central core 14 inches in diameter.

Velocities, based on gross area, ranged from 10^{-5} to 1.5 feet per second and hydraulic gradients from 10^{-4} to 15.

The velocity - hydraulic gradient (V-S) relationship plotted on logarithmic paper yielded, for each sample, a series of straight lines with sharp discontinuities of slope between each regime rather than a curved transition from the low Darcy-type flow to the high turbulent flow region. For each material, and each packing of the material, the V-S relationship is characterised by a discontinuous exponential relationship of the form

$$S = aV^n$$

Values of a and n have been determined for each material deposited without compaction and for several of the materials deposited so as to increase their porosities.

Each material yielded 3 or more regimes (sets of values of a

and n), the values of n ranging from 0.8 through unity (Darcy's law) and up to 1.9.

Changes in porosity produced large changes in a and small changes in n, in any particular regime.

No general unified relationship between S and V, or between the Darcy friction factor and Reynolds number was obtainable, owing to the impracticability of incorporating any effective allowance either for particle shape and grading or for porosity. The use of fall velocity as a parameter incorporating these characteristics was found to offer no significant advantage. In fact, it is shown that in the absence of geometrical similarity of particle size and arrangement any such generalisation cannot be expected.

The upper limit of Darcy's law could be predicted more accurately from a correlation between coefficient of permeability and limiting hydraulic gradient than from a Reynolds number. No method of predicting the lower limit of validity of Darcy's law was apparent.

1. Introduction

Many theoretical and experimental investigations into the characteristics of fluid flow through porous media have been undertaken since the results of Darcy's experiments were published in 1856. These investigations have arisen mainly from the necessity to calculate hydraulic gradients and flow rates in the fields of filtration, oil production, groundwater flow, chemical processing, soil mechanics and rockfill dam design.

The porous media involved in these investigations have ranged from naturally occurring cemented rocks and uncemented soils, sands and gravels and crushed aggregates through beds of spheres to beds of odd shaped particles such as Berl saddles and Raschig rings used in the chemical industry. The fluids used in the investigations have been mainly water and air.

Because of the wide range of particle sizes, shapes and gradings and porosities, the geometrical properties of the media varied greatly. It is little wonder, then, that attempts to obtain one general equation from which flow rates and hydraulic gradients may be calculated for all types of porous media, permeating fluids and flow rates have been unsuccessful. Until recently, even the form of the relationship between flow rate and hydraulic gradient for a particular porous medium has remained obscure.

The complex, but far simpler, problem of the flow rate - hydraulic gradient relationship for the flow of fluids through circular pipes has been

generalised only for flow through smooth pipes, pipes with a "uniform sand grain roughness" and pipes with a random type of roughness termed "commercial pipe roughness". Even then, flow rate - hydraulic gradient tests must be carried out on each type of pipe surface to determine the "roughness" before hydraulic gradients for other pipe diameters or flow rates can be calculated. Measurements of the physical characteristics of the roughness projections cannot as yet be used to calculate the "roughness" of a pipe surface.

When this is considered, the possibility of a single correlation between the permeability characteristics of porous media and the infinite range of possible physical characteristics of the media appears very remote. The most that can be expected is a number of correlations applicable to narrow ranges of porous media having approximate geometrical similarity.

Although the experimental investigation described in Sections 5 to 8 has been restricted to coarse granular media, which have been taken as those of coarse sand size or greater, it has been considered advisable to review the field of porous media flow in its entirety as all flow regimes which have been discovered in porous media may occur in coarse media, provided a wide enough range of flow rates is covered.

Emphasis is laid on those aspects of flow through coarse granular media which are of practical importance in civil engineering. The state of knowledge, within the civil engineering profession, of flow through

granular materials for conditions outside the range of validity of Darcy's law is poor. A great deal of further research and dissemination of information is required before a designer can confidently predict flow rates and hydraulic gradients for flows of this type.

The purpose of this thesis is to review existing information on the subject, to investigate experimentally some of the aspects requiring clarification and to set out what is considered to be the most rational approach to the use of present knowledge in civil engineering applications.

2. Literature Review

2.1 General

The review which follows is aimed at placing the particular study of flow through coarse granular media in perspective in the broader field of porous media flow. Of the few English language books available on flow through porous media, that by Scheidegger (1960) is the only one which devotes much space to the high flow rates which are pertinent to coarse materials. Muskat's classic reference work (1937) is now out of date on this topic and the recent work by Collins (1961) treats the topic only briefly.

Research work carried out since Darcy's results were published in 1856 falls into three main categories:

(i) That aimed at correlating permeability with physical characteristics of porous media.

(ii) That aimed at theoretical justification of Darcy's law and the permeability correlations, mentioned in (i), on the basis of various flow models.

(iii) That aimed at studying the upper limit of validity of Darcy's law and determining equations applicable to high flow rates.

Much of the more important recent research work has been carried out in East European and Soviet countries and the associated publications are either difficult to obtain or are obtainable only in untranslated form.

2. 2 Darcy's Law

(a) Darcy's Experiments

Hubbert (1940) reports that Darcy's experiments (1856) were carried out on a well compacted filter medium consisting mainly of sand but with a proportion of large shell particles included. Most of Darcy's tests were confined to the linear* flow regime but he recognised that there was an upper limit to the validity of his law. He defined this limit in terms of the velocity (approximately 10 to 11 cm/sec. for his material).

(b) Methods of Expression

Written in modern terms, Darcy's law states that:

$$Q = k\ A\ \frac{\Delta h}{\Delta l} \qquad 2.1$$

where Q is the discharge

A is the gross cross-sectional area of flow

Δh is the head loss over a distance Δl in the direction of flow

k is called the coefficient of permeability

The coefficient of permeability, k, depends on the physical characteristics of the porous medium and the viscosity of the permeating fluid.

Equation 2. 1 can be re-written as

$$V = k\ S \qquad 2.2$$

---

* The flow regime in which Darcy's law holds will be called the linear regime throughout this thesis.

*where $V = \frac{Q}{A}$ is called the "discharge velocity" or "filter velocity" or "flow velocity"

$S = \frac{\Delta h}{\Delta l}$ is the hydraulic gradient.

The fluid viscosity, μ, may be isolated from the coefficient of permeability and the hydraulic gradient expressed in terms of pressure by writing

$$V = \frac{K}{\mu} S_p \qquad 2.3$$

where $S_p = \gamma S = \gamma \frac{\Delta h}{\Delta l}$ is the pressure loss gradient

K is called the permeability of the porous medium and depends only on its physical properties

γ is the specific weight of the fluid.

Alternatively, $V = \frac{K \gamma S}{\mu}$ 2.4

Equations 2.1 to 2.4 are all frequently referred to as Darcy's law although Equation 2.1 is closest to Darcy's original expression.

Reference to Darcy's law is generally taken as a reference to a linear relationship between discharge velocity and hydraulic gradient in flow through porous media, however mathematically expressed.

(c) Theoretical Derivations

Attempts at theoretical justification of Darcy's law have been based on -

(i) the application of the Navier-Stokes equations neglecting

---

* Throughout this thesis the abbreviated term "velocity" will be used to refer to V.

inertial terms e.g. Philip(1957)

(ii) dimensional analysis e.g. Slepička (1961(a), 1961(b)

(iii) analogy with flow in capillary tubes (see Scheidegger (1960) pp. 114 to 130 for a comprehensive list which includes the work of Kozeny and Carman).

This is an indirect application of the Navier-Stokes equations.

(iv) The application of formulae derived by the application of the Navier-Stokes equations to other fluid flow problems (e.g. the use of Oseen's equations for viscous flow past a sphere by Iberall (1950) in his drag theory of permeability).

(v) the direction application of Newton's laws of motion and viscosity (Hall (1956)),

(vi) the application of statistical methods.

Dimensional analysis, without the use of additional physical equations, cannot prove the nature of the function relating discharge velocity, hydraulic gradient and the physical characteristics of porous media; and the solution of the Navier-Stokes equations for anything but very simple hypothetical models of porous media is not at present mathematically feasible. Thus the theoretical verification of Darcy's law for real porous media by methods (i) to (v) remains to be achieved.

Several papers have appeared on the application of statistical theory to the derivation of the relationship between discharge velocity

and hydraulic gradient. This approach recognises the random nature of most porous media instead of substituting for it an oversimplified ordered model.

The use of the "random walk" approach to produce a statistical model of flow through porous media is discussed by Scheidegger (1954, 1960) who has done a great deal of the original work on the subject.

The approach shows more promise than any other used to date but the mathematical difficulties are very great. A simplified model has allowed the derivation of a linear expression equivalent to Darcy's law.

(d) Limits of Validity.

(i) Theoretical Predictions

None of the theoretical derivations mentioned in Section 2. 2 gives a means of calculating either the upper or lower limit of validity of Darcy's law.

Derivations based directly on the Navier-Stokes equations imply an upper limit when the inertial terms become significant, while those based on analogy with flow in tubes suggest a breakdown of the law when turbulence commences. Watson (1963) has carried out a computer solution of the Navier-Stokes equations for two dimensional flow through a spaced array of squares to determine the value of Reynolds number at which the permeability becomes noticeably affected by the inertial terms.

The results show a rapid increase in the intertial effect between Reynolds numbers of 0. 2 and 5. These figures fall within the range 0. 1 to 75 quoted by Scheidegger (1960) as the extreme values of the limiting Reynolds number determined experimentally and reported in the literature. However, this approach does not allow limits to be calculated for anything but simple arrangements of simple geometrical shapes.

The assumption in all the attempts at theoretical derivation that the permeating fluid behaves as a Newtonian fluid under all flow conditions precludes any possibility of a lower limit to the law. However, experiment has shown that at least in some circumstances a lower limit exists.

(ii) Experimental Investigations

Upper Limit

Many experimental investigations have been carried out to determine the upper limit of validity of Darcy's law. A number of these have been associated with attempts to determine general equations for the discharge velocity - hydraulic gradient relationship at high flow rates. It has been customary to express the upper limit of validity in terms of a Reynolds number but the difficulty of determining a suitable characteristic length for the particles or pores of a porous medium, together with the fact that other factors such as particle shape and grading and porosity appear to affect the limit, has led to a wide range of limiting Reynolds numbers

being reported. Scheidegger (1960) quotes the range as from 0.1 to 75, a factor of 750 existing between the upper and lower values compared with a factor of approximately 2 for the corresponding limit in pipes for normal experimental set ups..

It appears very doubtful whether a Reynolds number will ever serve to characterise the upper limit except for geometrically similar packings of the same type of material.

Some of the investigations which express results in terms of Reynolds numbers are those of Fancher, Lewis and Barnes (1933) reported by Muskat (1937), Hickox (1934), Bakhmeteff and Feodoroff (1937), Rose (1945a, 1945c), Rose and Rizk (1949), Cohen de Lara (1955), Boreli and Batinic (1961), Yalim and Franke (1961), Karadi and Nagy (1961), Nagy (1961), Gerber and Perrin (1962), Anandakrishnan and Varadarajulu(1963), Ward (1964).

Experimental work by Slepička (1961) led to the expression of the limit in terms of a critical hydraulic gradient for a particular porous medium. This hydraulic gradient was then related to the permeability of the medium for the linear flow regime. However, the correlation between permeability and critical hydraulic gradient is poor, allowing differences of as much as 700 pc. between experimental results and the mean line drawn.

Lower Limit

Little attention has been paid to a lower limit of validity of Darcy's law for the flow of water, except for some work on flow through clayey materials, possibly because of the difficulty of carrying out accurate experimental work with low flow rates and hydraulic gradients.

Deviations from Darcy's law for the flow of gases through porous media are discussed by Scheidegger (1960) and Iffly (1960). They are thought to be due to the "Knudsen effect" or "molecular streaming" which causes head losses to be lower than those predicted by Darcy's law for low gas flow rates.

Fishel (1935) carried out tests on sands and claimed that the results showed that Darcy's law was valid down to hydraulic gradients of 2 to 3 inches per mile (or $S \doteq 5 \times 10^{-5}$).

There is, however, a great deal of scatter of his results at low gradients.

Swartzendruber (1962) reported that King (1898) detected deviations from Darcy's law at low hydraulic gradients. Expressed in modern terms, King's results indicate that on a linear plot the discharge velocity - hydraulic gradient relationship for the sands and sandstone tested consisted of straight lines intersecting the hydraulic gradient axis at values about 0. 2 for sand and 16 for sandstone. These results imply that the slope of the line changed at very low hydraulic gradients

to pass through the intersection of the axes, or that there was a "starting gradient" which had to be overcome before flow could occur. Swartzendruber attributed the deviations from Darcy's law to non-Newtonian behaviour of the permeating water at low hydraulic gradients and analysed these and similar results from the work of Von Engelhardt and Tunn (1955), Lutz and Kemper (1959) and Hansbo (1960) on this basis. It is important to note that all these results were from tests on fine grained materials and that Swartzendruber, in his summary, referred to "a modified equation for liquid flow in porous media containing clay", thus attributing the non-Newtonian behaviour of the fluid to the presence of clay particles. In adopting non-Newtonian fluid instead of Bingham plastic characteristics for the water he ruled out the possibility of "starting gradients" despite the fact that he reported claims by Derjaguin and Krylov (1944) for the occurrence of these in ceramic and charcoal filters.

Nagy (1961) also reported deviations from Darcy's law for low flow rates through materials containing clay.

In clayey materials, the deviations from Darcy's law at low hydraulic gradients are frequently referred to as being due to "electrochemical" or "electromolecular" effects.

The only reference found to suggest that this phenomenon might also occur for the flow of water through relatively coarse grained materials is that of Slepička (1961) who quotes the results of tests by Izbas (1953) on a gravel with a coefficient of permeability of 460 cms/sec.

These results indicate, for hydraulic gradients below 2×10^{-3}, a regime in which the head losses are much greater than those predicted by Darcy's law. There is, however, a large scatter of the experimental results.

Similar results are quoted by Slepička for a material with a coefficient of permeability of 60 cms/sec. (2 ft/sec.).

2.3 Application of Dimensional Analysis

Either by analogy with dimensional analysis for flow in pipes, or by direct application of dimensional analysis, the variables involved in flow through porous media are usually grouped into a Reynolds number involving some length term chosen as characteristic of the geometry of porous media and a friction factor which is usually arranged to follow the form of the friction factor in the Darcy-Weisbach equation for head losses in flow through circular pipes. A number of other parameters may enter the relationship if additional variables are included in the dimensional analysis.

Rose (1956(a)) and Rose and Rizk (1949) chose a large number of variables in an attempt to obtain a complete relationship. Assuming an exponential relationship they expressed their function in the form

$$H = \phi_1(v^{\alpha} h^{\beta} d^{\gamma} \rho^{\delta} D^{\varepsilon} \mu^{\theta} g^{\phi} e^{\eta} f^{\lambda} z^{\sigma} u^{\omega}) \qquad 2.5$$

where H = head loss

v = discharge velocity

d = particle diameter

ρ = fluid density

h = filter bed depth (in flow direction)

D = filter tube diameter

μ = fluid viscosity

g = acceleration due to gravity

e = surface roughness height of the particles

f = porosity

z = dimensionless shape factor

u = dimensionless particle size distribution factor.

By using dimensional analysis they obtained areorganized function in the form

$$\frac{H}{d} = \phi_2\left[\left(\frac{dv\rho}{\mu}\right)^{\theta} \left(\frac{dg}{v^2}\right)^{\phi} \left(\frac{h}{d}\right)^{\beta} \left(\frac{D}{d}\right)^{\varepsilon} \left(\frac{e}{d}\right)^{\eta} (f)^{\lambda} (z)^{\sigma} (u)^{\omega}\right] \qquad 2.6$$

The introduction of H and g instead of a pressure difference Δp caused unnecessary complications.

Other investigators omit one or more of the above variables. Some make the assumption of an exponential relationship, others retain the function in a more basic form.

Since dimensional analysis can be expected to give general relationships only for geometrically similar porous media, the use of variables such as porosity in conjunction with a characteristic particle diameter is not justified. If the porosity is changed independently of the particle size, geometrical similarity is not maintained. Similar arguments apply to the inclusion of shape factors and size distribution factors.

A simplified expression applicable to a particular geometrically similar series of porous media appears to be all that is warranted.

This takes the form -

$$\phi_1\left(\frac{\Delta p}{\Delta x}\ ,\ V,\ d,\ \rho,\ \mu\right) \quad = \quad 0 \qquad 2.7$$

where $\frac{\Delta p}{\Delta x}$ = pressure drop gradient

V = velocity = $\frac{\text{discharge}}{\text{gross cross-sectional area}}$

d = characteristic length

ρ = fluid density

μ = fluid viscosity

Using dimensional analysis, this expression may be rearranged to give

$$\phi_2\left(\frac{Vd\rho}{\mu}\ ,\ \frac{V^2\rho}{\Delta p/\Delta x\ d}\right) \quad = \quad 0 \qquad 2.8$$

which can be re-written as

$$\frac{\Delta p}{\Delta x} = \frac{V^2\rho}{d} \cdot \phi_2 \left(\frac{Vd\rho}{\mu}\right)$$

$$\text{or} \quad S = \frac{V^2}{gd} \quad \phi_2 \left(\frac{Vd\rho}{\mu}\right) \qquad 2.9$$

where S = hydraulic gradient = $\frac{1}{\gamma} \cdot \frac{\Delta p}{\Delta x}$

This corresponds to the Darcy-Weisbach equation

$$S = \frac{fV^2}{2gd} \qquad 2.10$$

where f is the Darcy friction factor.

Thus $f = \phi_3\ (\mathbb{R})$

where $\mathbb{R} = \frac{Vd\rho}{\mu}$ is the Reynolds number based on a characteristic length, d, such as the particle diameter.

Friction factor - Reynolds number plots can be expected to show a different graph for each geometrically similar series of porous media. Published experimental data indicate that this is so.

It should be noted that an alternative friction factor, f', called the Fanning friction factor may be defined by the equation

$$S = \frac{f'V^2}{gd} \qquad 2.11$$

Then $f' = \frac{f}{2}$

Slepička (1961(a), 1961(b)) used the permeability ($K = \frac{k\mu}{\gamma}$) to characterise the geometry of porous media instead of a length term such as particle diameter. He also included a term, σ, to represent the solid-liquid interfacial tension at the solid - liquid boundaries. However, he omitted to include the density, ρ, and was thus in error. His new dimensionless parameters, $\frac{KS\rho}{V\mu}$ and $\frac{KS\rho}{\sigma}$ intended to be applicable to all flow conditions are not valid. He also failed to state how σ might be determined and in calculations apparently took it to be constant. If ρ is introduced into Slepička's dimensional analysis the normal Reynolds number and Euler number parameters emerge and it is seen that the introduction of the permeability K is equivalent to using $K^{\frac{1}{2}}$ for the length term in the conventional dimensional analysis.

Ward (1964) following Harleman, Melhorn and Rumer (1963) actually used $K^{\frac{1}{2}}$ as the characteristic length.

The use of $K^{\frac{1}{2}}$ as the characteristic length is no more than a mathematical dodge which brings the linear sections of friction factor - Reynolds number graphs together. The values of K must still be derived from permeability tests and can be expected to correlate with physical characteristics only for geometrically similar porous media.

Dimensional analysis will only rearrange the variables chosen as applicable to the problem. It will not yield the nature of the relationship between the variables. If the nature of a physical relationship emerges from what is often loosely termed dimensional analysis, it is because additional assumptions or physical equations have been introduced in the process. The most common assumption is that inherent in the Rayleigh method of dimensional analysis in which the relationship between the variables is assumed to be an exponential one. The analysis of Rose and Rizk mentioned earlier in this section involves this assumption, as does that of Slepička (1961(a), 1961(b)) who claims to prove by dimensional analysis that the relationship between velocity and hydraulic gradient is an exponential one.

2. 4 Empirical Correlations

(a) General

Empirical correlations proposed by numerous investigators will be dealt with only briefly in this review since they give satisfactory results only for the limited range of particle sizes, shapes, gradings

and porosities and hydraulic gradients for which they were derived. Attempts to obtain correlations covering wide ranges of porous media characteristics have not been successful.

(b) Correlations between Permeability or Friction Factor and Physical Characteristics

Correlations of this type fall into four main groups:

(i) those based on theories postulating a capillary flow model;

(ii) those based on theories postulating flow in channels of more complicated form than parallel, series or branching capillaries. These may be called hydraulic radius theories;

(iii) those based on a friction factor approach;

(iv) those based on drag theories in which the flow is considered to be around a closely spaced system of particles rather than through a series of channels formed between the particles.

The first two are concerned mainly with flow in the linear regime while the last two deal with both linear and post-linear regimes.

(i) Correlations based on Capillary Flow Theories

Correlations based on capillary models may postulate series, parallel, series-parallel or branching tubes. The characteristic flow dimension adopted is the tube diameter. With the possible exception of special types of porous media in which the flow paths do resemble capillaries these correlations cannot be expected to yield results applicable outside the narrow range of conditions for which they were

derived. Flow through the tortuous paths in porous media with sudden expansions and contractions cannot be considered analogous to flow in capillaries. The disorder of natural porous media cannot be represented. Marshall (1962) gives a recent summary of various capillary theories and their equations.

(ii) Correlations Based on Hydraulic Radius Theories

In hydraulic radius theories, the characteristic pore dimension is taken as the hydraulic radius, a vague concept when applied to the flow channels in a porous medium. It is usually defined as the ratio of the surface area of the pores to the volume of the pore space.

The Kozeny equation

$$K = \frac{cP^3}{s^2} \qquad 2.12$$

and the Kozeny-Carman equation

$$K = \frac{P^3}{5s_o^{\,2}(1-P)^2} \qquad 2.13$$

or modifications of these, are equations which have been frequently used to calculate permeabilities for fine grained materials.

K = permeability

c = the Kozeny constant

P = porosity

s = specific surface = surface area/unit gross volume

s_o = Carman's "specific surface exposed to the fluid"
= surface area exposed to the fluid/unit solid volume

Frequently Equation 2.11 is modified by adding a tortuosity term, T, which in this case has no strictly defined meaning. The equation becomes

$$K = \frac{cP^3}{Ts^2} \qquad 2.14$$

The value of the constant c is doubtful although according to Kozeny's theory it varies only slightly with particle shape. The terms s and T have to be determined experimentally.

Equations such as the Kozeny equation should be used only for media of the same type as those for which the constants have been determined.

A recent attempt to prove the validity of the equation for simplified media has been made by Rose (1959).

Cohen de Lara (1955), Madhav and Subba Rao (1963), are among the more recent of those to report discrepancies between the experimentally determined relationship between permeability and porosity and that obtained from the Kozeny theory.

(iii) Correlations between Friction Factor and Physical Characteristics

Numerous investigators including Bakhmeteff and Feodoroff (1937), Muskat (1937), Cohen de Lara (1955) and Tek (1957) have quoted empirical relationships between friction factor, Reynolds number and physical characteristics of porous media such as particle mean diameter, porosity and surface area. No general agreement has been reached and it appears that each different type of porous medium requires a different

equation. This observation agrees with the discussion presented in Section 2.3.

(iv) Correlations based on Drag Theory

There can be no basic distinction between a particle drag theory and a theory assuming flow channels with diameters characterised by particle size, since the variables entering into both problems are the same whether the flow is laminar, with or without appreciable inertial effects, or turbulent.

Iberall (1950) assumed a random distribution of cylindrical fibres and laminar flow with no appreciable interaction between fibres. Assuming one third of the fibres to be oriented parallel to each of three mutually perpendicular axes, he used existing theoretical drag force equations to compute the flow resistance. His approach was thus an indirect application of the Navier-Stokes equations.

Watson's (1963) direct solution of the Navier-Stokes equations for a simplified two dimensional system of spaced squares was also a drag approach.

Cohen de Lara (1955) used the expression

$$S = \frac{\Delta H}{\Delta l} = \frac{C'V^2}{d\ 2g} \qquad 2.15$$

with $\frac{\Delta H}{\Delta l} = S$ = hydraulic gradient

C' = "coefficient of drag"

V = discharge velocity

to represent the head loss through a porous bed. However, this expression is analogous to the Darcy friction factor equation

$$S = \frac{f V^2}{2gd} \quad , \qquad 2.16$$

a fact which the author recognised. Cohen de Lara then compared the "drag coefficient" (or friction factor) - Reynolds number graphs for his tests on spheres and near spherical sand particles to the curve for the drag coefficient of a single sphere. Within his limited range of materials he obtained reasonably good agreement provided the "diameter", d, for heterogeneous sands was defined as that of a sphere having the same coefficient of drag as the mean drag coefficient of the individual grains of the mixture.

Van der Tuin (1960) attempted to express his results in the same way but had to choose an "opportune" diameter to fit his results to the drag coefficient curve. These results were for gravels and crushed basalt ranging in median size from 7 mm to 385 mm and covered short sections of the drag coefficient curve between Reynolds numbers of 10^2 and 10^5. Apart from illustrating that in the fully turbulent flow regime, the friction factor does not vary greatly with variation in Reynolds number based on some hypothetical "diameter", the comparison seems to be of little significance. It would certainly be surprising if the friction factor curve for flow through porous media composed of angular material dropped sharply for Reynolds numbers beyond 2×10^5 as does the drag

coefficient curve for a sphere, or even followed the gradual variation in coefficient from 0.4 to 0.5 in the "flat" part of the curve, since both of these phenomena are due to movements of the separation zone on a sphere.

(c) Empirical Relationships between Velocity and Hydraulic Gradient for High Flow Rates.

A number of empirical equations have been proposed for the discharge velocity-hydraulic gradient relationship for flow at velocities above the upper limit of validity of Darcy's law. Among these are:

(i) that proposed by Forcheimer (1901) and quoted by Bakhmeteff (1937). Using the notation adopted in this thesis, the equation states:

$$S_p = a V + b V^2 \qquad 2.17$$

This equation was later modified to agree better with experimental data to:

$$S_p = aV + bV^2 + cV^3 \qquad 2.18$$

where S_p = hydraulic gradient in terms of pressure

V = velocity

a, b, c are constants.

(ii) various exponential equations of the form

$$S = aV^n \qquad 2.19$$

such as those of White (1935) with n = 1.8, Escande (1953) with n = 2, Wilkins (1955) with n = 1.85, Parkin (1962) with n = 1.86. Scheidegger (1960, p. 163) reports a number of other investigators who obtained similar equations but a wide variation of the value of the exponent, n.

(iii) various correlations between the friction factor, f, and Reynolds number, mentioned in part (b). Typical of these is Bakhmeteff's (1937) equation for high flow rates

$$f = \frac{24.2}{\mathbb{R}_p^{0.2}} \qquad 2.20$$

with the Reynolds number, $\mathbb{R}_p$ based on a mean diameter and a "pore velocity" $V_p = \frac{V}{P^{2/3}}$, where P = porosity.

Equations such as this, expressed in terms of Reynolds number and friction factor, are intended to generalise the results of the more basic velocity-hydraulic gradient relationships.

Some equations of this type (e.g. that of Ward (1964)) cover both linear and post-linear flow regimes with the one expression.

The great variety of expressions that has been proposed (see Scheidegger (1960) pp. 163-168) is an indication that a friction factor - Reynolds number correlation, even with the introduction of other terms such as porosity and shape factors, is unable to yield one general relationship for high flow rates through all types of porous media.

2.5 Evidence for a General Exponential Velocity - Hydraulic Gradient Relationship

The recent papers by Slepička(1961) and Anandakrishnan and Varadarajulu (1963) indicate that an exponential relationship of the form $S = aV^n$ holds over a wide range of flows. In particular, the flow range is divided into a number of regimes each with its own value of a and n

which appear to vary from one porous medium to another. The results also show sharp divisions between regimes; i.e, abrupt changes in a and n at the limits of a regime.

Slepicka's results indicate only three regimes, a "linear" one in which Darcy's law holds, a "pre-linear" one for lower velocities and a "post-linear" one for higher velocities. His results do not, however, preclude the possibility of additional regimes for higher flow rates than those he achieved.

The results of Anandakrishnan and Varadarajulu's tests on sands indicate that there may be at least three regimes above the linear one.

A re-examination by the author of the results of other investigators such as Bakhmeteff and Feodoroff (1937), Fancher, Lewis and Barnes (1933) (see Muskat, 1937, p. 60), Karadi and Nagy (1961), Boreli and Batinic (1961), and Nagy (1961) shows that on a log-log plot, straight lines representing the equation $S = aV^n$ and sharp intersections fit the experimental results better than the curves drawn by the investigators where scatter due to experimental errors is not excessive.

In many cases, random experimental errors have masked the true nature of the relationship.

The numerous reports of an exponential relationship for high flow rates with a single value of n which varies from one investigation to another (e.g. Bakhmeteff (1937), Escande (1953), Wilkins (1955),

Parkin (1962) can be attributed to two causes. The first is the limited range of flow rates over which investigations have been carried out. Even if a change in regime occurred near the start or finish of a test series the fact that a few points lay off the single straight line on a log-log plot would probably be attributed to experimental errors. The second is the scatter of experimental results which hides changes in slopes of the velocity-hydraulic gradient lines plotted on log-log paper.

2.6 Experimental Investigations with Coarse Materials

Few experiments using very coarse grained porous media have been reported, no doubt because of the large test installations required and the physical difficulty of handling the materials.

Wilkins (1955) carried out tests in a pipe on materials having particle sizes up to 8 inches while Van der Tuin (1960) carried out tests in an open channel on basalt boulders weighing up to 200 kilograms (440 lbs.) and with a mean size about 385 mm (15 inches). Wilkins' test results yield an exponential relationship of the form $S = aV^n$ with $n = 1.85$ for crushed dolerite up to 3 inches in size and marbles up to 1 inch in diameter. The results show a greater value of n for 8 inch crushed dolerite, but the exact value is not given.

Van der Tuin's results are expressed in a number of ways, one of which is by the relationship $S = aV^n$. For his very large material, values of n of 1.92 and 2.23 were reported.

Slepička (1961(a)) quoting the results of Izbas (1953), indicates values of n between 1.37 and 2.49 for tests on gravels.

Escande's (1953) tests were carried out on media composed of crushed rock particles with a mean size of approximately 2 inches. He stated that the value of n must be equal to 2 on the assumption that fully turbulent flow must occur for high Reynolds numbers. There is no theoretical justification for the value of 2, even if the state of flow is fully turbulent. The relationship between the hypothetical velocity V and the actual velocities which occur in the pores has not been established. Escande's results do not conclusively support his assumption as experimental errors mask the true value of n for his tests.

The tests reported by Parkin (1962) were carried out on 3/8 inch and 3/4 inch crushed blue metal over a limited range of flow rates for each material. A value of n equal to 1.86 was determined.

2.7 Summary

If coarse granular media are defined as those made up of particles the size of coarse sand and larger, the review occupying Sections 2.1 to 2.6 shows that all aspects of the general problem of flow through porous media must be considered when dealing with flow through coarse granular media. There is evidence to show that, for low flow rates, Darcy's law may be relevant and that for even lower flow rates so called "molecular" effects may be significant, even for materials much coarser than coarse

sand, and Darcy's law may not apply. For flow rates above the upper limit of validity of Darcy's law the same form of velocity - hydraulic gradient relationship appears to apply to flow through coarse grained as to flow through fine grained materials.

Theoretical treatments have not advanced the knowledge of the nature of flow through porous media to any appreciable extent. Dimensional analysis has, however, been useful in arranging the pertinent variables into dimensionless parameters which are of assistance in organizing and plotting the results of experiments.

Empirical correlations which have been determined for various types of porous media and flow conditions are applicable only to the conditions under which they were derived and should not be extrapolated beyond these conditions. The only really reliable method of determining the velocity hydraulic gradient relationship for a coarse granular medium encountered in engineering practice is to carry out permeability tests over the relevant range of flow rates. Careful comparison of materials with those described in conjunction with published head loss data may, however, allow useful estimates to be made.

In engineering investigations the importance of the various aspects discussed depends on the nature of the problem being investigated. Various civil engineering applications will be discussed in the next section.

3. Porous Media Problems in Civil Engineering

3. 1 General

A number of porous media flow problems are met in civil engineering practice. The main differences between these lie in the size and type of particles of which the media are composed, the range of hydraulic gradients involved and whether or not a free surface is present. Almost invariably the permeating fluid is water whose temperature lies in such a narrow range that the viscosity variation over the range may be neglected in many circumstances.

3. 2 Typical Examples

(a) Filtration

Filtration may involve fine or coarse granular media and all flow regimes may occur in practice.

However, trickling filtration through coarse granular filters such as those found in sewage disposal systems must be treated as a separate problem as the voids are not completely filled with water.

(b) Percolation through Earth Retaining Structures

Earth retaining structures, such as earth dams, may be composed of a number of zones of different granular media with different permeability characteristics. The same form of velocity-hydraulic gradient relationship will apply to the flow through each zone but the flow regimes may differ from one zone to the other or even within each zone.

(c) Groundwater Flow

Naturally occurring groundwater flow through gravel or coarse sand beds will usually be at very low hydraulic gradients and a linear (Darcy) flow regime, or even a pre linear regime may occur.

The assumption, commonly made, that Darcy's law will not be applicable to flow through materials as coarse as gravels will result in overestimates of head losses or underestimates of flow rates if a linear regime does occur. There is evidence to show that linear regimes may occur in gravels for Reynolds numbers much greater than the limiting value between 1 and 5 which is usually adopted.

The assumption that Darcy's law is always valid for low flow rates will, on the other hand, result in underestimates of head losses and overestimates of flow rates if a pre-linear regime occurs.

A particular problem is the estimation of flows through gravel beds in river channels where the average slope of the water surface may be as low as a few inches per mile. In such cases either linear or pre-linear flow regimes might be expected to occur and estimates of flow rates made on the assumption that the flow through gravels is "turbulent" may be grossly in error.

(d) Flow into Pumped Wells

A number of flow regimes may be expected in the vicinity of wells sunk into gravel beds. High gradients can be expected near a well, with

post-linear flow regimes and with changes to linear and possibly pre-linear regimes further away from the well.

(e) Field Permeability Tests

The calculations associated with field permeability tests assume that Darcy's law is applicable in all cases. This may not be so, with the result that such determinations may be in error, particularly if pre-linear flow regimes are encountered.

(f) Flow through Rockfill Dams

The passage of water through rockfill dams may be allowed either as a planned or an emergency measure during construction or to meet part or all of the overspill requirements of the completed structure.

Because of the disastrous nature of a dam failure, the ability to make accurate predictions of flow rates and hydraulic gradients is of vital importance in the design of such structures. The important aspect of stability of the rockfill under the action of the flowing water is also related to the hydraulic gradient.

Flows through prototype structures will usually be at very high Reynolds numbers and problems of extrapolating model results to give predictions of prototype conditions arise. The requirements of geometrical similarity are difficult to meet and the possible existence of a number of post-linear flow regimes for different ranges of Reynolds number makes the attainment of dynamic similarity equally difficult.

33. Difficulties in Determing Flow Rates and Hydraulic Gradients

(a) Form of the Velocity-Hydraulic Gradient Relationship

Apart from the linear flow regime to which Darcy's law applies, the form of the general relationship linking velocity and hydraulic gradient for a particular porous medium has remained obscure. The main reasons for this are:-

(i) The plotting together of the results from many different porous media for limited test ranges in an attempt to define a common or mean curve rather than first defining clearly the relationship for a particular medium.

(ii) The limited flow ranges over which most of the tests were carried out.

(iii) The experimental errors which caused a scatter in the experimental results sufficient to hide significant features of the relationship.

(iv) The tendency to fit curves to experimental results rather than straight lines even though the straight lines give a better fit. This tendency may be attributed to theoretical notions requiring gradual changes from laminar to turbulent flow or the gradual appearance of inertial effects in laminar flow.

No standard engineering reference book is yet sufficiently up to date to give the form of the velocity - hydraulic gradient relationship over a wide range of flow rates.

(b) Prediction of Constants in the Velocity-Hydraulic Gradient Relationship

Whether an exponential relationship or some other empirical equation is used, constants have to be determined before flow rates or hydraulic gradients can be predicted. In general, the only accurate determination of these constants can come from tests on the particular porous medium under consideration. Empirical correlations discussed in Chapter 2 are useful only for the narrow ranges of particle characteristics and porosities for which they were developed.

There is as yet no known way of taking any granular material, determining certain physical characteristics, and making accurate estimates of the required constants.

(c) Prediction of Regime Changes

When the knowledge of flow through porous media was restricted mainly to the linear regime, a serious problem was to predict accurately the flow rate at which Darcy's law ceased to hold. Only a rough estimate could be made in terms of a Reynolds number.

The use of a discontinuous exponential relationship with sharp breaks between a number of flow regimes makes the problem even more difficult as only a poor correlation exists (Slepicka (1961(a), 1961(b)) between the hydraulic gradients at which the changes occur and the permeability of the medium.

(d) Anisotropic Porous Media

The problem of calculating flow rates and hydraulic gradients through anisotropic beds becomes very complex when different flow regimes may be expected for different flow rates and different directions. Anisotropy is the rule rather than the exception in natural gravel deposits so the difficulty occurs frequently.

(e) Application of Similarity and Models to the Solution of Porous Media Problems

Except in the case of simple particles such as spheres the attainment of geometrical similarity between one porous medium and another medium composed of apparently similar particles at the same porosity is very unlikely. This is reflected in the variability of the velocity - hydraulic gradient and friction factor - Reynolds number graphs for apparently similar materials at the same porosities.

In addition, the different flow regimes which may occur for the same hydraulic gradient in, say, medium and very coarse grained media, means that the criterion of obtaining "turbulent" flow and the same porosity in model and prototype is insufficient to guarantee that flow patterns, flow rates and hydraulic gradients in the model will represent those in the prototype, even if geometrical similarity were achieved.

(f) Flow Nets

The problem of how to draw flow nets for flow regimes other than

the linear one in which Darcy's law holds is serious. None of the analogies or graphical procedures applicable to Darcy type flow is valid for either the pre-linear or post-linear regimes. Should a number of regimes occur in various regions of a rock or gravel structure because of a considerable variation of hydraulic gradients the difficulty would be even greater.

4. Purpose of Experimental Investigation

The experimental investigation described in Chapters 5 to 7 was intended to clarify ideas on a number of aspects of flow through coarse granular media. The research was oriented towards the application of the results to civil engineering investigations.

The investigation was intended to determine

(i) whether a general velocity - hydraulic gradient relationship was applicable over a wide range of flow rates to coarse as well as fine grained granular media of the type commonly met in civil engineering practice. River gravel and crushed rock were chosen as representative of these materials and glass marbles were chosen to allow comparison of results with many published results for flow through beds of spheres;

(ii) for what types of coarse granular media and what range of flows Darcy's law might be encountered;

(iii) whether "molecular" effects might cause a deviation from Darcy's law at very low hydraulic gradients, even for relatively coarse grained materials;

(iv) the magnitude of "wall effects" in permeameters

(v) whether the physical characteristics of the particles of a coarse granular medium could be characterised by the mean velocity of fall through water of the particles of the medium;

(vi) whether a simple relationship between porosity and permeability

is applicable over a wide range of flow conditions for a particular porous medium;

(vii) whether the onset of turbulence coincided with the upper limit of validity of Darcy's law.

5. Experimental Apparatus

5.1 General

The main criteria adopted for the design of the permeameter and associated apparatus used in the experiments were:

(i) the ability to carry out permeability tests on granular material ranging from coarse sands to coarse gravels;

(ii) the ability to cover a range of hydraulic gradients from approximately 10^{-4} to 10 and velocities from near zero to approximately one foot per second;

(iii) the necessity of determining or removing "wall effects" in the permeameter.

5.2 Permeameter

(a) Basic Requirements

(i) Tube Diameter. It has been stated in literature dealing with permeameters (Rose and Rizk, (1949), Zenz and Othmer (1960)) that provided the ratio of particle diameter to tube diameter does not exceed 10 pc. "Wall effects" may be neglected. The only justification found for this statement is that given by Rose and Rizk (1949) whose graphs of "wall effect" against diameter ratio and Reynolds number, obtained by a correlation procedure and not direct measurement, are open to question.

In the absence of other information, a tube diameter of approximately 2 feet was decided on to allow materials with nominal diameters up to 2 inches to be tested. Additional precautions to exclude, and to determine

the effect of, the flow adjacent to the walls of the permeameter are described in Section 5. 2(b).

(ii) Direction of Flow. Preliminary investigation of a design of permeameter intended to eliminate "wall effects" showed that a downflow model would be simpler to operate, as the outflow section would need to be relatively heavy and have a number of pipe outlets and would be better placed in a permanent position at the bottom. The simpler inflow and test sections could then be placed at the top and arranged for easy removal and replacement for leading samples.

In addition, the lower the outlets could be placed without unnecessary pipework, the greater the maximum head there would be available for dissipation in the sample under test.

(ii) Sample and Test Lengths. Provision was made for sample lengths up to 4 feet with test lengths of 2 feet and 3 feet to depend on the particle size of the material under test. The relatively short lengths were chosen to reduce the weight of material required and the permeameter height to a minimum and allow the greatest possible energy gradients to be obtained with the available head while still retaining a length sufficient to give representative results.

(b) Permeameter Details

Details of the construction of the permeameter and the arrangement of outlets are shown in Figures 1 and 2. The permeameter and associated

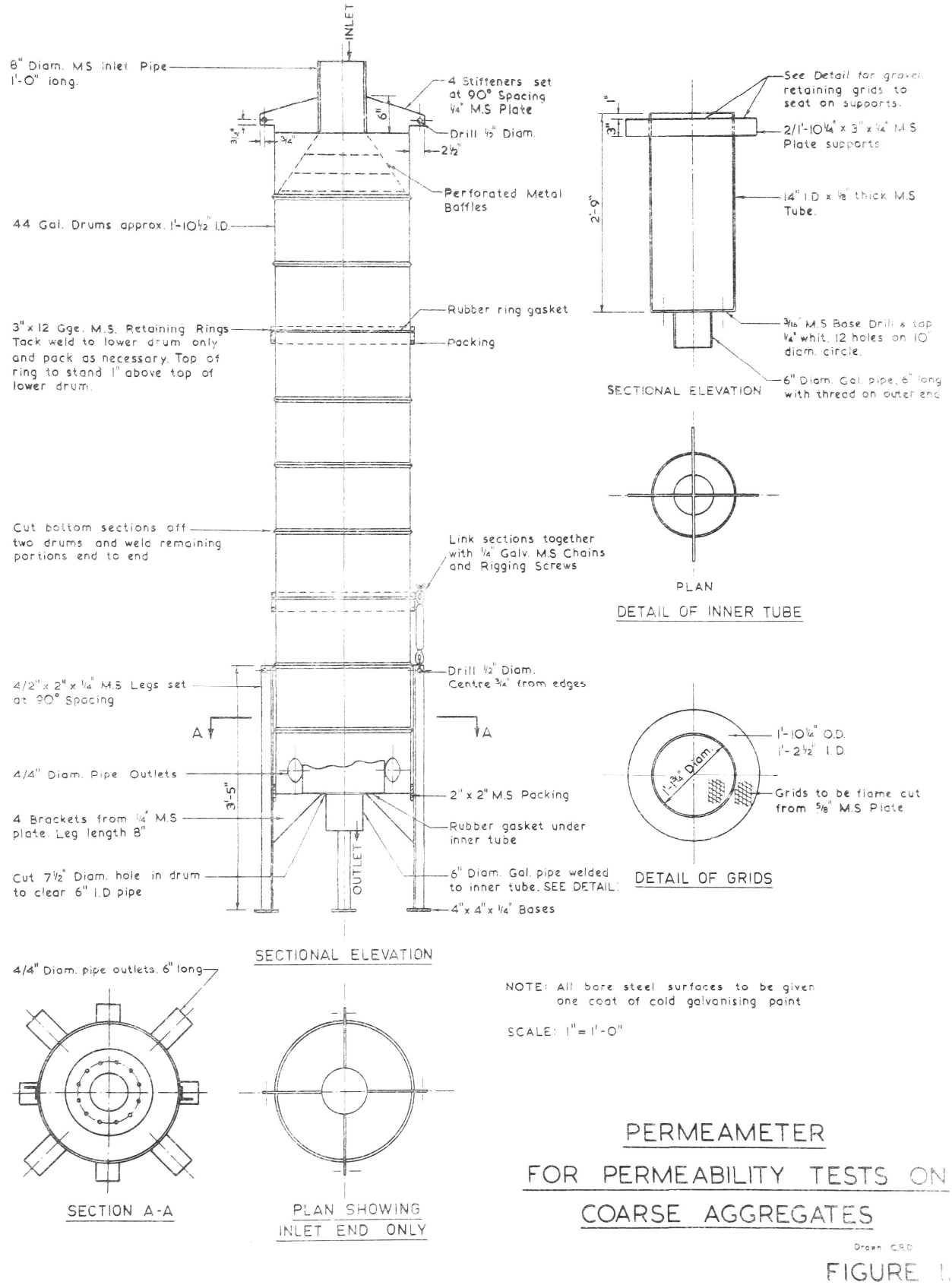

PERMEAMETER

FOR PERMEABILITY TESTS ON COARSE AGGREGATES

Drawn C.R.D

FIGURE 1.

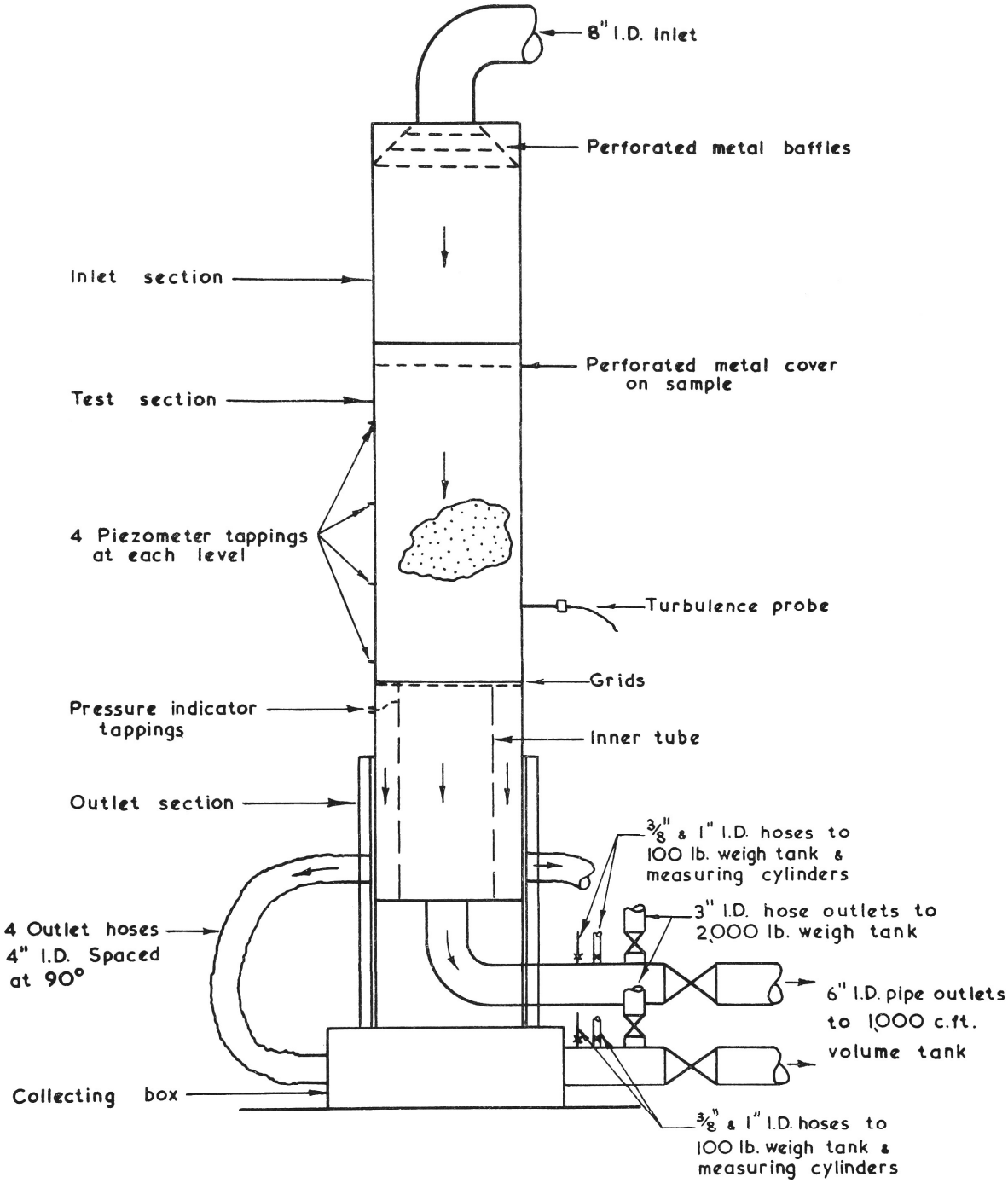

DIAGRAM OF PERMEAMETER AND OUTLETS

FIGURE 2.

apparatus are shown in Photograph 1.

The body of the permeameter was fabricated from open ended 44 gallon drums. These afforded a cheap circular section about the diameter required and their light weight allowed the permeameter to be assembled and dismantled by one operator with the aid of a block and tackle positioned overhead.

The main features of the permeameter are:

(i) Inlet Section. A 3 feet long inlet section was used. It was fitted with perforated metal baffles to break up the jet of water entering from the 8 inch diameter inlet pipe at high flow rates.

(ii) Test Section. The 4 feet long test section was provided with a number of glands made from 1/4 inch double ended petrol unions. Four of these were spaced at 90° intervals around the test section at each of a number of levels to allow the insertion of 1/4" O.D. pressure tapping tubes. Neoprene rings were used to seal the tubes in the glands.

A 6 inch square perspex window was fitted to allow visual observation of the sample in the test section.

(iii) Outlet Section. The 3 feet long outlet section was designed to enable the flow down a 14 inch diameter central core of the test material to be isolated from the flow down the annular section between this core and the wall of the permeameter.

An inner 14 inch diameter thin walled tube was bolted to the bottom

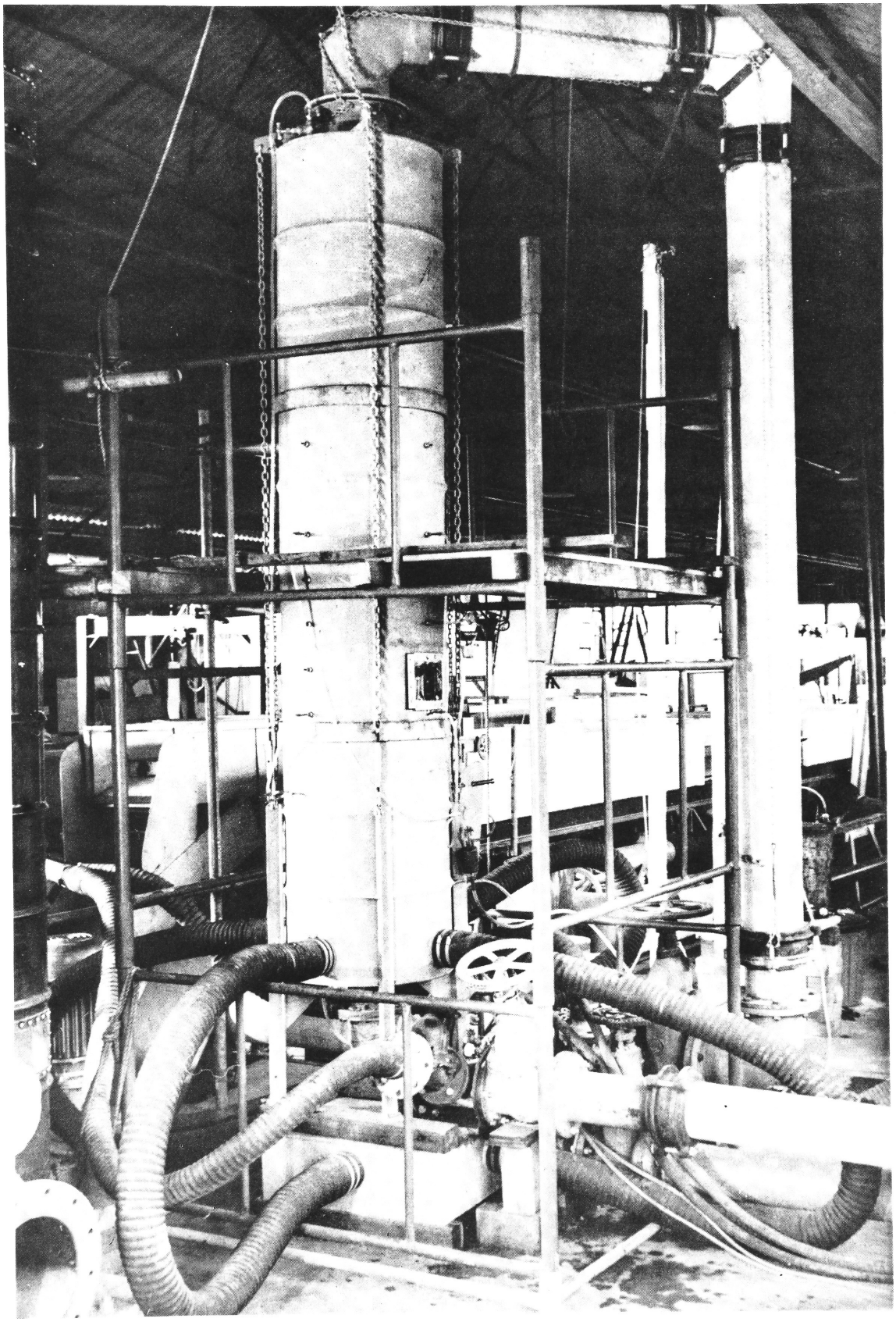

Photograph 1: General View of Permeameter.

of the outlet section and a 6 inch diameter outlet provided through the base. A view of this tube is shown in Photograph 2.

Four 4 inch I. D. outlets were spaced at 90^{o} around the outer wall of the outlet section near its base to allow the flow through the outer section to be drawn off uniformly without causing eccentricity in the pattern of flow in this section at high flow rates. The aim was to provide a practically constant flow distance and head loss to the outlets for all water particles emerging from the outer portion of the base of the sample under test.

(iv) Sample Supports. Heavy steel grids flame cut from 5/8 inch thick steel plate were used to support the weight of the sample and the force of up to 2 tons caused by the pressure difference at high flow rates. These grids were supported on steel beams set into the inner tube. A layer of perforated metal and, for finer materials, a layer of fly gauze, rested on the grid.

The grids are shown on Photograph 3.

(v) Pressure Equality Indicator. To enable the piezometric heads to be kept the same in the inner and outer portions of the outlet section, a visual indicator was installed. Two tappings were drilled at the same level in the walls of the inner and outer tubes a short distance below the supporting grids. This distance was chosen to be great enough to eliminate trouble from local jets emerging from the grids and yet not be so great

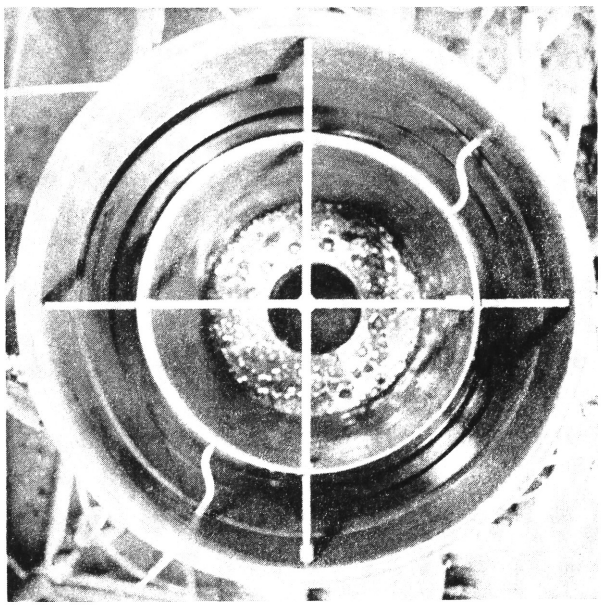

Photograph 2. Outlet Section of Permeameter showing inner tube.

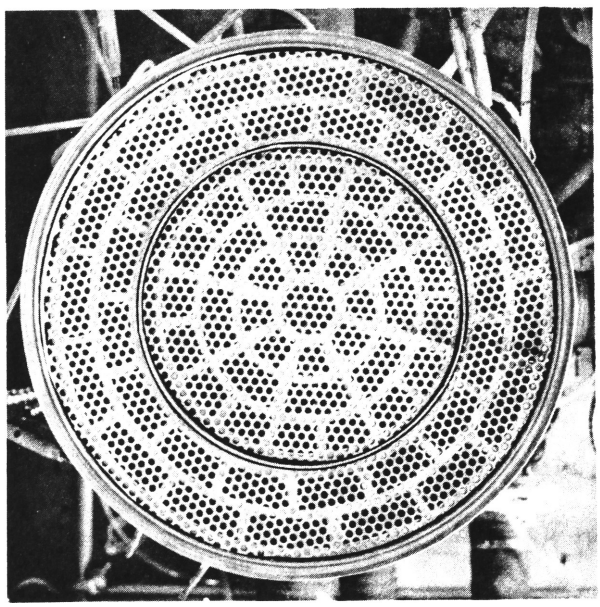

Photograph 3. Material-supporting Grids in Permeameter.

for there to be any appreciable head loss due to pipe friction between the base of the specimen and the tappings. Copper tubes with internal diameters of approximately 1/8 inch were set into the walls so that they were accurately flush with the inner surfaces. Plastic tubing with an internal diameter of approximately 1/4 inch was used to connect these tappings via a loop outside the permeameter. A short length of 1/8 inch I. D. plastic tubing was inserted as a constriction into this loop at its mid point and a hypodermic needle inserted through the wall of the constriction to allow dye to be injected.

Head differences between the inner and outer portions of the outlet sections could then be detected by movement of the dye.

The indicator and internal connections are shown on Photographs 2, 4 and 5.

(vi) Joints and Seals. Cutting and welding of the 44 gallon drums were arranged so that the rolled over edges of the test section mated with the rolled over edges of the inlet and outlet sections. Guide rings with very small clearances were fitted around the drums at each joint. These were tack welded to one drum only, the other drum being a light push fit into the guide ring. A rubber ring was used in each joint as a seal. The use of a grease which would not attack rubber was found to be necessary to facilitate assembling and dismantling the joints.

The joints were held together by four chains spaced at 90^{o} around the permeameter with four additional light chains to hold the test section on

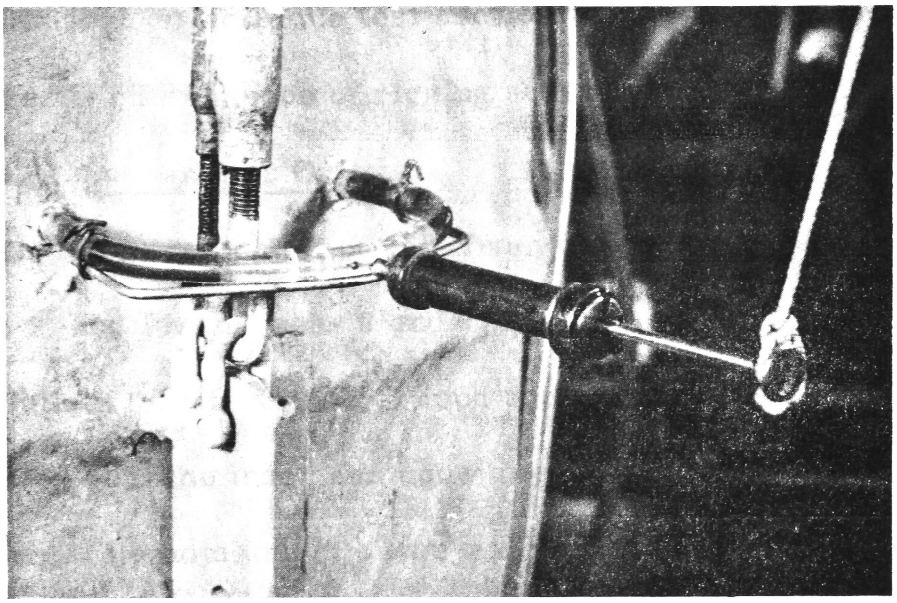

Photograph 4 (above).
Pressure Equality
Indicator.

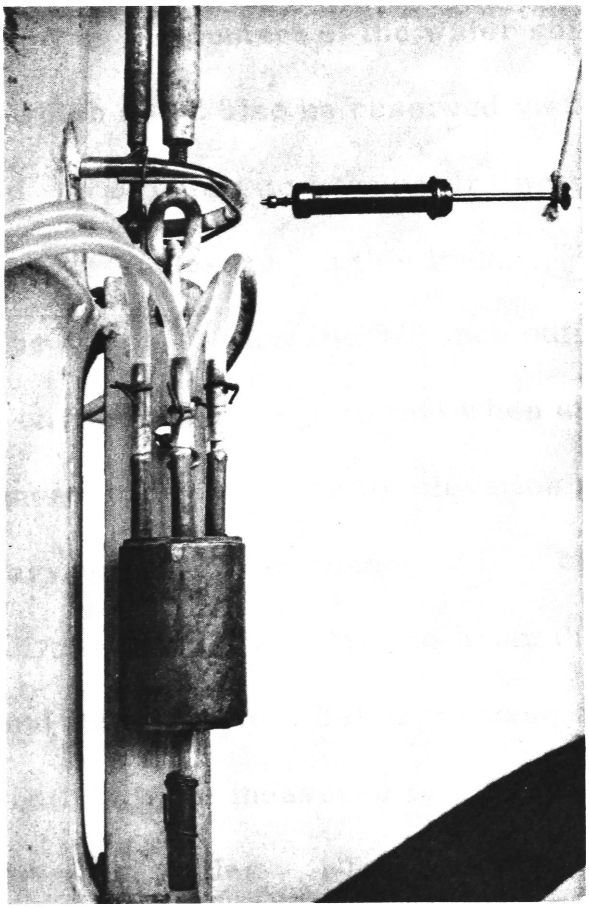

Photograph 5 (left).
Piezometer Tapping
Junction Box.

the outlet section while the test section was being loaded. All chains were tensioned by means of rigging screws.

(c) Permeameter Outlets

The arrangement of outlets from the permeameter is shown in Figure 2. and Photographs 6 and 7.

Outlets 6 inch, 3 inch, 1 inch and 3/8 inch in diameter were required for both the inner and outer portions of the outlet section to allow accurate adjustment of the wide range of flow rates.

The pair of 6 inch outlets were fixed in position above a 1,000 cubic feet calibrated volume measuring tank equipped with an electrical device for indicating the contact of the water surface with a number of hook gauges which could also be observed visually. The outer flow was diverted via a chute into a waste drain when required. Flow rates up to 4 c f s were measured in this tank.

The 3 inch, 1 inch and 3/8 inch outlets were provided with pipe bends sliding on horizontal bars so that when an outlet was moved to direct water into a measuring container its elevation remained constant. This was necessary to retain the balance of flow between the outer and inner outlets, preset by adjusting the valves to make the piezometric heads equal in the inner and outer sections below the base of the sample. Flows from the 3 inch outlets were measured in a 30 cubic feet capacity tank on a 3,000x$\frac{1}{2}$ lb. capacity set of scales. Flows from the 1 inch and 3/8 inch outlets were

Photograph 6. 6 inch, 1 inch, and 3/8 inch diameter Permeameter Outlets.

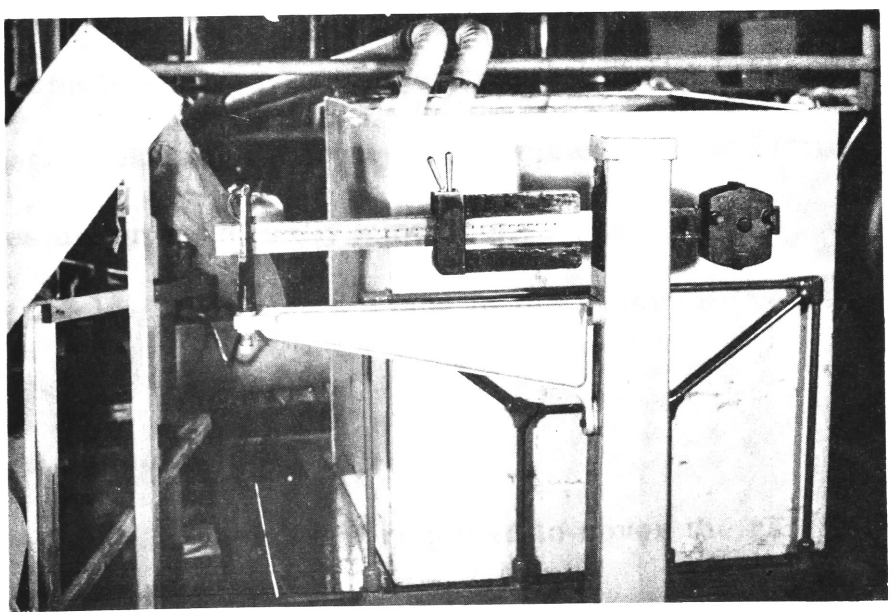

Photograph 7. 3 inch diameter Permeameter Outlets.

measured in a 10 gallon bin on a 1,000 lb. x 1/4 lb. set of scales. Small flows from the 3/8 inch outlets could also be measured in measuring cylinders or by counting and timing drops for very small flows.

(d) Pressure Tapping Junction Boxes

Plastic tubes of equal lengths were led from the four tappings at each level of the permeameter test section into junction boxes from which single tubes were led to the manometers. The justification for adopting the pressure in the junction box as the mean pressure at a given level is given in Appendix 1. Photograph 5 shows a junction box in position.

(e) Water Supply

Water was supplied to the permeameter from a large reservoir via approximately 300 feet of 18 inch diameter and 50 feet of 10 inch diameter pipe. The distances were sufficiently short to allow pressure fluctuations caused by small wind waves on the reservoir to be transmitted to the permeameter, causing difficulty in the measurement of small head differences under even mildly windy conditions.

The level of the water surface in the reservoir remained constant during tests.

5.3 Manometers

Three manometers were required to cover the range of hydraulic gradients with the required accuracy. A mercury-water U-tube was used for head differences from 25 to 10 feet of water, a water U-tube

for head differences from 10 feet to 0.5 feet of water and a pair of Casella micromanometers for head differences from 15 centimetres to 0.01 centimetre of water.

The micromanometers were connected at the bottoms of the sight glasses to the permeameter pressure tappings and at the tops to an air reservoir. The pressure in this reservoir was controlled by either adding air from an auxiliary cylinder pressurised by a foot pump or bleeding off water contained in the bottom of the reservoir. Water was found to be necessary to give a sufficiently sensitive control of pressure as it could be bled off in very small quantities.

The micromanometers were thus used to measure accurately the water levels in an inverted air-water U-tube.

The manometer setup is shown in Photograph 8.

5.4 Piezo-electric Turbulence Detector

Several methods of detecting the onset of turbulence in the permeameter were investigated and a detector using a piezo-electric crystal as the detecting element was decided on. The design of this detector is shown in Figure 3.

Pressure fluctuations were led through a short length of flexible tubing connected to the permeameter at one end and the cover of the detector at the other. Water in the tube was isolated from the crystal by a thin metal diaphragm sealed between the cover and body of the detector.

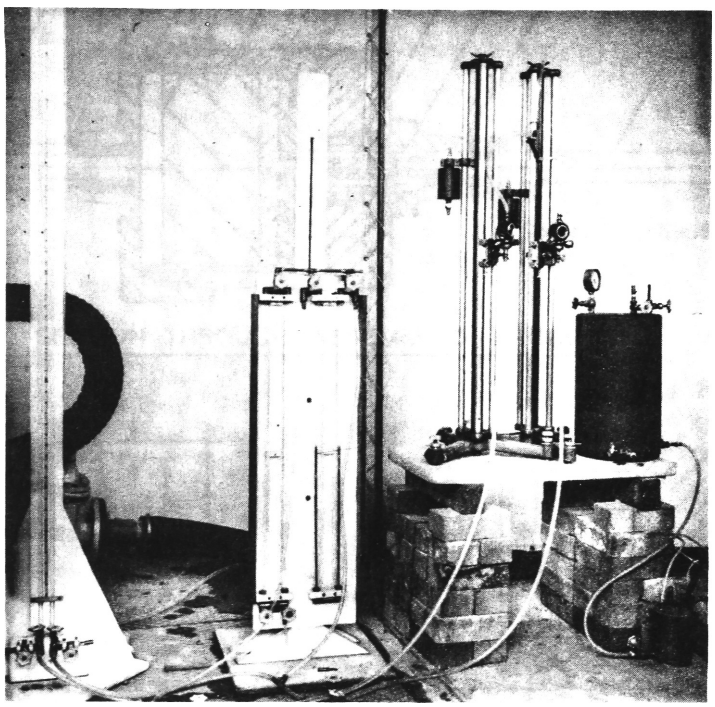

Photograph 8. Arrangement of Manometers.

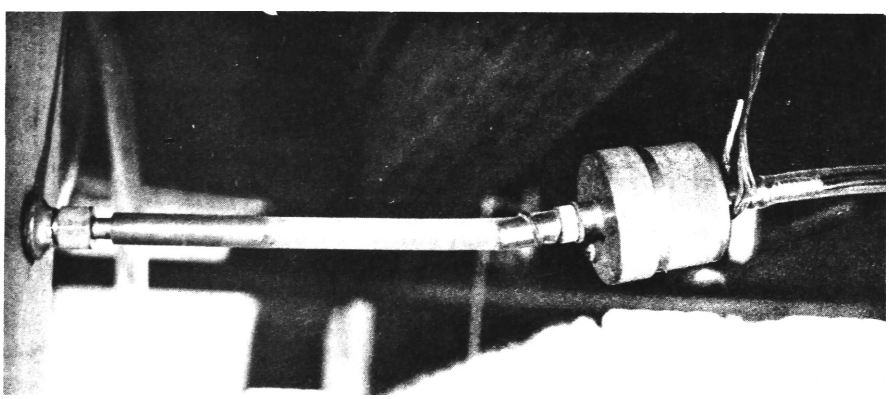

Photograph 9. Piezo-electric Turbulence Detector.

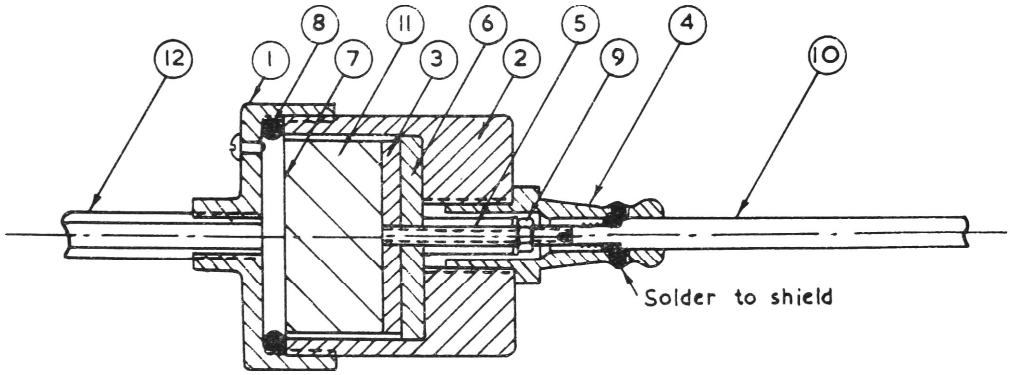

SECTION THROUGH ASSEMBLED PROBE

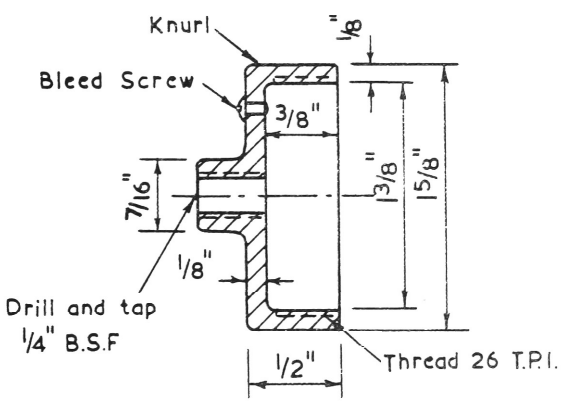

(1) COVER (Brass)

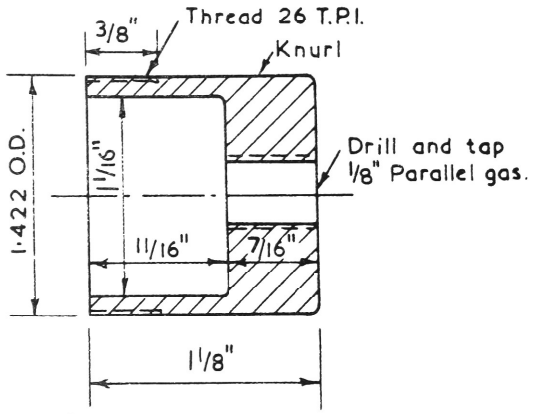

(2) BODY (Brass)

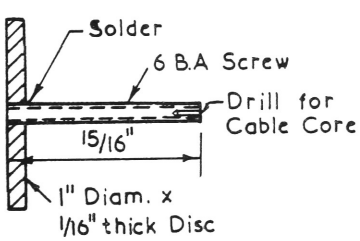

(3) CRYSTAL BASE
(Brass)

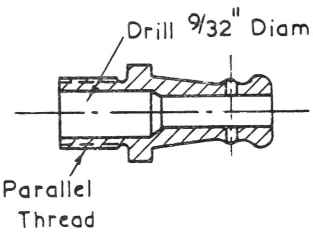

(4) CABLE CONNECTOR
(Brass, from 1/8" Gas Nipple)

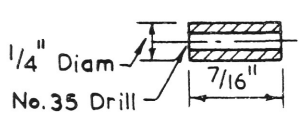

(5) SPACER
(Bakelite Fibre)

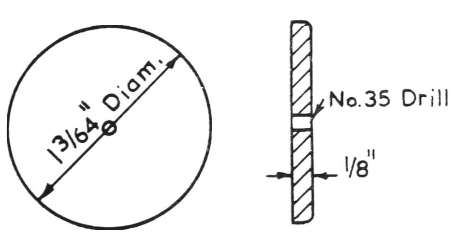

(6) INSULATING WASHER
(Bakelite Fibre)

(7) Brass shim cover 1 23/64" Diam, ·0015" thick
Glue to crystal with epoxy resin

(8) 1 3/8" O.D Neoprene sealing ring

(9) 1–6 B.A Brass nut and washer

(10) 6 ft. noise-free co-axial cable

(11) Barium titanate crystal, 1" Diam. x 1/2" thick
Glue to base

(12) 1/4" O.D Copper tube

SCALE – FULL SIZE

PIEZO-ELECTRIC TURBULENCE DETECTOR

FIGURE 3.

Voltage fluctuations produced by the pressure fluctuations on the crystal were transferred through a noise-free co-axial cable direct to a cathode ray oscilloscope with a maximum sensitivity of 1 mV per cm or through an intermediate low frequency amplifier to an oscilloscope with a maximum sensitivity of 30 mV per cm.

Since detection, and not measurement, of turbulence fluctuations was the aim, the circuitry was kept as simple as possible.

A photograph of the detector in position is shown in Photograph 9.

5.5 Fall Velocity Tanks

A 12 feet long, 22 inch diameter tank for measuring fall velocities of particles was welded together from open ended 44 gallon drums with the bottoms cut out. Perspex windows were fitted in the tank to allow falling particles to be observed and a 45^{o} mirror was placed in front of the top window to allow an observer at the base to time the fall of particles near the top and bottom of the tank.

A 3 feet x 3 feet x 6 feet high tank with one perspex wall and an 8 feet x 8 feet x 10 feet high tank were also used for fall velocity tests.

6. Details of Tests and Procedures

6.1 Permeability Tests

(a) General. The first series of tests in the permeameter was carried out on a sample of 3/4 inch crushed blue metal. It was intended to determine the relationship between flow velocity and hydraulic gradient and to investigate differences between results obtained for increasing and decreasing flows, wall effects in the permeameter, the effect of spreading tests over a period of a number of days, the effect of variation of water pressure in the permeameter and to develop techniques required to minimise experimental errors. A large number of tests were included in this series to investigate these aspects.

Using the techniques developed in the first series, tests were then undertaken to determine the head loss - velocity relationships for 7 gradings of Nepean River Gravel (including Nepean River Sand), 5 gradings of crushed blue metal, 3 sizes of glass marbles and one mixture of the 3 sizes of marbles.

Further tests were performed on 3/4 inch crushed blue metal and 16 mm diameter marbles to check existing formulae for the relationship between permeability and porosity.

(b) Loading and Unloading the Permeameter. Between 0.8 and 1.0 tons of test material were handled each time the permeameter was loaded and unloaded. The material was weighed before loading and elevated in

4 gallon containers. It was distributed evenly over the entire cross-section of the test section by pouring from a height of approximately 4 feet. No tamping or other form of compaction was attempted. When the test section was filled to the required height the surface was levelled and its height measured before it was covered with a perforated metal grid to prevent displacement of the surface particles by water while the permeameter was being filled.

The unloading procedure consisted of removing the inlet section and lifting one side of the test section to allow material to spill down a chute into drums.

The use of a rubber ring joint in the inlet pipe and rigging screws in the tensioning chains allowed one operator to dismantle and unload the permeameter in half an hour.

Two operators were needed to load the permeameter, the time required for the complete loading and reassembly operation being approximately $1\frac{1}{2}$ hours.

The loading and unloading procedures are illustrated by photographs 10 and 11.

(c) Pre-Test Procedure. Before carrying out tests, water was run through the permeameter at the maximum flow rate for some time to wash out any very fine material from coarse material and to allow the sample to settle. Settlement was checked by observing the head

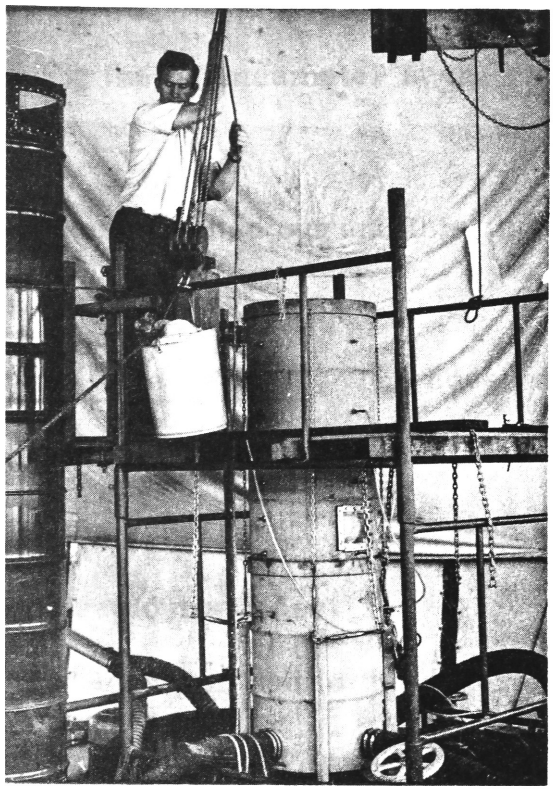

Photograph 10. Loading the Permeameter.

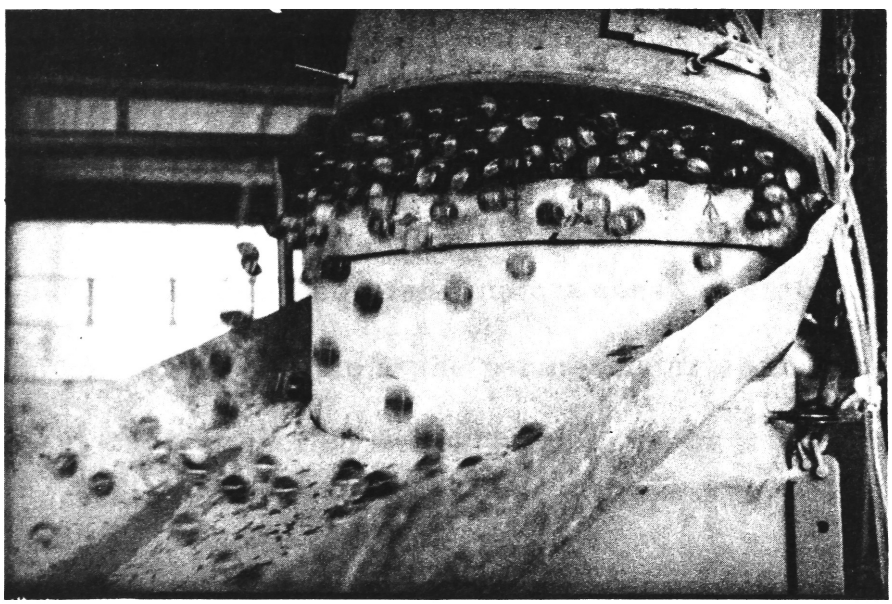

Photograph 11. Unloading the Permeameter.

loss over the test length during this initial period and by checking the sample height when unloading the permeameter at the end of a series of tests.

All manometer tubes were flushed out and this flushing repeated at intervals during the tests.

(d) Balancing Inner and Outer Flows. The necessity for separate control of the flows through the inner and outer outlets, even though each outlet of a pair was kept at the same level, was caused by the inequality of the head losses in the paired outlet lines.

This difference in head loss was due to the different rates of flow in the two outlets and the impracticability of adjusting the shapes and sizes of the inner and outer valves, pipes and hoses to allow for this effect.

Each of the pairs of valves in use for a particular test was adjusted until the required head difference over the test length was obtained and dye injected into the pressure indicator constriction remained stationary.

This procedure was intended to maintain a constant piezometric head across the base of the sample in the permeameter so that the distribution of flow in the test section would be the same as if the inner outlet were not present.

A constant rate of head loss between the top and bottom surfaces

of the sample were also ensured by this procedure. Thus head differences measured between piezometer tappings near the outer walls could be expected to represent head differences for the entire cross section of the flow

(e) Measurement of Flow Velocities. Velocities of flow through the inner core and the total cross-sectional area of the permeameter were calculated by dividing measured flow rates by the appropriate cross-sectional areas.

These flow rates were measured by weighing or measuring the volume of water discharged during a measured time interval. Times were measured by means of a stop watch. Details of the outlets from the permeameter and the corresponding measuring facilities are listed in Section 5. 2(c).

A comparison of the velocities determined for the total cross section and the inner core allowed wall effects to be studied.

When the large volume tank was being used with the fixed 6 inch outlets a pump was used to keep it empty while the flow was set. When conditions were steady, the pump was stopped and the time taken for the water surface to rise from one hook gauge to another was measured. For all other measuring containers, the flow was directed into, or diverted from, the container by sliding the appropriate 3 inch, 1 inch or 3/8 inch outlets along the horizontal bar provided.

Very small flows from the 3/8 inch outlets were measured by counting the number of drops discharged in a measured time. The drop volume was determined independently by measuring the volume deposited in a measuring cylinder by a counted number of drops. This procedure was found to be necessary because at these low flow rates the minute valve openings required tended to be unstable and it was difficult to maintain the correct balance between the inner and outer flows. Simultaneous counting of drops from both outlets over a short period was the only way repeatable results could be obtained. The drop volume could be checked over a much longer period, despite the variations in flow rate, since the drop volume was practically constant provided discrete drops were formed.

(f) Measurement of Hydraulic Gradient

(i) Test Lengths. Piezometer tappings used in the tests were set accurately 2 feet and 3 feet apart. The 2 feet test length was used for all tests except those on materials of nominal size greater than $1\frac{1}{2}$ inches for which the 3 feet length was used.

Hydraulic gradients were calculated from the head losses measured over the test lengths.

(ii) Piezometer Tappings. For tests on fine materials the 1/4 inch O.D., 1/8 inch I.D. piezometer tubes were inserted through glands approximately 1/2inch into the permeameter and covered with cylinders of fly gauze which projected inwards a further 1/2 inch leaving small shielded

cavities in front of the openings. This was done to prevent the small particles from blocking the ends of the tubes.

For tests on medium sized materials, the gauze covers were omitted and for very coarse materials the ends of the tubes were set flush with the inside of the permeameter.

Investigators have used a number of types of piezometer tappings ranging from flush openings to tubes inserted to the middle of the permeameter and turned upwards to face the flow (Wilkins, 1955). Provided the velocity effects at the upper and lower tappings are the same it appears that the type of tapping is immaterial as these effects cancel when the head difference is determined. The main point to watch is that the flow conditions at each opening are the same. A device to average the heads at a number of tappings, such as that used in this investigation, is useful in minimising the effect of differences in flow around the openings.

An important advantage of tappings set close to the permeameter wall is that their positions can be measured accurately and will remain constant.

(iii) Measurement of Head Loss. Details of the mercury-water and water manometers and the Casella micromanometers used to measure head losses are given in Section 5.3. The use of the mercury-water and water U-tubes was according to normal practice but the micro-manometer setup was non-standard, the sight glasses and point gauges being used to measure

accurately the water levels in the two legs of an inverted air-water U-tube. No ideal micromanometer is available for this application and the measurement of head losses, not flow rates, set the limit below which the hydraulic gradient-velocity relationship could not be investigated.

To minimise errors, the point of one of the micromanometers was kept at a constant level and the water surface brought level with this point by adjusting the air pressure in the top of the U tube. The apparatus for carrying out this procedure is described in Section 5.3. The level of the point in the other micromanometer was adjusted to be equal to that of the water surface in the other leg of the manometer.

By adopting this procedure two pointings and one vernier reading were involved whereas two points and two vernier readings would have been involved had the level of both points been altered. One source of accidental error was thus eliminated.

The main difficulties met in using the micromanometers were:

(i) The separation of the eyepieces of the micrometers required the eye to be moved and re-focussed to check the water surface at both points. This caused particular difficulty if the levels were oscillating slightly.

(ii) Because the levels of the points were fixed in the sight glasses, adjustment of the level of one point caused a re-adjustment of the level of the water in the leg containing the fixed point. This necessitated the

development of good judgment in adjusting both the level of the moving point and the air pressure in the U-tube, or the measurement of small head losses became very time consuming.

(iii) The separate stands supporting the point gauges could not be placed closer together than approximately 9 inches so that slight tilting of the supporting surface due to temperature and moisture changes caused the zero levels to wander.

(iv) Because the position of a point could not be seen through the optical system when it was above the water surface, the mean position of fluctuating levels could not be judged accurately. Damping in the test sample caused pressure fluctuations originating in the water supply line to be greater at the upstream than at the downstream tapping, thus preventing the troughs of fluctuating levels being used as guides when setting the points. This made the measurement of small head differences difficult when there was the slightest pressure fluctuation in the supply main. Such measurements had to be restricted to periods when there was practically no wind.

Difficulties (i) to (iii) could possibly be overcome or minimised for head differences up to 1 or 2 inches by using a pair of sight glasses and movable points attached to one stand and with a common optical system so that both points could be viewed simultaneously. The use of points attached to micrometer drums and sliding in glands in the

bottoms of the sight glasses would allow more accurate measurement of levels and would overcome the problems caused by having points fixed in level in the sight glasses.

(g) Measurement of Temperature and the Control of Temperature Differences within the Permeameter

Water temperatures were measured initially by thermometer to $0.1^{\circ}C$ to determine the viscosity of the water for each test.

However, several discrepancies which occurred for low flow rates showed that for these tests the temperatures within the inner and outer sections of the permeameter had to be maintained constant within approximately $0.1^{\circ}C$ to prevent convection currents being set up in the test section and through the pressure equality indicator. It was found that if a temperature difference as small as 0.2 or $0.3^{\circ}C$ existed between the outer and the inner portions of the outlet section a definite flow was set up through the pressure indicator device when no flow was passing through the permeameter. This flow caused an incorrect balance of the flows from the outer and inner outlets when the valves were adjusted to stop the dye movement during a test.

Once the trouble had been detected the water was flushed out of the permeameter each time a series of small flow tests was to be carried out. It was noticed that the most consistent results were obtained at times when the temperatures of the water supply and the atmosphere were approximately equal. Under these conditions there

was no tendency for the water near the outer surface of the permeameter to gain heat from or lose heat to the surroundings.

(h) Checking the Onset of Turbulence in the Permeameter

The piezo-electric detector described in Section 5. 4 was inserted through the side wall of the test section at right angles to the flow. For fine materials the tapping tube was allowed to project approximately $\frac{1}{2}$ inch inside the wall and was covered with a fly gauze cylinder which projected inwards a further $\frac{1}{2}$ inch. For medium size materials the fly gauze was omitted and for the coarsest materials the tube was left flush with the inner surface.

One of two available cathode ray oscilloscopes was used to detect and display the output of the probe. One of these was sufficiently sensitive to allow the probe to be connected directly to its input. The other was used with a low frequency amplifier with a response down to approximately 5 c. p. s. between it and the probe. The latter setup was used for most tests.

The apparatus was used during a number of the permeability tests in an attempt to detect the velocity or hydraulic gradient at which irregular fluctuations became apparent on the oscilloscope trace. Checks were carried out with both increasing and decreasing flow rates.

(i) Measurement of Porosity

The porosities of the porous media as placed in the permeameter

were checked by two methods.

In the first method the porosity was calculated from the weight of material loaded and the gross volume occupied in the permeameter. Since the material was allowed to settle under the action of the maximum flow before tests were carried out, the height of the sample determined after the tests was used to calculate the gross volume.

In the second method, water was drained from the permeameter until no more flowed from the upper piezometer tappings. The water between the upper and lower piezometer tappings was then drained off and weighed. The volume of drained water was taken as the volume of voids.

It was anticipated that the two methods would agree closely only for coarse smooth materials because of interstitial and surface retention effects.

6.2 Tests to check the effect of Porosity on the Velocity - Hydraulic Gradient Relationship

The tests described in Section 6.1 (a) were aimed at determining the hydraulic gradient - velocity relationships for a number of materials for one porosity for each material. To allow a comparison of the results for different porosities a limited number of tests were carried out on 3/4 inch blue metal and 16 mm diameter marbles at a number of porosities. These tests were intended to check the applicability of a number of published relationships connecting

porosity and permeability characteristics (see Cohen de Lara (1955)).

Porosities greater than those obtained by pouring material into the permeameter were obtained by mixing approximately 25 pc. by weight of crushed ice of maximum size $1\frac{1}{2}$ inches with the test material before it was loaded into the permeameter. The ice was allowed to melt and the surface was levelled before the permeameter was re-assembled. Settlement was then allowed to occur under the action of the maximum test flow until a stable packing was formed.

Intermediate porosities were obtained by vibrating the permeameter, rodding, and applying impact loading to the upper surface after the loose packing tests had been completed.

In all cases the methods of measuring porosity described in Section 6.1 (i) were adhered to.

6.3 Tests to Determine the Physical Characteristics of the Particles of the Granular Media

(a) Description of Materials

(i) River Gravels. The river gravels came from the Nepean River between Penrith and Richmond, N.S.W. They were composed mainly of water worn particles of hard igneous and metamorphic rocks and minerals derived from these.

The coarse and medium gravels consisted entirely of well rounded fragments of quartzite and intermediate igneous rocks such as granodiorite and porphyry. Although rounded, many of the

particles were somewhat flat.

The fine gravels consisted of small angular rock particles and separate mineral grains. Quartz was the predominant separate mineral present with some feldspar. The proportion of quartz increased with increasing fineness until for sand it was approximately 98 pc. The angularity of the particles increased with increasing fineness but the tendency towards flatness decreased until for sand it had almost disappeared.

(ii) Crushed Blue Metal. The crushed blue metal came from Prospect, N.S.W. All sizes consisted of angular particles of crushed dolerite. The smaller sizes had a higher proportion of the lighter minerals as these tend to crush more easily. This was reflected in the results of specific gravity tests. Of the two samples of 3/4 inch blue metal, sample BM3-2, used in test series No. 1, was more flaky than sample BM3-1.

The sizes and shapes of particles of the various materials are in Photographs 12 to 24. Photographs 25 and 26 show 3 inch and 6 inch river gravel in position in the permeameter.

(b) Particle Size Analyses

Sieve analyses of all river gravels and crushed rock materials used in the permeability tests were carried out according to A.S.T.M. Tentative Standard D422-54T.

(12) BM4. 3 inch Blue Metal.

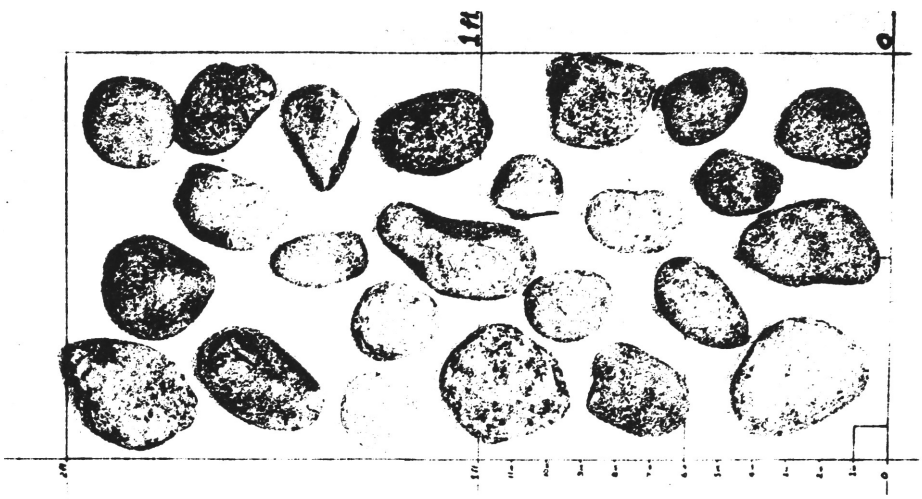

(13) C6. 3 inch River Gravel

(14) C7. 6 inch River Gravel.

Photographs (12) to (14) showing materials used in Permeability Tests.

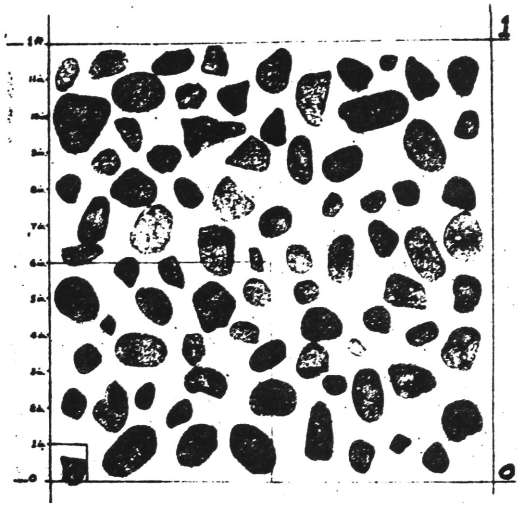

(15) G4 3/4 inch River Gravel.

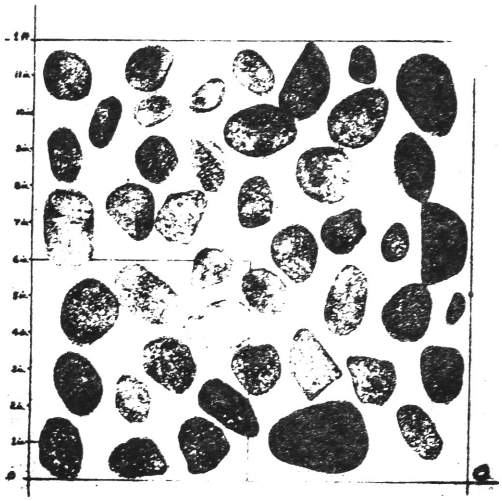

(16) G5. $1\frac{1}{2}$ inch River Gravel.

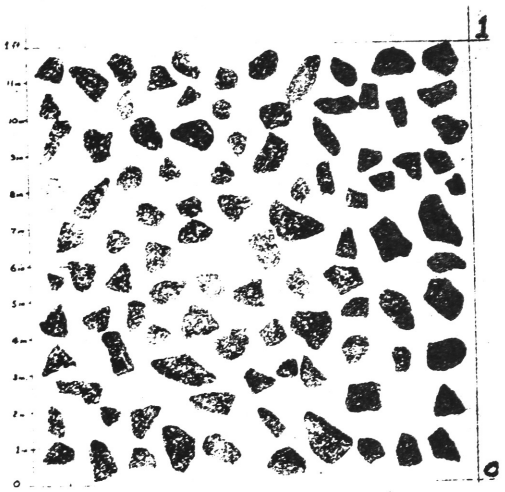

(17) BM3 - 2. 3/4 inch Blue Metal

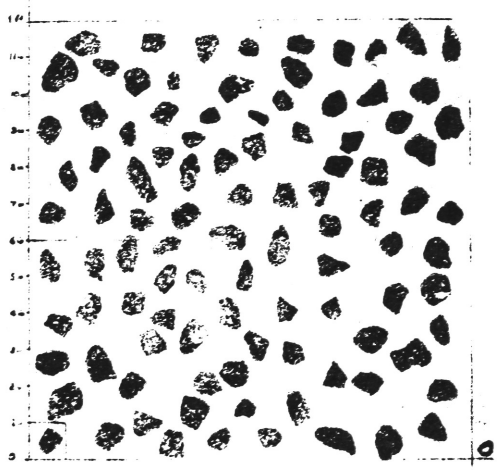

(18) BM 3-1.3/4 inch Blue Metal.

Photographs 15 to 19 showing materials used in Permeability tests.

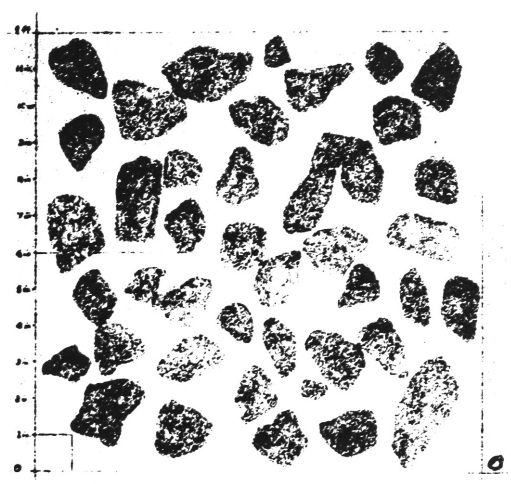

(19) BM4. $1\frac{1}{2}$ inch Blue Metal.

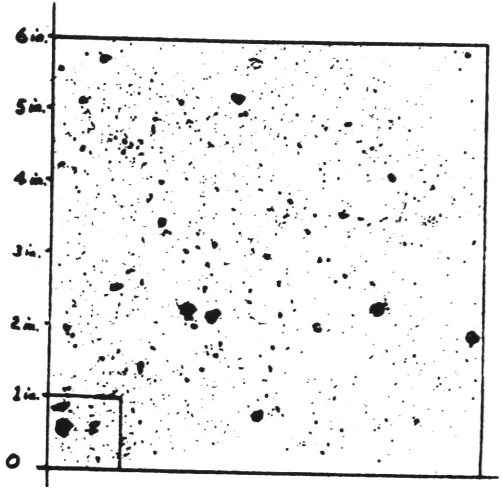

(20) G1 Nepean River Sand

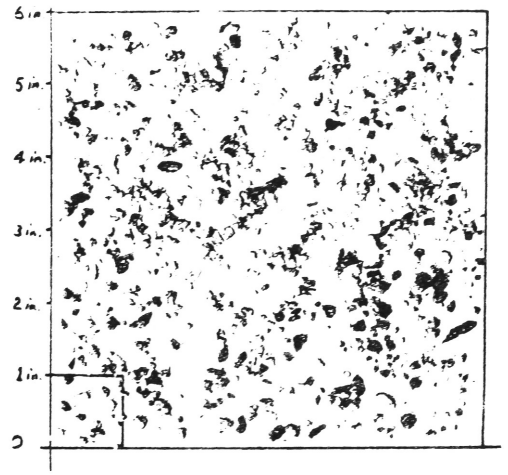

(21) G2 - 1/4 inch River Gravel

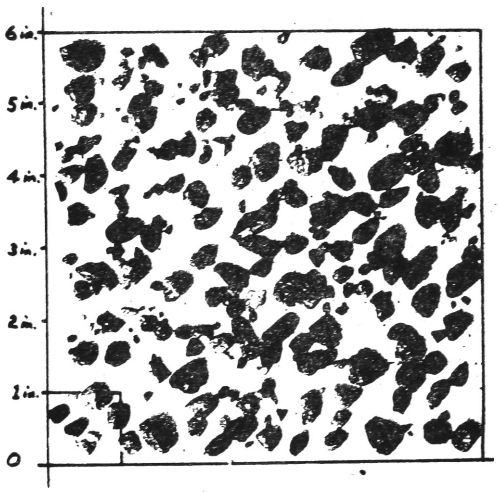

(22) G3 3/8 inch River Gravel

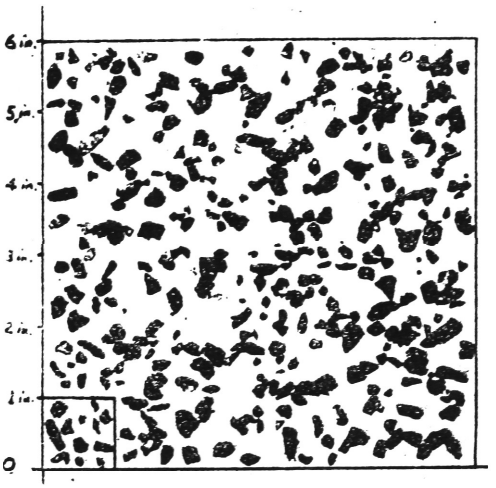

(23) BM1 3/16 inch Blue Metal

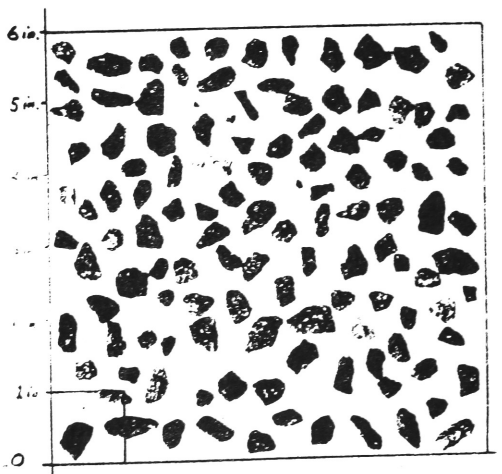

(24) BM 2 3/8 inch Blue Metal

Photographs (20) to (24) showing materials used in Permeability Tests.

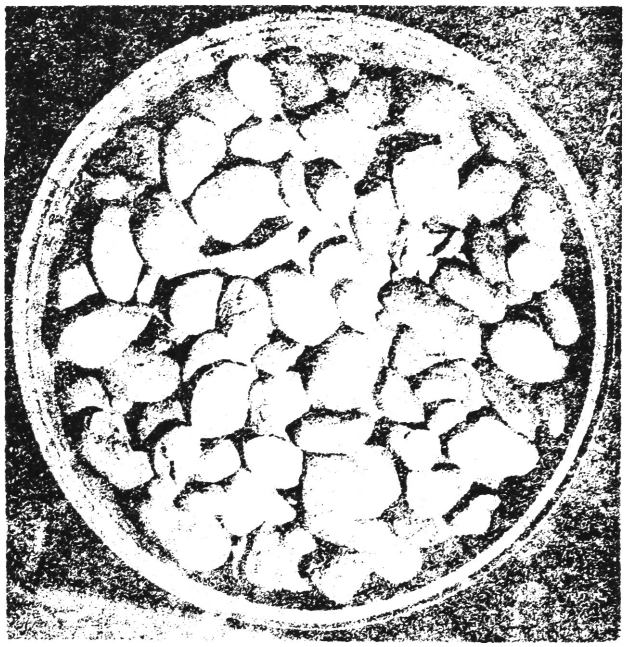

Photograph 25. 3 inch River Gravel in Permeameter.

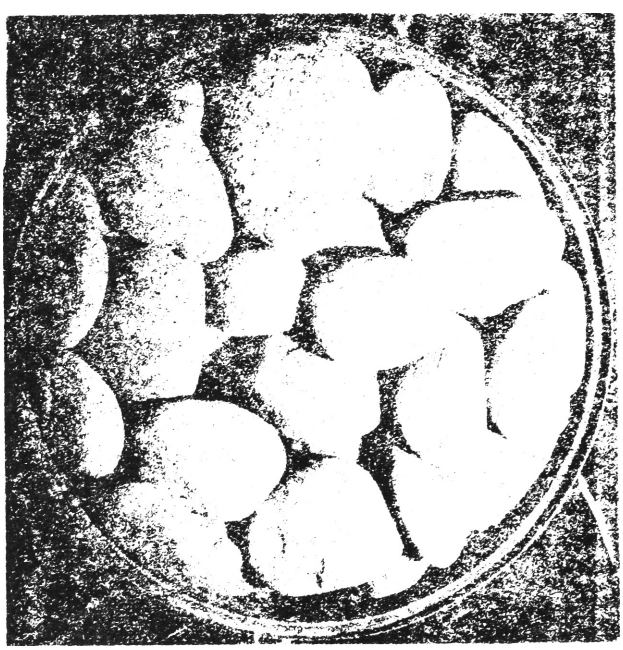

Photograph 26. 6 inch River Gravel in Permeameter.

The samples used for the sieve analyses were taken as the materials were being unloaded from the permeameter to avoid including any fines in the material originally loaded and which might have been washed out by the high pre-test flows.

The sizes of marbles were measured using vernier calipers and micrometers. Eccentricity was checked by measuring three mutually perpendicular diameters.

(c) Specific Gravity Tests

Specific gravities of the materials were required for the calculation of solid volumes from weights and for adjustment of fall velocity results. Determinations were made using the method set out in A. S. T. M. Standard C127.

(d) Fall Velocity Tests

Fall velocities were measured in an attempt to determine a factor for the particles of a material which would characterise their size, shape and grading.

Approximately 100 particles of each material used in the permeability tests were dropped individually in a fall velocity tank. Fall times over a fixed distance were measured with a stopwatch. The tanks listed in Section 5. 5 were used for these tests.

Additional tests were carried out on some materials to determine the differences between fall velocities in the various tanks and to check

the consistency of fall and timing of individual particles.

An approximate check on the distance required for particles to reach terminal velocity was made by photographing the fall of particles with a movie camera.

The tests on the 6 inch river gravel had to be performed in a concrete tank in which the fall of the particles could not be observed. These particles were dropped from a height sufficient to allow them to reach the approximate terminal velocities expected in water. Fall times were measured over a 10 feet fall distance from the water surface to the bottom of the tank.

7. Experimental Results

7.1 Permeability Tests

Detailed summaries of the results of the permeability tests on glass marbles, river gravels and crushed blue metal aggregates are listed in Tables 8 to 27 in Appendix II. Velocities and hydraulic gradients determined in these tests are plotted in Figures 4 to 10. On these figures filled-in symbols represent flows through the innter section of the permeameter while open symbols represent flows through the total cross sectional area.

In the drawing of the graphs for low flow rates, less weight has been placed on the results with very low hydraulic gradients since the possible error in these is high. This is illustrated by the scatter of the lowest points on the graphs.

A brief summary of test numbers, materials, median diameters and porosities is given in Table 3. A loose-leaf copy of this table is provided for ease of reference throughout the text.

7.2 Material Characteristics

(a) Sieve Analyses

A summary of sieve analysis results is presented in Table 4. These results are plotted on conventional grading sheets in Figures 11 and 12, on logarithmic probability paper in Figures 13 and 14 and on linear probability paper in Figures 15 and 16.

(b) Fall Velocities

Fall velocity test results are summarized in Table 5. The results are plotted on logarithmic probability paper in Figures 17 to 19 and on linear probability paper in Figures 20 to 22.

Median fall velocities have been adjusted to allow for the different specific gravities of the materials. These velocities, adjusted to a specific gravity of 2.65 (that of quartz) are tabulated in Table 7.

It should be noted that fall velocities for the same particles in different tanks differed because of the effect of wall proximity in the smaller tanks. In general, the results from the 3 ft. x 3 ft. tank were accepted as the most accurate as wall effects were a minimum for this tank.

8. Analysis of Experimental Results

8.1 Permeability Tests

(a) Form of Velocity - Hydraulic Gradient Relationship.

The results of permeability tests plotted in Figures 4 to 10 show that for a wide range of coarse granular media and hydraulic gradients between 10^{-4} and 15, the velocity - hydraulic gradient relationship is a discontinuous exponential one. In all cases a number of flow regimes which plot as straight lines on the log log plots are apparent. This is true for both the flow through the inner section and the flow through the total cross-section of the permeameter. The equation for each regime may be written

$$S = aV^n$$

where S = hydraulic gradient

V = velocity

a, n are constants for each regime for a particular granular medium.

For each regime of a medium, the value of a is equal to the value of S for which V is unity, (the S-V curve being extended to this region if necessary), and the corresponding value of n is the slope of the S-V line.

Table 1 gives a summary of the values of velocity and hydraulic gradient for the limits of experimental data, and the intersection points of the straight line sections of the graphs, together with calculated

values of a and n. The latter were obtained algebraically and, where possible, checked graphically on the original plotting sheets.

Figure 10 shows all of the velocity-hydraulic gradient graphs drawn on the one sheet to facilitate a comparison of the graphical forms.

In accordance with Slepička's (1961(a)1961(b)) notation, regimes for which $n = 1$ will be called linear regimes; those for which $n < 1$ will be called pre-linear regimes and those for which $n > 1$ will be called post-linear regimes.

(i) Linear Regimes

Linear regimes were obtained for the 3/16 inch and 3/8 blue metal, sand, -1/4 inch and 3/8 inch gravel samples, 17 mm diameter marbles and the marble mixture containing 17 mm diameter marbles. The apparatus available for head loss measurements precluded the possibility of determining linear regimes for crushed rock and gravel aggregates with nominal sizes greater than approximately $\frac{1}{2}$ inch, as sufficiently low hydraulic gradients could not be measured.

Within the limits of accuracy of the experimental results, values obtained for n for the linear regimes did not differ significantly from 1.00. The most accurate determinations were for the less coarse materials and yielded values of 1.00 ± 1 pc.

It should be noted that the linear regime is the only one for which the exponent, n, remained sensibly constant despite changes in

TABLE I. SUMMARY OF DATA DEFINING FLOW REGIMES.

Test	Material	Porosity P pc.	Post-Linear Regimes												Linear Regime								Pre-Linear Regime					
			V ft/sec	S	a	n	V ft/sec	S	a	n	V ft/sec	S	a	n	V ft/sec	S	a	n	V ft/sec	S	a	n	V ft/sec	S	a	n	V ft/sec	S
1	BM3-2.3/4" Bl. Metal	45.5	*0.805	*10.0	15.0	1.87	9.8×10^{-2}	0.194	12.7	1.73	3.31×10^{-2}	2.96×10^{-2}	6.25	1.57	1.12×10^{-2}	5.45×10^{-3}	1.70	1.28	1.8×10^{-3}	5.2×10^{-4}	0.253	0.98	$*5.4\times10^{-4}$	$*1.6\times10^{-4}$				
2	M123 Marble Mix.	37.9	*1.25	*11.5	7.51	1.87	0.138	0.188	6.16	1.76					2.61×10^{-2}	1.00×10^{-2}	3.03	1.57	9.9×10^{-3}	2.19×10^{-3}	0.239	1.02	$*7.0\times10^{-4}$	$*1.48\times10^{-4}$				
4	G1 Nepean Sand	38.7													4.50×10^{-2}	11.5	442	1.18	1.50×10^{-2}	3.13	211	1.00	6.1×10^{-5}	1.28×10^{-2}	69	0.89	$*2.0\times10^{-6}$	$*6.2\times10^{-4}$
5	G3 3/8" River Gravel	39.2					*0.209	*10.0	147	1.72	4.35×10^{-2}	0.675	71.8	1.49	1.12×10^{-2}	8.95×10^{-2}	23.3	1.24	3.27×10^{-3}	1.95×10^{-2}	6.40	1.01	1.74×10^{-4}	1.00×10^{-3}				
6	G2-1/4" River Gravel	41.8					*0.200	*13.4	210	1.71	0.141	7.37	128	1.46	4.60×10^{-2}	1.44	60.1	1.21	7.5×10^{-3}	0.160	21.3	1.00	1.30×10^{-4}	2.78×10^{-3}	6.1	0.86	$*6.0\times10^{-6}$	$*1.97\times10^{-4}$
8	BM1 3/16"Bl.Metal	47.7					*0.350	*12.7	76.7	1.71					2.91×10^{-2}	0.179	12.4	1.20	4.6×10^{-3}	1.96×10^{-2}	4.63	1.01	1.54×10^{-3}	6.45×10^{-3}	1.10	0.79	$*4.5\times10^{-5}$	$*3.9\times10^{-4}$
9	BM2 3/8"Bl. Metal	45.8					*0.463	*12.5	47.6	1.74					3.90×10^{-2}	0.170	16.9	1.42	6.70×10^{-3}	1.40×10^{-2}	2.02	0.99	1.04×10^{-3}	2.20×10^{-3}	0.55	0.80	$*9.0\times10^{-5}$	$*3.07\times10^{-4}$
10	G6 3"River Gravel	36.9	*1.02	*5.04	4.85	1.86	3.27×10^{-2}	8.0×10^{-3}	2.62	1.69					$*9.0\times10^{-3}$	$*9.0\times10^{-4}$												
11	BM5 3" Blue Metal	48.3	*0.94	*10.0	11.3	1.88	3.59×10^{-2}	2.00×10^{-2}	7.89	1.80					7.5×10^{-3}	1.2×10^{-3}	0.92	1.36	$*1.7\times10^{-3}$	$*1.6\times10^{-4}$								
12	G5 1½"River Gravel	37.2	*0.855	*10.0	13.4	1.85	5.90×10^{-2}	7.17×10^{-2}	7.97	1.67					6.1×10^{-3}	1.64×10^{-3}	1.31	1.31	$*1.4\times10^{-3}$	$*2.38\times10^{-4}$								
13	G4 3/4"River Gr.	36.7	*0.63	*10.0	25.4	1.83	4.6×10^{-2}	9.0×10^{-2}	11.9	1.59	1.36×10^{-2}	1.30×10^{-2}	7.20	1.47	5.35×10^{-3}	3.30×10^{-3}	2.74	1.29	$*1.2\times10^{-3}$	$*4.83\times10^{-4}$								
14	BM4 1½" Bl. Metal	43.8	*0.95	*10.0	11.0	1.89	7.1×10^{-2}	7.5×10^{-2}	7.60	1.75					1.23×10^{-2}	3.5×10^{-3}	2.27	1.47	$*5.0\times10^{-3}$	$*9.3\times10^{-4}$								
15	BM3-1.3/4"Bl. Met.	42.8	*0.69	*10.0	19.7	1.82					4.10×10^{-2}	5.85×10^{-2}	6.66	1.48	4.4×10^{-3}	2.14×10^{-3}	1.79	1.24	$*1.2\times10^{-3}$	$*4.27\times10^{-4}$								
16	M1 16mm Marbles	36.9	*0.895	*8.0	9.80	1.83	9.4×10^{-2}	0.131	6.91	1.68					2.80×10^{-2}	1.72×10^{-2}	2.88	1.43	5.17×10^{-3}	1.53×10^{-3}	0.309	1.01	$*8.0\times10^{-4}$	$*2.33\times10^{-4}$				
17	M2 25 mm Marbles	36.9	*1.06	*7.00	6.28	1.87	0.180	0.255	5.40	1.78					3.92×10^{-2}	1.69×10^{-2}	2.70	1.57	$*1.00\times10^{-3}$	$*5.4\times10^{-5}$								
18	G7 6"River Gravel	40.6	*1.35	*2.50	1.41	1.91	7.0×10^{-2}	8.8×10^{-3}	1.07	1.80					$*5.85\times10^{-3}$	$*1.00\times10^{-4}$												
19	M1 16 mm Marbles	41.5	*0.510	*1.60	5.55	1.85	0.172	0.215	4.52	1.73					1.72×10^{-2}	4.00×10^{-3}	1.22	1.41	7.7×10^{-3}	1.29×10^{-3}	0.205	1.04	$*1.16\times10^{-3}$	$*1.8\times10^{-4}$				
20	M1 16 mm Marbles	37.2	*0.450	*1.88	7.98	1.81	9.1×10^{-2}	0.104	6.29	1.71					1.80×10^{-2}	6.5×10^{-3}	2.00	1.43	$*6.5\times10^{-3}$	$*1.52\times10^{-3}$								
21	BM3-1.3/4"Bl. Met.	51.5	*0.400	*1.50	8.45	1.89	8.0×10^{-2}	7.2×10^{-2}	5.33	1.70	2.33×10^{-2}	8.8×10^{-3}	2.05	1.45	5.2×10^{-3}	1.00×10^{-3}	0.712	1.25	$*2.00\times10^{-3}$	$*3.05\times10^{-4}$		-						
22	M3 29 mm Marbles	38.5	*1.13	*6.00	4.79	1.85	5.80×10^{-2}	2.45×10^{-2}	2.30	1.60					$*3.90\times10^{-3}$	$*3.30\times10^{-4}$												

TABLE 2

ANALYSIS OF PERMEABILITY TEST RESULTS.

Test Series	Material	Porosity P pc.	Characteristic Particle Lengths d 10 pc. mm	d 10 pc. ft.	d 50 pc. mm	d 50 pc. ft.	Water Kinematic Viscosity $\nu \times 10^5$ $ft^2/sec.$	Critical Values from experimental graphs V ft/sec.	Critical Values from experimental graphs S	Reynolds Number $\frac{Vd_{50}}{\nu}$	Friction Factor $\frac{2gd_{50}S}{V^2}$	Adjusted mean particle fall velocity V_f ft/sec.	$\frac{V}{V_f}$	$\frac{V^3\rho}{\gamma S\nu}$
1	BM3-2 3/4" Blue Metal	45.5	11	3.6×10^{-2}	16	5.2×10^{-2}	1.25	0.805	10.0	3.35×10^{3}	5.17×10^{1}	1.56	0.516	130
								9.8×10^{-2}	0.194	4.07×10^{2}	6.77×10^{1}		6.3×10^{-2}	12.1
							+0.17	3.31×10^{-2}	2.96×10^{-2}	1.38×10^{2}	9.01×10^{1}		2.12×10^{-2}	3.05
				$\frac{d_{10}}{d_{50}}$ = 0.69			-0.02	1.12×10^{-2}	5.45×10^{-3}	4.66×10^{1}	1.46×10^{2}		7.2×10^{-3}	0.642
								1.8×10^{-3}	5.2×10^{-4}	7.5	5.38×10^{2}		1.15×10^{-3}	2.79×10^{-2}
								5.4×10^{-4}	1.6×10^{-4}	2.25	1.84×10^{3}		3.46×10^{-4}	2.45×10^{-3}
2	M123 Marble Mixture	37.9	15.8	5.2×10^{-2}	24.9	$8\ 2\times10^{-2}$	1.34	1.25	11.5	7.65×10^{3}	3.89×10^{1}	3.02	0.414	394
								0.138	0.188	8.45×10^{2}	5.22×10^{1}		4.57×10^{-2}	32.4
							+0.03	2.61×10^{-2}	1.00×10^{-2}	1.60×10^{2}	7.75×10^{1}		8.65×10^{-3}	4.13
				$\frac{d_{10}}{d_{50}}$ = 0.63			-0.05	9.9×10^{-3}	2.19×10^{-3}	6.06×10^{1}	1.18×10^{2}		3.28×10^{-3}	1.03
								7.0×10^{-4}	1.48×10^{-4}	4.28	1.59×10^{3}		2.32×10^{-4}	5.38×10^{-3}
4	G1 Nepean Sand	38.7	0.27	8.9×10^{-4}	0.53	1.74×10^{-3}	1.42	4.50×10^{-2}	11.5	5.51	6.35×10^{2}	-		
								1.50×10^{-2}	3.13	1.84	1.56×10^{3}			
				$\frac{d_{10}}{d_{50}}$ = 0.51			+0.03	6.1×10^{-5}	1.28×10^{-2}	7.47×10^{-3}	3.86×10^{5}			
							-0.02	2.0×10^{-6}	6.2×10^{-4}	2.45×10^{-4}	1.74×10^{7}			
5	G3 3/8" River Gravel	39.2	2.0	6.6×10^{-3}	5.8	1.9×10^{-2}	1.42	0.209	10.0	2.80×10^{2}	2.80×10^{2}	0.91	0.230	2.00
								4.35×10^{-2}	0.675	5.82×10^{1}	4.37×10^{2}		4.78×10^{-2}	0.267
							+0.01	1.12×10^{-2}	8.95×10^{-2}	1.50×10^{1}	8.77×10^{2}		1.23×10^{-2}	3.44×10^{-2}
				$\frac{d_{10}}{d_{50}}$ = 0.35			-0.02	3.27×10^{-3}	1.95×10^{-2}	4.38	2.23×10^{3}		3.59×10^{-3}	3.92×10^{-3}
								1.74×10^{-4}	1.00×10^{-3}	2.33×10^{-1}	4.03×10^{4}		1.91×10^{-4}	1.15×10^{-5}
6	G2-1/4" River Gravel	41.8	0.95	3.1×10^{-3}	2.3	7.5×10^{-3}	1.40	0.200	13.4	1.07×10^{2}	1.62×10^{2}	0.67	0.299	1.33
								0.141	7.37	7.55×10^{1}	1.79×10^{2}		0.210	8.45×10^{-1}
							+0.01	4.60×10^{-2}	1.44	2.46×10^{1}	3.28×10^{2}		6.86×10^{-2}	1.50×10^{-1}
				$\frac{d_{10}}{d_{50}}$ = 0.41			-0.00	7.5×10^{-3}	0.160	4.02	1.37×10^{3}		1.12×10^{-2}	5.86×10^{-3}
								1.30×10^{-4}	2.78×10^{-3}	6.96×10^{-2}	7.95×10^{4}		1.94×10^{-4}	1.76×10^{-6}
								6.0×10^{-6}	1.97×10^{-4}	3.21×10^{-3}	2.65×10^{6}		9.0×10^{-6}	2.44×10^{-9}
8	BM1 3/16" Blue Metal	47.7	1.9	6.2×10^{-3}	3.2	1.05×10^{-2}	1.41	0.350	12.7	2.61×10^{2}	6.98×10^{1}	0.63	0.556	7.45
								2.91×10^{-2}	0.179	2.17×10^{1}	1.43×10^{2}		4.62×10^{-2}	3.04×10^{-1}
							+0.03	4.6×10^{-3}	1.96×10^{-2}	3.43	6.25×10^{2}		7.3×10^{-3}	1.10×10^{-2}
				$\frac{d_{10}}{d_{50}}$ = 0.59			-0.01	1.54×10^{-3}	$6\ 45\times10^{-3}$	1.15	1.84×10^{3}		2.45×10^{-3}	1.25×10^{-3}
								4.5×10^{-5}	3.9×10^{-4}	3.35×10^{-2}	1.30×10^{5}		7.1×10^{-5}	5.15×10^{-7}
9	BM2 3/8" Blue Metal	45.8	4.7	1.54×10^{-2}	6.4	2.10×10^{-2}	1.41	0.463	12.5	6.90×10^{2}	7.90×10^{1}	0.89	0.520	17.5
								3.90×10^{-2}	0.170	5.81×10^{1}	1.51×10^{2}		4.38×10^{-2}	7.70×10^{-1}
							+0.02	6.70×10^{-3}	1.40×10^{-2}	9.98	4.21×10^{2}		7.53×10^{-3}	4.74×10^{-2}
				$\frac{d_{10}}{d_{50}}$ = 0.73			-0.04	1.04×10^{-3}	2.20×10^{-3}	1.55	2.76×10^{3}		1.17×10^{-3}	1.13×10^{-3}
								9.0×10^{-5}	3.07×10^{-4}	1.34×10^{-1}	5.12×10^{4}		1.01×10^{-4}	5.24×10^{-6}
10	G6 3" River Gravel	36.9	40	1.31×10^{-1}	55	1.80×10^{-1}	1.37	1.02	5.04	1.34×10^{4}	5.62×10^{1}	3.48	0.290	478
							+0.04	3.27×10^{-2}	8.0×10^{-3}	4.30×10^{2}	8.67×10^{1}		9.40×10^{-3}	9.92
				$\frac{d_{10}}{d_{50}}$ = 0.73			-0.04	9.0×10^{-3}	9.0×10^{-4}	$1\ 18\times10^{2}$	1.29×10^{2}		2.58×10^{-4}	1.84
11	BM5 3" Blue Metal	48.3	25	8.2×10^{-2}	37	1.21×10^{-1}	1.39	0.94	10.0	8.18×10^{3}	8.82×10^{1}	2.36	0.398	186
								3.59×10^{-2}	2.00×10^{-2}	3.13×10^{2}	1.21×10^{2}		1.52×10^{-2}	5.18
							+0.04	7.5×10^{-3}	1.2×10^{-3}	6.53×10^{1}	1.66×10^{2}		3.18×10^{-3}	7.87×10^{-1}
				$\frac{d_{10}}{d_{50}}$ = 0.68			-0.04	1.7×10^{-3}	1.6×10^{-4}	1.48×10^{1}	4.32×10^{2}		7.2×10^{-4}	6.87×10^{-2}

TABLE 2 (cont'd.)

ANALYSIS OF PERMEABILITY TEST RESULTS

Test Series	Material	Porosity P pc.	Characteristic Particle Lengths d 10 pc. mm	d 10 pc. ft.	d 50 pc. mm	d 50 pc. ft.	Water Kinematic Viscosity $\nu \times 10^5$ ft^2/sec.	Critical Values from experimental graphs V ft/sec.	Critical Values from experimental graphs S	Reynolds Number $\frac{Vd_{50}}{\nu}$	Friction Factor $\frac{2gd_{50}S}{V^2}$	Adjusted mean particle fall velocity V_f ft/sec.	$\frac{V}{V_f}$	$\frac{V^3\rho}{\gamma S\nu}$
12	G5 1½" River Gravel	37.2	19	6.2×10^{-2}	26	8.5×10^{-2}	1.40	0.855	10.0	5.19×10^{3}	7.49×10^{1}	2.20	0.388	139
								5.9×10^{-2}	7.17×10^{-2}	3.58×10^{2}	1.13×10^{2}		2.68×10^{-2}	6 36
				$\frac{d_{10}}{d_{50}} = 0.73$			+0.00)	6.1×10^{-3}	1.64×10^{-3}	3.70×10^{1}	2.41×10^{2}		2.77×10^{-4}	3.07×10^{-1}
							-0.00)	1.4×10^{-3}	2.38×10^{-4}	8.5	6.65×10^{2}		6.4×10^{-4}	2.56×10^{-2}
13	G4 3/4" River Gravel	36.7	12	3.9×10^{-2}	16	5.2×10^{-2}	1.40	0.63	10.0	2.34×10^{3}	8.43×10^{1}	1.80	0.350	55.5
								4.6×10^{-2}	9.0×10^{-2}	1.71×10^{2}	1.42×10^{2}		2.55×10^{-2}	2. 40
				$\frac{d_{10}}{d_{50}} = 0.75$			+0.017)	1.36×10^{-2}	1.30×10^{-2}	5.05×10^{1}	2.35×10^{2}		7.55×10^{-3}	4.30×10^{-1}
							-0.001)	5.35×10^{-3}	3.30×10^{-3}	1.99×10^{1}	3.86×10^{2}		2.97×10^{-3}	1.03×10^{-1}
								1.2×10^{-3}	4.83×10^{-4}	4. 46	1.12×10^{3}		6.7×10^{-4}	7.95×10^{-3}
14	BM4 1½" Blue Metal	43.8	19	6.2×10^{-2}	25	8.2×10^{-2}	1.41	0.95	10.0	5.52×10^{3}	5.85×10^{1}	2.03	0.468	189
								7.1×10^{-2}	7.5×10^{-2}	4.13×10^{2}	7.85×10^{1}		3.49×10^{-2}	10.5
				$\frac{d_{10}}{d_{50}} = 0.76$			+0.02)	1.23×10^{-2}	3.5×10^{-3}	7.15×10^{1}	1.22×10^{2}		6.06×10^{-3}	1. 17
							-0.01)	5.0×10^{-3}	9.3×10^{-4}	2.91×10^{1}	1.96×10^{2}		2.46×10^{-3}	2.96×10^{-1}
15	BM3-1 3/4" Blue Metal	42.8	10.5	3.4×10^{-2}	14	4.6×10^{-2}	1.39	0.69	10.0	2.28×10^{3}	6.22×10^{1}	1.74	0.396	73.5
								4.10×10^{-2}	5.85×10^{-2}	1.36×10^{2}	1.03×10^{2}		2.35×10^{-2}	2.64
				$\frac{d_{10}}{d_{50}} = 0.75$			+0.02)	4.4×10^{-3}	2.14×10^{-3}	1.46×10^{1}	3.26×10^{2}		2.53×10^{-3}	8.9×10^{-2}
							-0.03)	1.2×10^{-3}	4.27×10^{-4}	3.97	8.80×10^{2}		6.9×10^{-4}	9.05×10^{-3}
16	M1 16 mm Marbles	36.9	15.6	5.11×10^{-2}	16.0	5.24×10^{-2}	1.38	0.895	8.0	3.40×10^{3}	3.38×10^{1}	2.64	0.339	202
								9.4×10^{-2}	0.131	3.57×10^{2}	5.01×10^{1}		3.56×10^{-2}	14.3
				$\frac{d_{10}}{d_{50}} = 0.98$			+0.02)	2.80×10^{-2}	1.72×10^{-2}	1.06×10^{2}	7.4×10^{1}		1.06×10^{-2}	2. 88
							-0.03)	5.17×10^{-3}	1.53×10^{-3}	1.96×10^{1}	1.94×10^{2}		1.96×10^{-3}	2.03×10^{-1}
								8.0×10^{-4}	2.33×10^{-4}	3.04	1.23×10^{3}		3.03×10^{-4}	7.56×10^{-4}
17	M2 25 mm Marbles	36.9	24.6	8.06×10^{-2}	24.9	8.16×10^{-2}	1.37	1.06	7.00	6.31×10^{3}	3.28×10^{1}	3.10	0.342	386
								0.180	0.255	1.07×10^{3}	4.13×10^{1}		5.80×10^{-2}	51.9
				$\frac{d_{10}}{d_{50}} = 0.99$			+0.03)	3.92×10^{-2}	1.69×10^{-2}	2.34×10^{2}	5.77×10^{1}		1.26×10^{-2}	8.09
							-0.02)	1.00×10^{-3}	5.4×10^{-5}	5.95	2.84×10^{2}		3.23×10^{-3}	4.20×10^{-2}
18	G7 6" River Gravel	40.6	84	2.75×10^{-1}	110	3.60×10^{-1}	1.37	1.35	2.50	3.55×10^{4}	3.19×10^{1}	5.96	0.227	2, 233
								7.0×10^{-2}	8.8×10^{-3}	1.84×10^{3}	4.16×10^{1}		1.18×10^{-2}	88.5
				$\frac{d_{10}}{d_{50}} = 0.76$			+0.03)	5.85×10^{-3}	1.00×10^{-4}	1.54×10^{2}	6.78×10^{1}		9.82×10^{-4}	4. 54
							-0.05)							
19	M1 16 mm Marbles	41.5	15.6	5.11×10^{-2}	16.0	5.24×10^{-2}	1.30	0.510	1.60	2.06×10^{3}	2.08×10^{1}	2.64	0.193	198
							+0.05)	0.172	0.215	6.94×10^{2}	2.46×10^{1}		6.52×10^{-2}	56.6
							-0.07)	1.72×10^{-2}	4.00×10^{-3}	6.94×10^{1}	4.57×10^{1}		6.52×10^{-3}	3.04
				$\frac{d_{10}}{d_{50}} = 0.98$				7.7×10^{-3}	1.29×10^{-3}	3.11×10^{1}	7.33×10^{1}		2.92×10^{-3}	8.47×10^{-1}
								1.16×10^{-3}	1.8×10^{-4}	4.68	4.50×10^{2}		4.40×10^{-4}	2.07×10^{-2}
20	M1 16 mm Marbles	37.2	15.6	5.11×10^{-2}	16.0	5.24×10^{-2}	1.24	0.450	1.88	1.90×10^{3}	3.13×10^{1}	2.64	0.170	122
								9.1×10^{-2}	0.104	3.85×10^{2}	4.25×10^{1}		3.45×10^{-2}	18. 2
				$\frac{d_{10}}{d_{50}} = 0.98$			+0.00)	1.80×10^{-2}	6.5×10^{-3}	7.60×10^{1}	6.78×10^{1}		6.82×10^{-3}	2. 25
							-0.00)	6.5×10^{-3}	1.52×10^{-3}	2.75×10^{1}	1.21×10^{2}		2.46×10^{-3}	4.53×10^{-1}

TABLE 2 (Cont'd.)

ANALYSIS OF PERMEABILITY TEST RESULTS.

Test Series	Material	Porosity p pc.	Characteristic Particle Lengths d 10 pc. mm	d 10 pc. ft.	d 50 pc. mm	d 50 pc. ft.	Water Kinematic Viscosity $\nu \times 10^5$ ft²/sec.	Critical Values from experimental graphs V ft/sec.	Critical Values from experimental graphs S	Reynolds Number $\frac{Vd_{50}}{\nu}$	Friction Factor $\frac{2gd_{50}S}{V^2}$	Adjusted mean particle fall velocity V_f ft/sec.	$\frac{V}{V_f}$	$\frac{V^3\rho}{\gamma S\nu}$
21	BM3 – 1.3/4" Blue Metal	51.5	10.5	3.4×10^{-2}	14	4.6×10^{-2}	1.23	0.400	1.50	1.50×10^{3}	2.78×10^{1}	1.74	0.230	108
								8.0×10^{-2}	7.2×10^{-2}	2.99×10^{2}	3.33×10^{1}		4.59×10^{-2}	18.0
				$\frac{d_{10}}{d_{50}}$ =			+0.00)	2.33×10^{-2}	8.8×10^{-3}	8.71×10^{1}	4.80×10^{1}		1.34×10^{-2}	3.63
					0.75		-0.01)	5.2×10^{-3}	1.00×10^{-3}	1.95×10^{1}	1.10×10^{2}		2.99×10^{-3}	3.55×10^{-1}
								2.00×10^{-3}	3.05×10^{-4}	7.48	2.26×10^{2}		1.15×10^{-3}	6.63×10^{-2}
22	M3.29 mm Marbles	38.5	28.5	9.35×10^{-2}	29.0	9.5×10^{-2}	1.20	1.13	6.00	8.95×10^{3}	2.87×10^{1}	3.31	0.341	623
								5.80×10^{-2}	2.45×10^{-2}	4.59×10^{2}	4.46×10^{1}		1.75×10^{-2}	20.6
				$\frac{d_{10}}{d_{50}}$ =			+0.04)	3.90×10^{-3}	3.30×10^{-4}	3.09×10^{1}	1.33×10^{2}		1.18×10^{-3}	4.66×10^{-1}
					0.98		-0.02)							

TABLE 3.

Summary of Permeability Test Data.

Test Series No.	Material	Median Diameter mm	Median Diameter ft.	Porosity pc By weighing Solids	Porosity pc By draining Voids
1	BM3-2.3/4" B. Metal	16	5.2×10^{-2}	45.5	42.6
2	M123 Marble mixture	24.9	8.2×10^{-2}	37.9	35.8
4	G1 Nepean R. sand	0.53	1.74×10^{-3}	38.7	27.2
5	G3 3/8" R. Gravel	5.8	1.9×10^{-2}	39.2	36.9
6	G2 –1/4" R. Gravel	2.3	7.5×10^{-3}	41.8	37.1
8	BM1 3/16" B. Metal	3.2	1.05×10^{-2}	47.7	45.9
9	BM2 3/8" Blue Metal	6.4	2.10×10^{-2}	45.8	41.6
10	G6 3" R. gravel	55	1.80×10^{-1}	36.9	37.3
11	BM5 3" Blue Metal	37	1.21×10^{-1}	48.3	46.3
12	G5 $1\frac{1}{2}$" R. gravel	26	8.5×10^{-2}	37.2	34.9
13	G4 3/4" R. gravel	16	5.2×10^{-2}	36.7	33.9
14	BM4 $1\frac{1}{2}$" Blue Metal	25	8.2×10^{-2}	43.8	41.8
15	BM3-1. 3/4" Blue Metal	14	4.6×10^{-2}	42.8	39.5
16	M1 16 mm Marbles	16.0	5.24×10^{-2}	36.9	36.9
17	M2 25 mm Marbles	24.9	8.16×10^{-2}	36.9	38.0
18	G7 6" R. Gravel	110	3.60×10^{-1}	40.6	40.4
19	M1 16 mm Marbles	16.0	5.24×10^{-2}	41.5	41.3
20	M1 16 mm Marbles	16.0	5.24×10^{-2}	37.2	37.8
21	BM3-1. 3/4" B. metal	14	4.6×10^{-2}	51.5	48.5
22	M3 29 mm Marbles	29.0	9.5×10^{-2}	38.5	38.0

Note: (a) Porosities shown on Figures 4 to 10 are those obtained by weighing solids.

(b) Marble mixture M123 consists of 16, 25 and 29 mm marbles in the proportions 1.23: 1.05: 1.00 by weight.

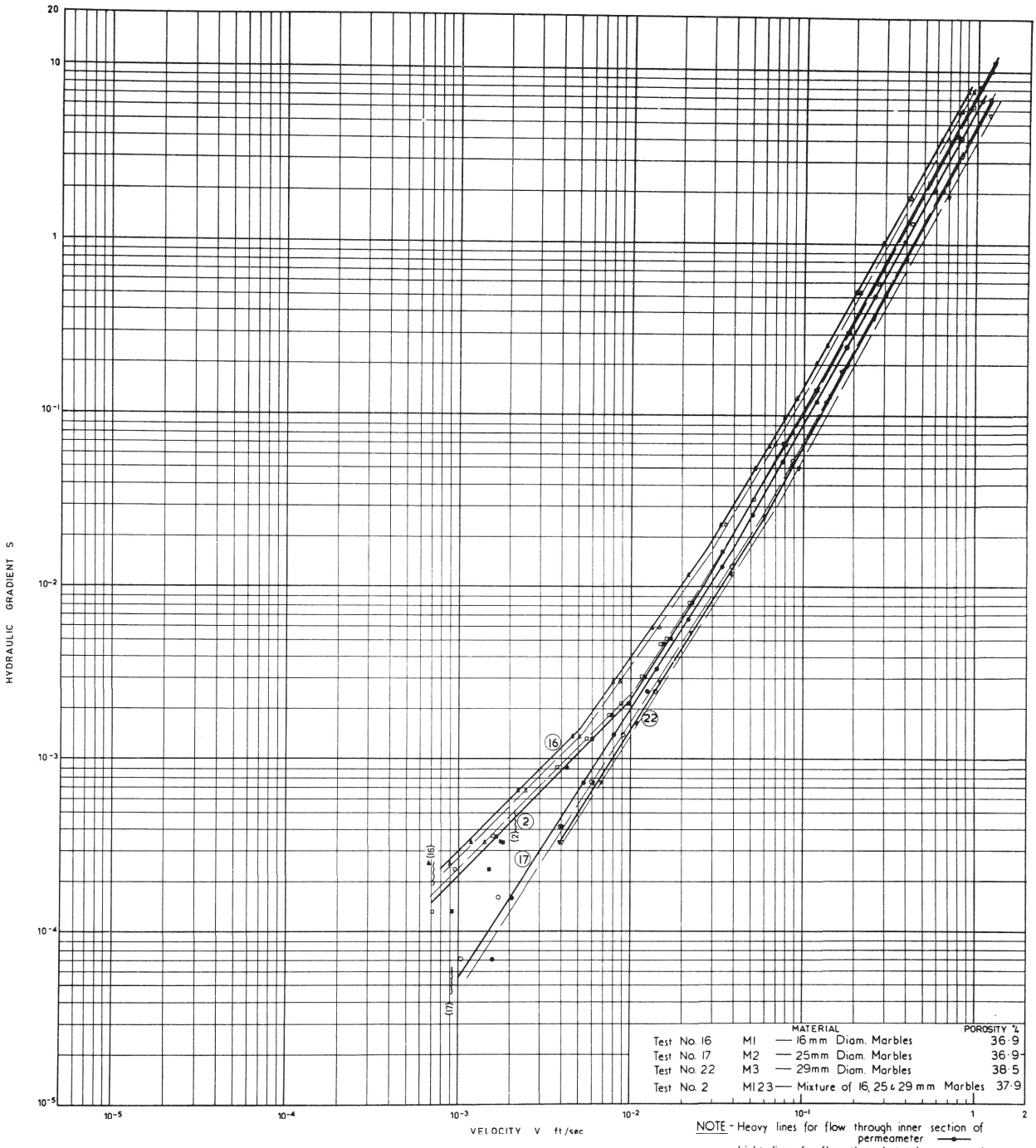

PERMEABILITY TESTS ON GLASS MARBLES

FIGURE 4.

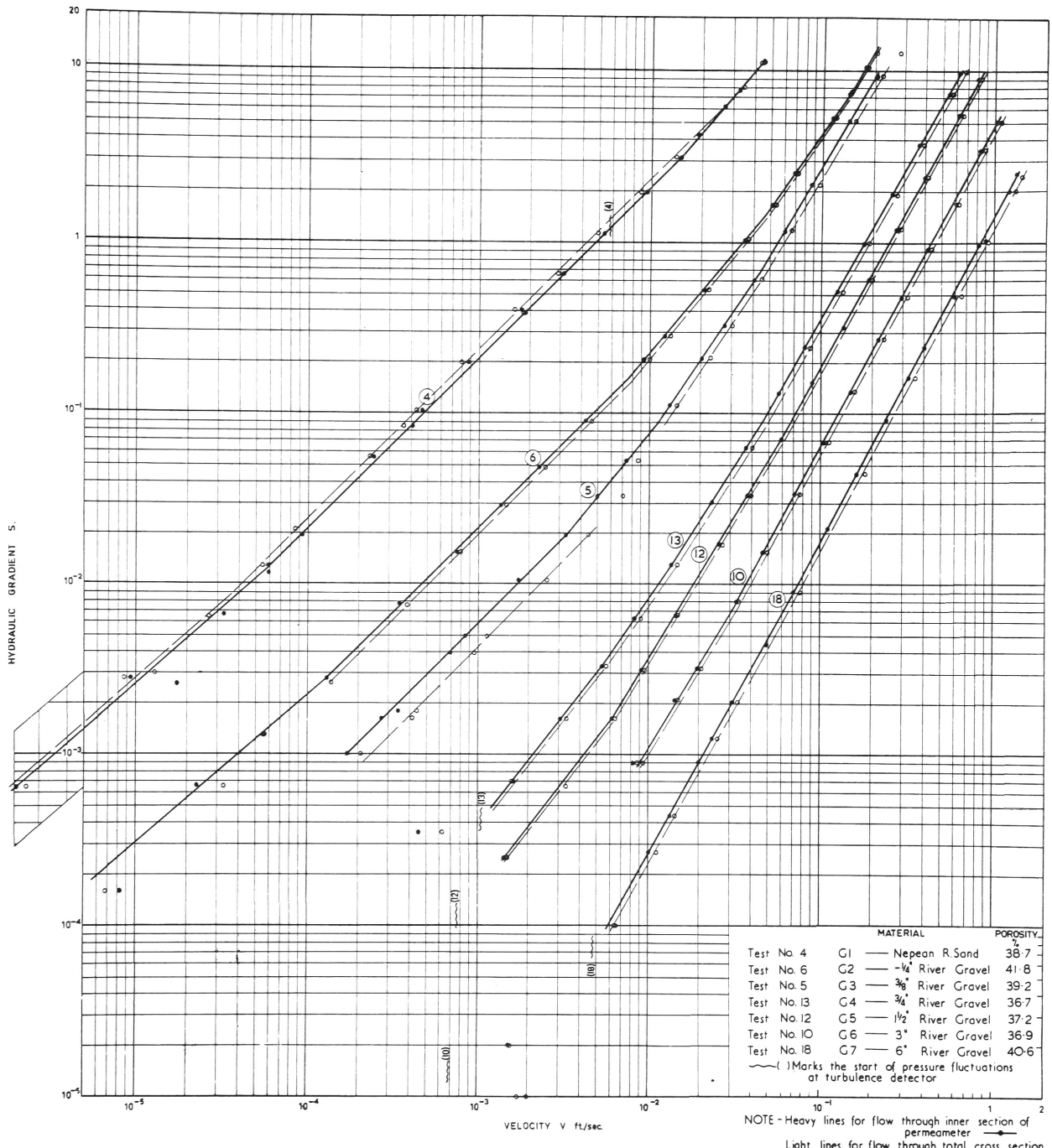

PERMEABILITY TESTS ON NEPEAN RIVER GRAVEL

FIGURE 5

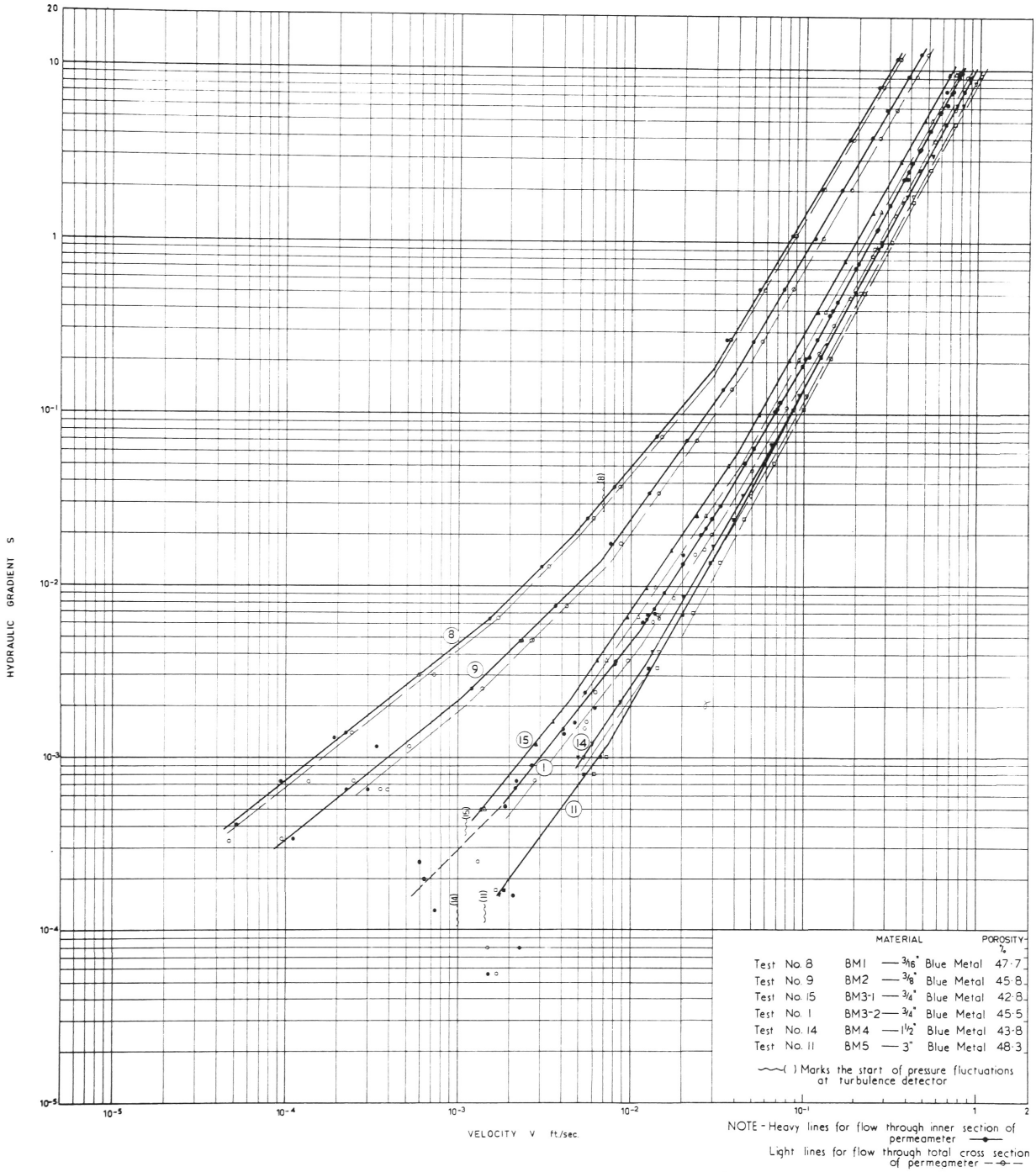

PERMEABILITY TESTS ON CRUSHED BLUE METAL

FIGURE 6

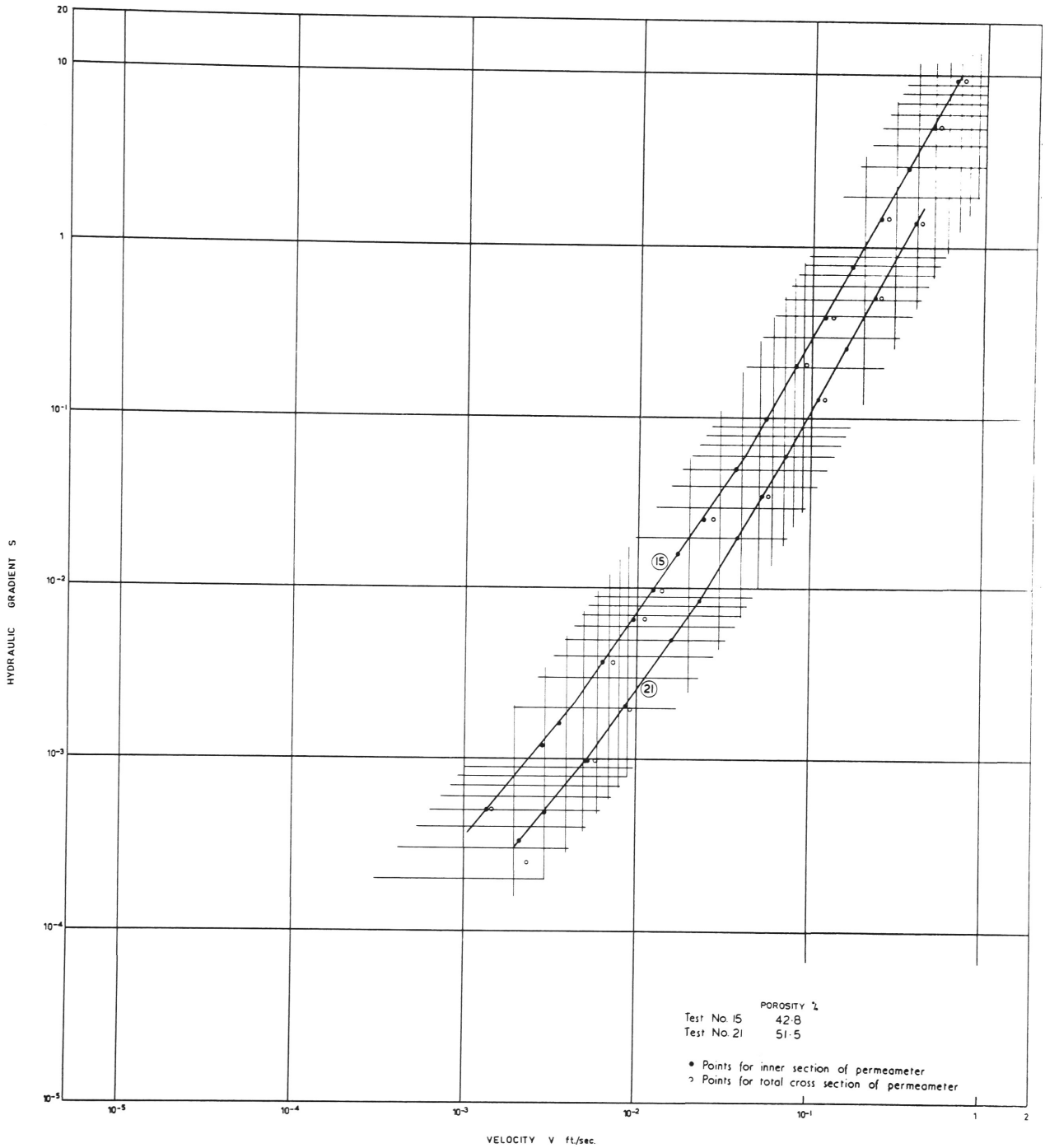

PERMEABILITY TESTS ON BM3-1 3/4" BLUE METAL FOR DIFFERENT POROSITIES

FIGURE 7

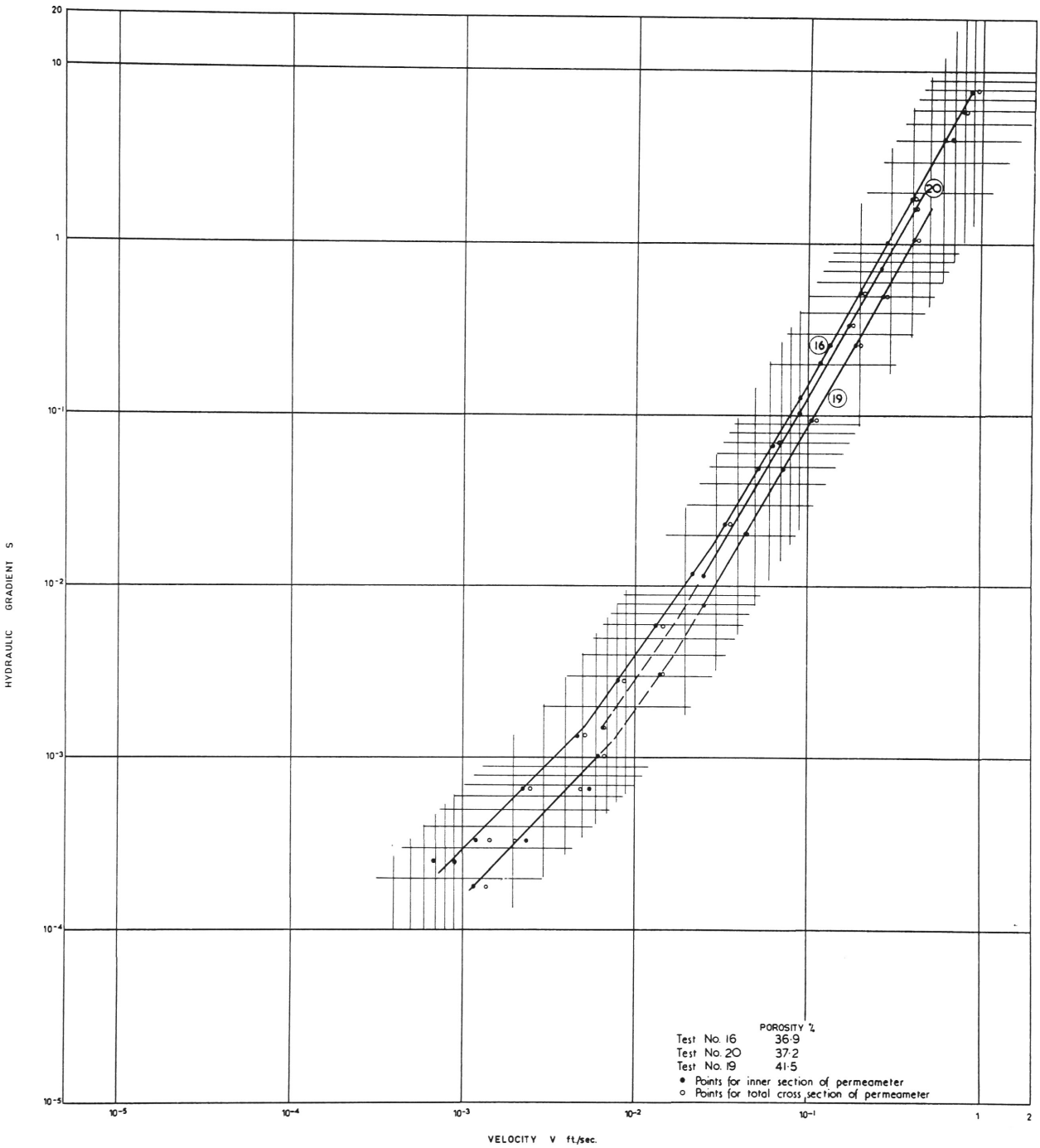

PERMEABILITY TESTS ON MI 16mm DIAM. MARBLES FOR DIFFERENT POROSITIES

FIGURE 8

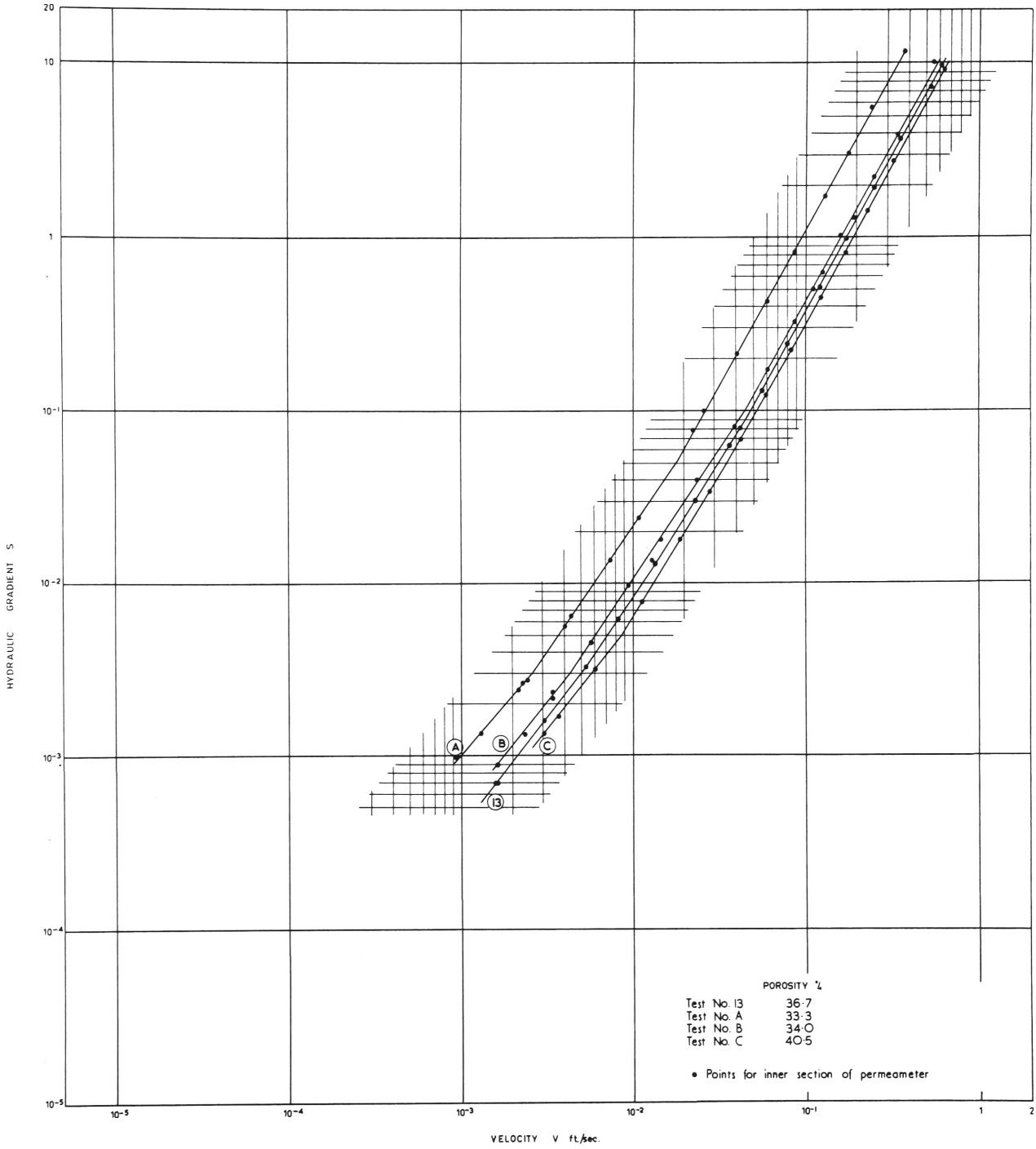

PERMEABILITY TESTS ON G4 3/4" RIVER GRAVEL FOR DIFFERENT POROSITIES

FIGURE 9

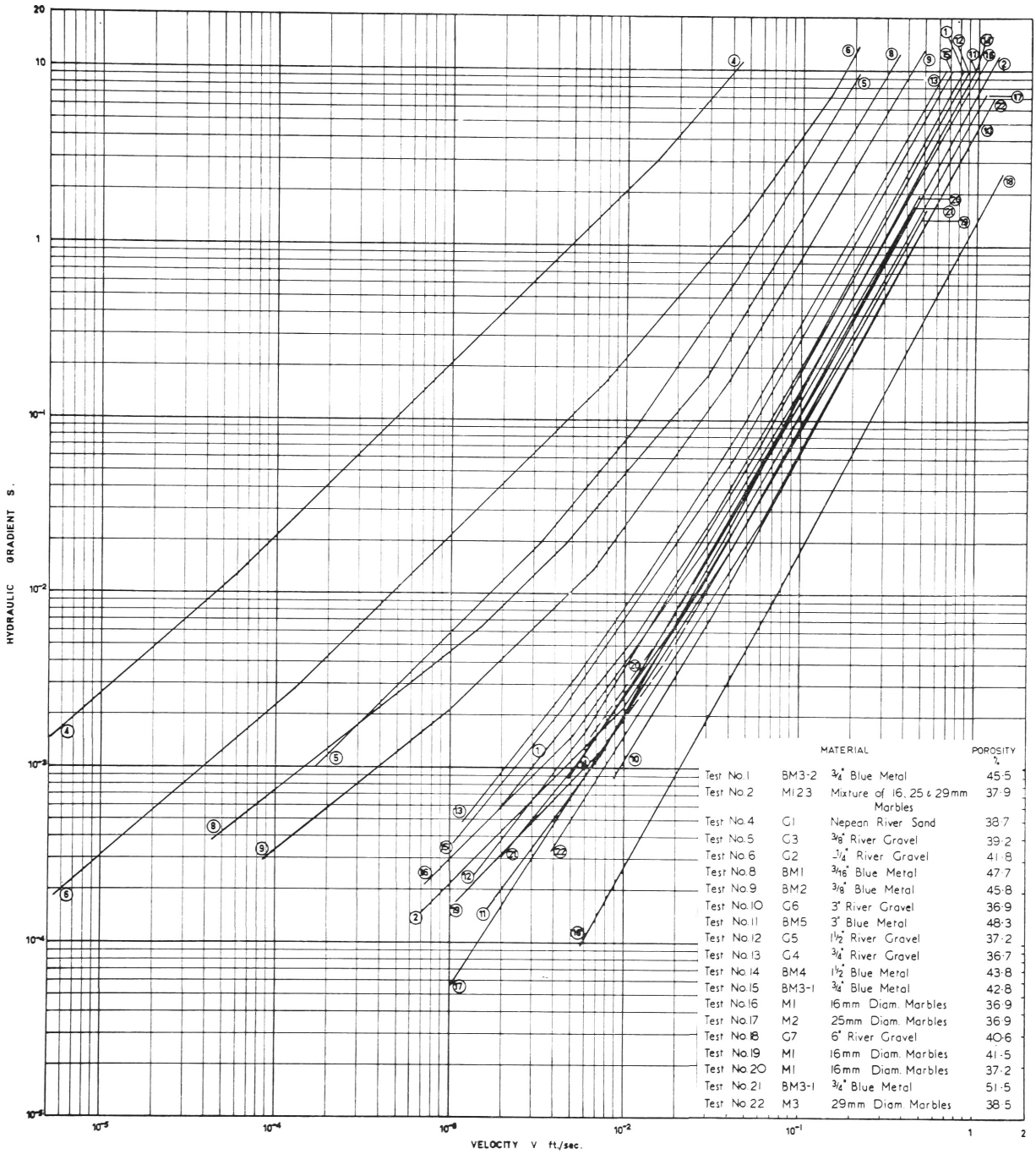

		MATERIAL	POROSITY %
Test No.1	BM3-2	3/4" Blue Metal	45·5
Test No.2	M123	Mixture of 16, 25 & 29mm Marbles	37·9
Test No.4	G1	Nepean River Sand	38·7
Test No.5	G3	3/8" River Gravel	39·2
Test No.6	G2	1/4" River Gravel	41·8
Test No.8	BM1	3/16" Blue Metal	47·7
Test No.9	BM2	3/8" Blue Metal	45·8
Test No.10	G6	3" River Gravel	36·9
Test No.11	BM5	3" Blue Metal	48·3
Test No.12	G5	1 1/2" River Gravel	37·2
Test No.13	G4	3/4" River Gravel	36·7
Test No.14	BM4	1 1/2" Blue Metal	43·8
Test No.15	BM3-1	3/4" Blue Metal	42·8
Test No.16	M1	16mm Diam. Marbles	36·9
Test No.17	M2	25mm Diam. Marbles	36·9
Test No.18	G7	6" River Gravel	40·6
Test No.19	M1	16mm Diam. Marbles	41·5
Test No.20	M1	16mm Diam. Marbles	37·2
Test No.21	BM3-1	3/4" Blue Metal	51·5
Test No.22	M3	29mm Diam. Marbles	38·5

VELOCITY—HYDRAULIC GRADIENT LINES FROM FIGURES 4 TO 9

FIGURE 10

porosity and particle shape, size and gradings.

In the linear regime, laminar flow with negligible inertial effects is postulated, but no conclusive evidence appears to have been published to show experimental confirmation of this. The turbulence tests reported later in this section were inconclusive.

The occurrence of a linear regime in fine gravels and crushed rock aggregates for hydraulic gradients between 10^{-1} and 10^{-2} is of practical significance since many engineers consider that for hydraulic gradients within their range of interest, Darcy's law is not applicable for materials coarser than coarse sand. This impression is apparently the result of the widespread belief that the "critical" Reynolds number lies between 1 and 5, whereas in fact it may be as high as 75 (Scheidegger (1960)). Values up to 60 were obtained in these experiments.

(ii) Post-linear Regimes

Each test series which covered an appreciable range of flows above the upper limit of the linear regime revealed the existence of a number of post-linear regimes, each with an exponent, n, between 1 and 2. The maximum values of n obtained for each of the coarser media were between 1.8 and 1.9. Those media for which linear regimes and regimes with exponents between 1.8 and 1.9 were obtained mostly exhibited two intermediate regimes, but in some cases three such regimes were observed. Figure 7 is of particular

interest as it shows both two and three intermediate regimes for 3/4 inch blue metal packed with low and high porosity.

The results of these tests alone might suggest that the regimes for which the value of n lay between 1.8 and 1.9 represented a state of fully turbulent flow and that intermediate regimes represented transition states between laminar and turbulent flows. However, the results of Izbas (1953) (quoted by Slepicka (1961 (a)) show values of n as high as 2.49 for a regime above the linear regime and Van der Tuin (1960) quotes an exponential relationship for tests on gravel and basalt boulders, of mean size 62 mm, 225 mm and 385 mm, with values of n equal to 1.92 and 2.23. It is possible, therefore, that additional regimes above those detected might have been found if a higher range of hydraulic gradients had been covered. The stage at which complete turbulence and perhaps an upper limiting value of n is reached is not apparent from the nature of the graphs.

(iii) Pre-linear Regime

The experimental results of tests on 3/16 inch and 3/8 inch blue metal, Nepean River sand and -1/4 inch river gravel indicated the existence of a lower limit to the linear regime and an adjacent pre-linear regime. Only one pre-linear regime could be detected for each material but additional pre-linear regimes might have been found had it been possible to measure lower hydraulic gradients. At the low

hydraulic gradients the scatter of experimental results is greater than for higher hydraulic gradients but there is a significant departure from Darcy's law in the cases mentioned. The results for 3/16 inch blue metal, in particular, for which test conditions were very favourable, plot closely on the pre-linear line.

The hydraulic gradients marking the lower limit of validity of Darcy's law varied from approximatly 10^{-2} for the Nepean River sand to 2×10^{-3} for the 3/8 inch blue metal. These gradients are well within the range of practical significance to engineers.

Reynolds numbers based on median diameters for the lower limit of the linear regime varied from approximately 8×10^{-3} for the Nepean River sand to 2 for the 3/8 inch blue metal.

It is interesting to note that the 3/16 inch blue metal, which many engineers would consider too coarse for Darcy's law to be applied, not only showed a linear regime, but a pre-linear regime as well for hydraulic gradients below 6×10^{-3} (approx. 1 in 150).

Current ideas in the engineering field on the validity of Darcy's law at low hydraulic gradients are based more on speculation than on experimental evidence. They are typefied by a statement by Jacob (1950) in Chapter 5 of "Engineering Hydraulics" (Editor Rouse); "Regarding the lower limit of applicability of Darcy's law, it may safely be stated that there is no perceptible lower limit in a sand whose smallest pores are

several thousands of molecular diameters across. That is to say, since water behaves as a viscous liquid at vanishingly low hydraulic gradients, it will flow through pores in sand in obedience to Darcy's law at gradients far smaller than those which can be measured in the laboratory".

The occurrence of pre-linear regimes possibly can be attributed to the interaction between solid and liquid molecules at the solid-liquid boundaries within porous media. This interaction gives rise to the phenomenon called " contact tension" or interfacial tension" by those who work in the fields of the chemistry and physics of surfaces. It is analogous to the surface tension which is familiar to engineers as a phenomenon occurring at liquid - gas interfaces. Reference texts such as those of Schwartz, (1949), Harkins (1952) and Bikerman (1958) discuss interfacial tension at solid liquid boundaries in the general context of surface chemistry.

The net result of surface effects appears to be non-Newtonian behaviour of the water at low flow rates in the interstices of at least some porous media.

Swartzendruber (1962) analysed results obtained for fine grained porous media by a number of investigators on the basis of water acting as a non-Newtonian fluid at low flow rates. Those who claim the existence of "starting" or "threshold" hydraulic gradients imply that

water acts as a Bingham plastic type material under these conditions, rather than as a non-Newtonian fluid with a stress-strain rate graph passing through zero.

The only reference found by the author to this effect being noticeable for flow through coarse granular materials is that of Slepička (1961 (a)) who quotes the results of tests on two gravel materials which, despite a large scatter of experimental results, appeared to show a deviation from Darcy's law at low flow rates.

The effect has normally been reported for tests on fine grained clayey materials and has been attributed to "clay-water" interaction or "electro-molecular" action. The fact that it has not been reported more often for coarse materials may be due to the infrequency of very low hydraulic gradient measurements.

The results of this investigation show that pre-linear regimes can occur for gravels and crushed rock aggregates as well as for clayey materials. They support the hypothesis of non-Newtonian rather than Bingham plastic type behaviour of the permeating water, since the equations for the pre-linear regimes determined have the origin of co-ordinates as a possible solution. However, the velocity-hydraulic gradient graphs for hydraulic gradients lower than those covered in the tests might deviate from the exponential form, and not pass through the origin. The possibility of Bingham type behaviour of the water and

the existence of "threshold" hydraulic gradients is thus not entirely ruled out. If this type of behaviour did occur, the "threshold" gradient would have to be overcome before flow would occur. Claims by Derjaguin and Krylov in support of this have been quoted by Swartzendruber (1962).

(iv) Abrupt Changes between Regimes

The velocity-hydraulic gradient graphs show what are for all practical purposes abrupt changes between regimes. In particular, the results of test series 1, for which a large number of readings was taken show no significant curvature or additional scatter of plotted points at changes of regime. The results of Slepička (1961(a)) and Anandakrishnan and Varadarajulu (1963) show equally abrupt changes.

The appearance of these abrupt changes conflicts with the frequently stated assertion that the change from laminar to turbulent flow in porous media must be gradual. For instance, Jacob, in Chapter 5 of "Engineering Hydraulics" (1950, editor Rouse) states that "The transition from laminar to turbulent flow in sands is quite gradual, requiring at least a thousandfold increase in velocity to reach the limit of fully established turbulence" In the light of the results of this investigation and those reported above such statements are apt to be misleading without additional qualification regarding the nature of the transition.

The assumption of gradual changes in all porous media may be attributed to the scatter of experimental results which characterise many investigations, the development of general equations from data for a relatively narrow range of flow conditions and frequently to the plotting together of experimental results from tests on a number of porous media and drawing a curve of best fit between the scatter of points which results (See Carman's (1937) plot of the results of Fancher, Lewis and Barnes; Bakhmeteff and Feoderoff (1937); Rose and Rizk (1949) Cohen de Lara (1955); Karadi and Nagy (1961).

No evidence is available as to the reason for the abrupt changes. Actual measurements of local conditions such as the nature of the separation zones and levels of turbulence in the flow channels are required before any theory can be established. It seems unlikely that the changes are due to local packing irregularities in the permeameter, with consequent local zones of turbulence, since the same material replaced in the permeameter at a different porosity shows changes identical in nature with those which occur for the original filling although the hydraulic gradients at which they occur may differ. Abrupt changes were found to occur for all media tested including those composed of spherical, rounded, angular, uniform sized and graded particles.

The changes may be caused by the occurrence of a number of stable flow patterns around the particles of the media with sudden

changes from one to another.

(b) Turbulence Detector Results

The velocities at which random pressure fluctuations were registered by the piezo-electric turbulence detector are marked on the velocity - hydraulic gradient plots in Figures 5 and 6. There is no significant correlation between the median grain sizes of the media and the velocities at which the fluctuations were found to commence. As a result, no constant Reynolds number based on median diameters was found to apply. Calculated Reynolds numbers varied from approximately 1 to 150.

Since the velocities are not constant they do not correspond to any particular flow rate or approach velocity in the inlet section of the permeameter. The flow rate corresponding to a critical Reynolds number of 2,000 in the approach section is approximately 3.5×10^{-2} c.f.s., approximately 3 to 13 times as great as the flow rates equivalent to the indicated velocities. It is, therefore, unlikely that the response of the indicator was connected with the onset of turbulent conditions in the inlet section and associated vibration of the permeameter.

The results do appear to give a general indication of the onset of turbulence in the test section corresponding to the upper limit of the linear regime, particularly for the finer materials. The erratic results, particularly for the coarser materials, can probably be attributed to the use of only one pressure tapping which gave an

indication only of local flow conditions, not the average of conditions prevailing throughout the test section. This distinction is particularly noteworthy in the tests on the 6 inch and 3 inch gravels where one particle could significantly affect the flow over a large area around the tapping.

The indicator was extremely sensitive and could be used only when the laboratory was free from vibrations caused by wind, model construction work or large flows falling into drainage channels. It is felt that with refinement of the electronic circuitry to increase the signal to noise ratio and allow changes in the nature of the trace on the oscilloscope to be observed more accurately, a piezo-electric detector would yield useful information on the nature of flow in the interstices of granular media. The development of a probe to pick up pressure fluctuations from a number of points in the permeameter or the use of dummy particles as sensing elements might overcome the difficulty of determining average conditions. Measurements of pressure distributions on dummy particles, such as those of Wentz and Thodos (1963), but for a wider range of flow rates, might be useful.

(c) Permeameter Wall Effects

(i) Differences between Inner and Total Flow Velocities

The heavy and light lines in Figures 4, 5 and 6 respectively represent velocity-hydraulic gradient relationships determined for the inner section and total cross-section of the permeameter. Filled in symbols are experimental points plotted for the inner section and open

symbols are points plotted for the total cross-section flows. It will be seen that in almost all cases the velocity through the inner section is less than the velocity averaged over the total cross-sectional area. The difference is presumably caused by a disproportionate flow of water passing down the zone immediately adjacent to the wall of the test section. Against this wall no "interlocking" of the particles is possible and voids of nature different from those present in the material away from the wall must occur.

For the tests on the coarser materials the difference between the two calculated velocities is of the order of 5 pc. to 10 pc. Since there are no appreciable differences in slopes of the corresponding lines on the log-log plots for these materials the equation $S = aV^n$ holds for both velocities with values of n unchanged. A parallel shift in the V direction means a constant change in the logarithm of a for each regime of each test series. Thus the results of the experiments indicate that the values of n determined for coarse granular media in a permeameter in which the whole of the flow is measured should not be in error to any significant extent but the values of a will be in error by a constant proportion which may be as high as 15 pc.

For the finer materials, sand , -1/4 inch river gravel and 3/16 inch blue metal, the percentage error decreased with increasing hydraulic gradient and values of n for corresponding lines differed

slightly. It is noteworthy that these were the only materials with a large proportion of fine material which might have altered the nature of the voids.

The results of the tests on sand were exceptional in that the velocity through the inner section was greater than the overall velocity for all but the higher flows. This material was subjected to a water pressure from underneath during the pre-test procedure to help remove entrapped air and was accidentally reduced to a "quick" condition. Large bubbles of air trapped beneath the sample were forced upwards around the sides of the permeameter. The permeameter was dismantled and the top of the sand re-levelled before tests were carried out but the packing of the sand was undoubtedly altered by the accident. It is possible that this caused the altered relationship between the measured velocities.

Test series 5 on 3/8 inch river gravel showed a sudden change in the percentage difference between velocities. At the end of the tests a small flaky particle of gravel, which had passed through the retaining grid, was found in one of the pressure equaliser tappings and projecting approximately 1/16" inch into the flow. It appears that this particle became lodged during the test run and that all pressure equalisations after this were in error.

Two other test series, numbers 3 and 7 for which results are

not listed, had to be discontinued because of large discrepancies between the inner and overall velocities. Measured overall velocities were up to twice the inner velocities. The materials involved were -1/4 inch river gravel and 3/16 inch blue metal both of which contained a lot of fine particles. These were loaded into the permeameter without fly gauze on top of the punched metal grid so that fine particles washed out by the pre-test flows would not block the grid. Examination of the permeameter in each case after dismantling showed that the level of the upper surface of the sample at one side of the permeameter had fallen as the result of material escaping down the side of the punched metal grid. This had not been mated correctly with the outlet section which was slightly eccentric as the result of welding distortion. Both test series were repeated with the fly gauze in position to give the results listed in series 6 and 8.

(ii) Comparison with Published Results

The results do not support the conclusions drawn by Rose (1945) and Rose and Rizk (1949) from tests on assemblages of spheres of various diameters in a permeameter tube of fixed diameter. Their results, plotted in the form

$$\frac{\text{Head loss for finite bed}}{\text{Head loss for infinite bed}} \quad \text{versus} \quad \frac{D_T}{D_p} = \frac{\text{tube diameter}}{\text{particle diameter}}$$

are shown in abbreviated form in the diagram overleaf

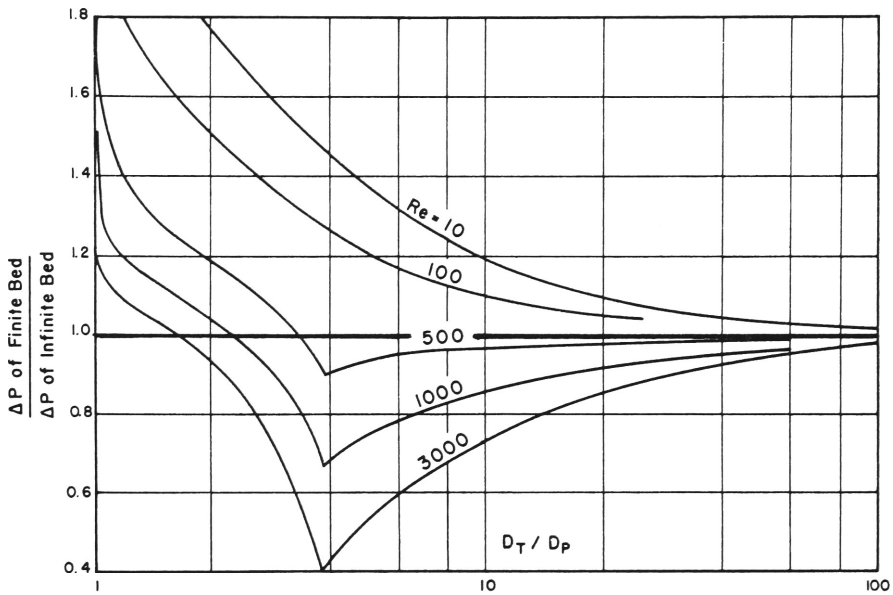

Wall effect correction factor correlated by Rose and Rizk

reproduced from Zenz and Othmer (1960). The original plot of Rose and Rizk shows a much greater number of lines for different Reynolds numbers and were plotted by computing, on the basis of a friction factor - Reynolds number relationship previously determined by them, the hydraulic gradients for various Reynolds numbers and various diameter ratios. It is important to note that the results were not obtained by varying the diameter of the test bed and keeping the sphere size and porosity constant, a procedure which would have yielded direct head loss comparisons. This would have eliminated the assumptions involved in allowing for porosity variations and using one velocity hydraulic gradient relationship for flow through spheres of various

sizes at various porosities (i. e. for media not geometrically similar). The results of the author's tests on marbles, plotted in friction factor versus Reynolds number form in Figure 23, show that a single equation will not accurately describe this relationship for geometrically dissimilar media.

It appears probable, then, that the curves of Rose and Rizk depend on other factors as well as wall effects.

The small variation in percentage wall effect with flow rate and the insensitivity to tube diameter to particle median size ratios down to 5 apparent in this investigation is explicable when the nature of the porosity change near the wall is considered. Provided the permeameter is loaded by distributing the material evenly over the whole area in the same manner, porosity changes should be restricted to a narrow zone adjacent to the wall. In this zone no particles project from the wall to interlock with the voids between the adjacent layer of particles so a relatively free passage for water is provided. As the particle size increases the size of the voids increases but the same proportional increase can be expected in the voids near the wall as in those nearer the centre of the permeameter. A relatively constant velocity distribution and percentage wall effect can therefore be expected to apply to each flow regime. Variations in the wall effect for the various materials can probably be attributed to the effect of local packing

variations and variations of particle shape and grading which affect the nature of the voids.

The hypothesis that wall effects are restricted to a narrow zone adjacent to the permeameter wall is supported by the results of a pitot traverse by Saunders and Ford (1940) across the outlet face of a circular porous bed. They found that the velocity across the bed was approximately constant except for an annular area approximately one particle diameter wide adjacent to the tube wall in which the velocity was as much as 50 pc higher than the inner velocity. This evidence supports the assumption that the flows through the inner section of the permeameter used by the author represented flows through a bed of infinite extent, since in all cases the median particle size was less than the distance between the inner tube and the outer wall.

8. 2 Physical Characteristics of Materials Tested

(a) Lithological Descriptions

Lithological descriptions of the river gravels and blue metals are given in Section 6. 3(a). By engineering standards they are hard inert materials and their mineralogical properties would not be expected to influence the flow of water through them.

(b) Particle Sizes and Gradings

The conventional plots of particle gradings given in Figures 11 and 12 are included to allow comparison with materials for which

TABLE 4
SUMMARY OF SIEVE ANALYSIS RESULTS.

A. S. T. M. Sieve No.	Opening in mm.	Percentages finer than sizes shown for listed samples.				
		G1 Nepean R. Sand	G2 -1/4" River Gravel	G3 3/8" River Gravel	G4 3/4" River Gravel	G5 1½" River Gravel
6 inch	152.4					
4 inch	101.6					
3 inch	76.2					
2 inch	50.8					100.0
1½ inch	38.1				100.0	98.7
1 inch	25.4				99.4	49.2
3/4 inch	19.1				68.2	7.5
1/2 inch	12.7			100.0	15.5	1.3
3/8 inch	9.52	100.0	100.0	99.2	2.8	0.6
4	4.76	99.6	98.4	28.9	0.3	0.5
10	2.00	93.4	37.9	8.9	0.0	0.2
20	0.84	81.4	5.9	3.1		0.0
40	0.42	34.0	1.2	1.5		
60	0.25	5.8	0.5	0.9		
140	0.105	0.4	0.0	0.0		
200	0.074	0.2				
Pan	-	0.0				

TABLE 4 (cont'd.)

A. S. T. M. Sieve No.	Opening in mm.	Percentages finer than sizes shown for listed samples.				
		G6 3" River Gravel	G7 6" River Gravel	BM1 3/16" Blue Metal	BM2 3/8" Blue Metal	BM3-1 3/4" Blue Metal
6 inch	152.4		100.0			
4 inch	101.6		34.7			
3 inch	76.2	100.0	0.0			
2 inch	50.8	35.9				
$1\frac{1}{2}$ inch	38.1	4.6				
1 inch	25.4	0.3				100.0
3/4 inch	19.1	0.0				99.5
1/2 inch	12.7				100.0	25.6
3/8 inch	9.52			100.0	99.4	3.1
4	4.76			77.9	8.5	1.2
10	2.00			10.3	2.0	
20	0.84			3.4	1.3	
40	0.42			2.0	0.9	
60	0.25			1.3	0.7	
140	0.105			0.5		
200	0.074			0.4		
Pan	-			0.0		

TABLE 4 (cont'd.)

A. S. T. M. Sieve No.	Opening in mm.	Percentages finer than sizes shown for listed samples.		
		BM3-2 3/4" Blue Metal	BM4 1½" Blue Metal	BM5 3" Blue Metal
6 inch	152.4			
4 inch	101.6			
3 inch	76.2			100.0
2 inch	50.8			96.4
1½ inch	38.1		100.0	51.9
1 inch	25.4	100.0	51.1	8.7
3/4 inch	19.1	91.1	10.1	4.4
1/2 inch	12.7	17.5	2.0	2.5
3/8 inch	9.52	1.7	1.8	1.9
4	4.76	0.4	1.6	1.5
10	2.00	0.4		
20	0.84			
40	0.42			
60	0.25			
140	0.105			
200	0.074			
Pan	-			

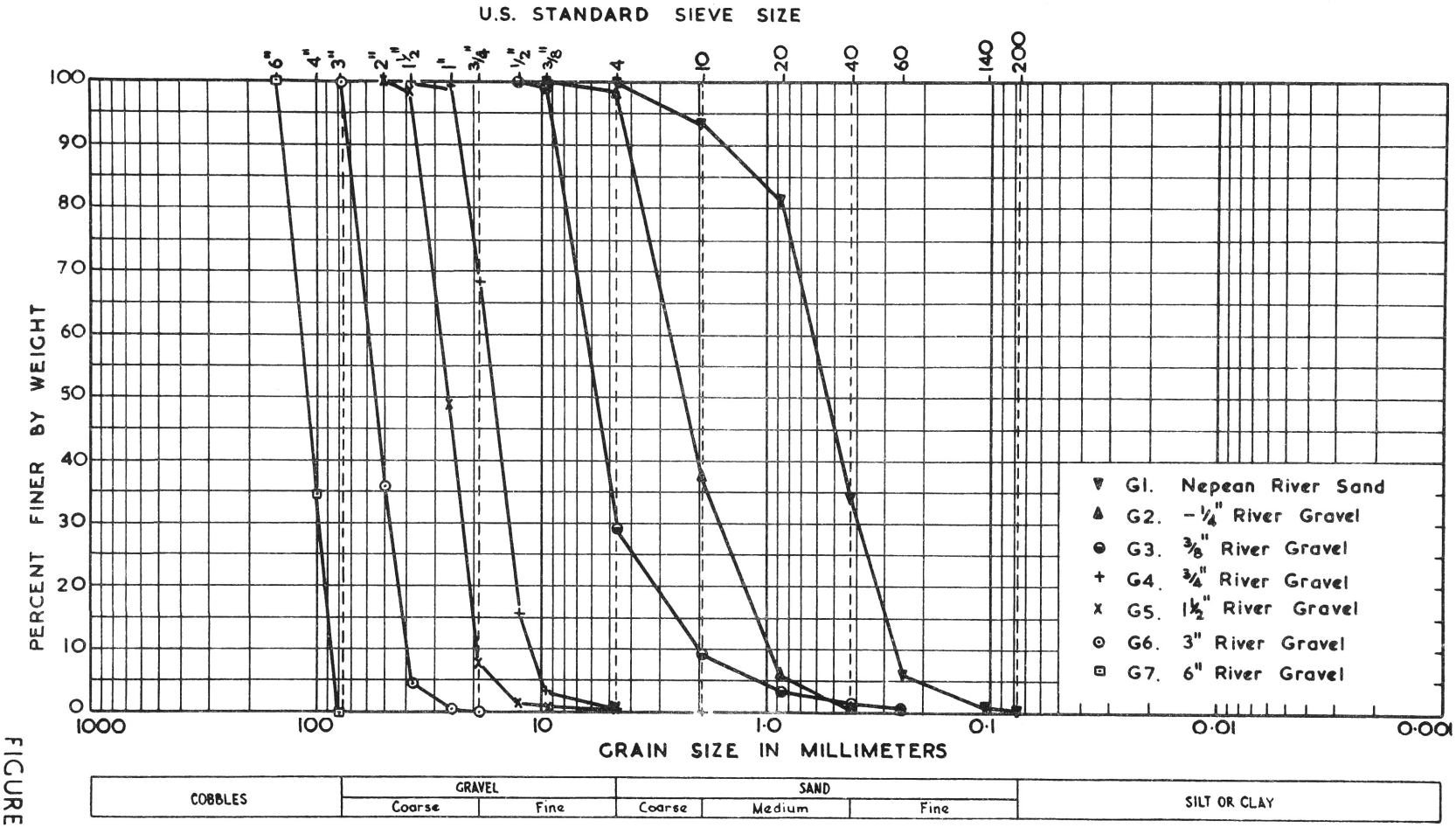

FIGURE 11

SIEVE ANALYSES OF NEPEAN RIVER GRAVEL MATERIALS

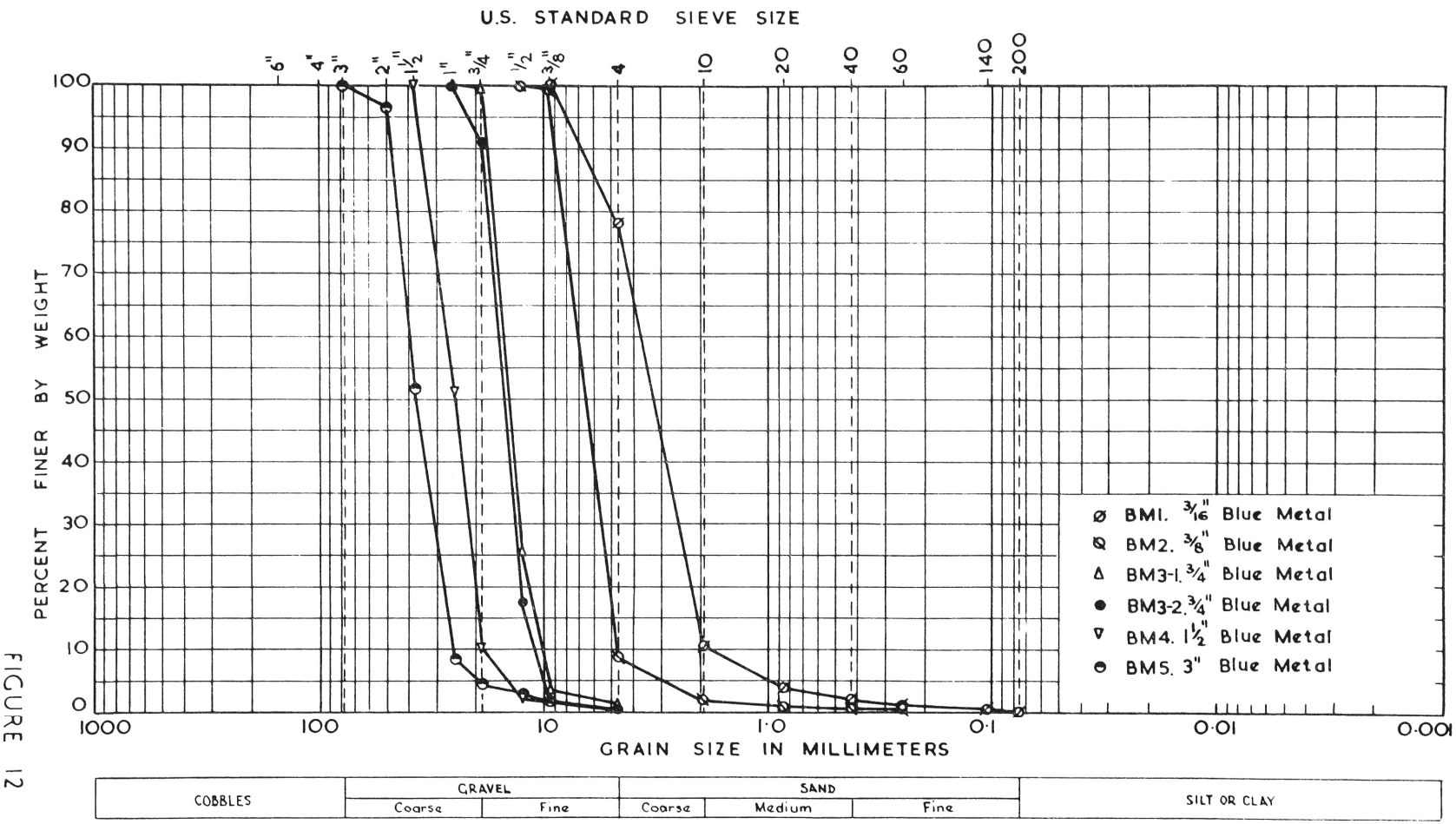

FIGURE 12

SIEVE ANALYSES OF CRUSHED BLUE METAL MATERIALS

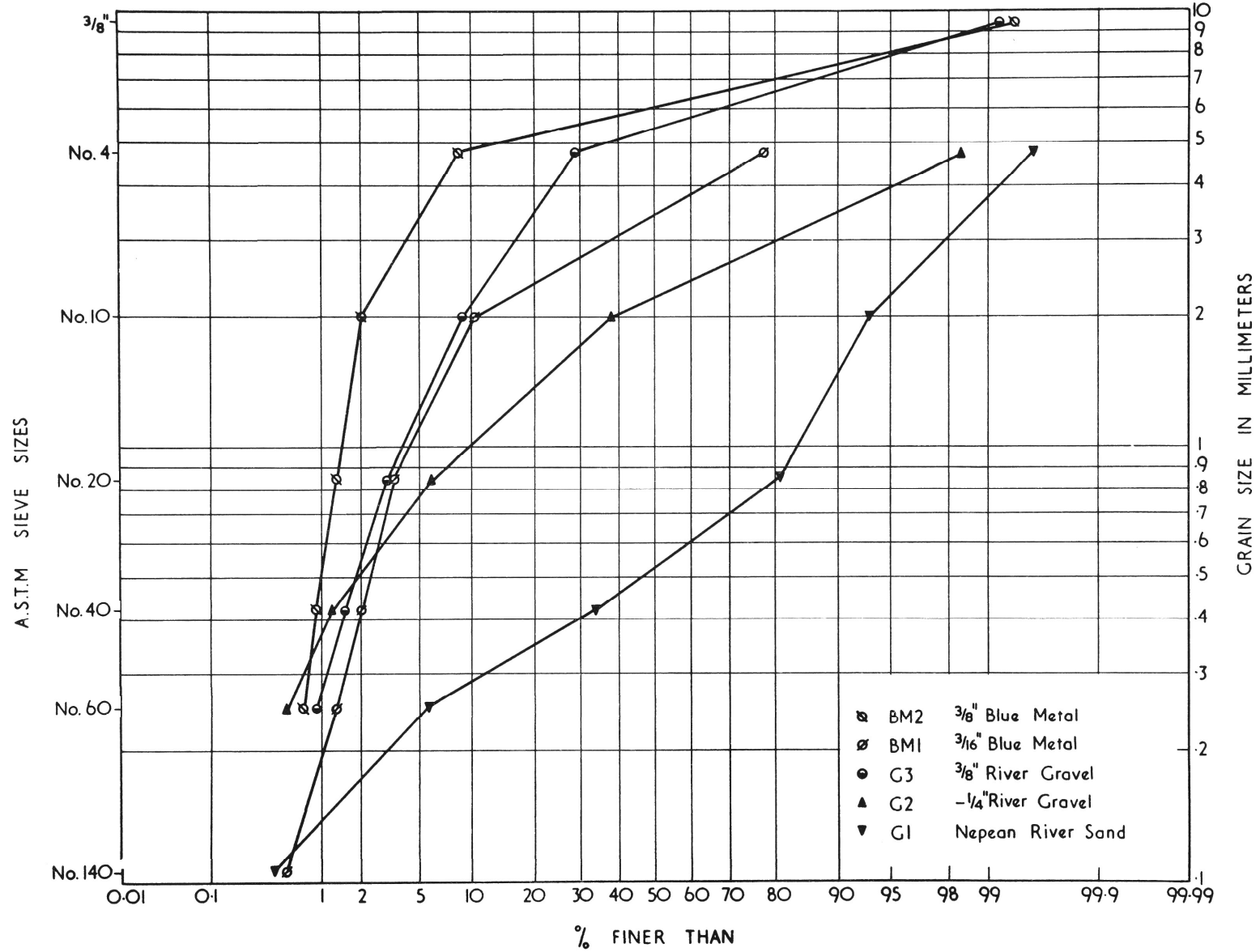

FIGURE 13

LOG PROBABILITY PLOT OF SIEVE ANALYSES—

3/8" & FINER MATERIALS

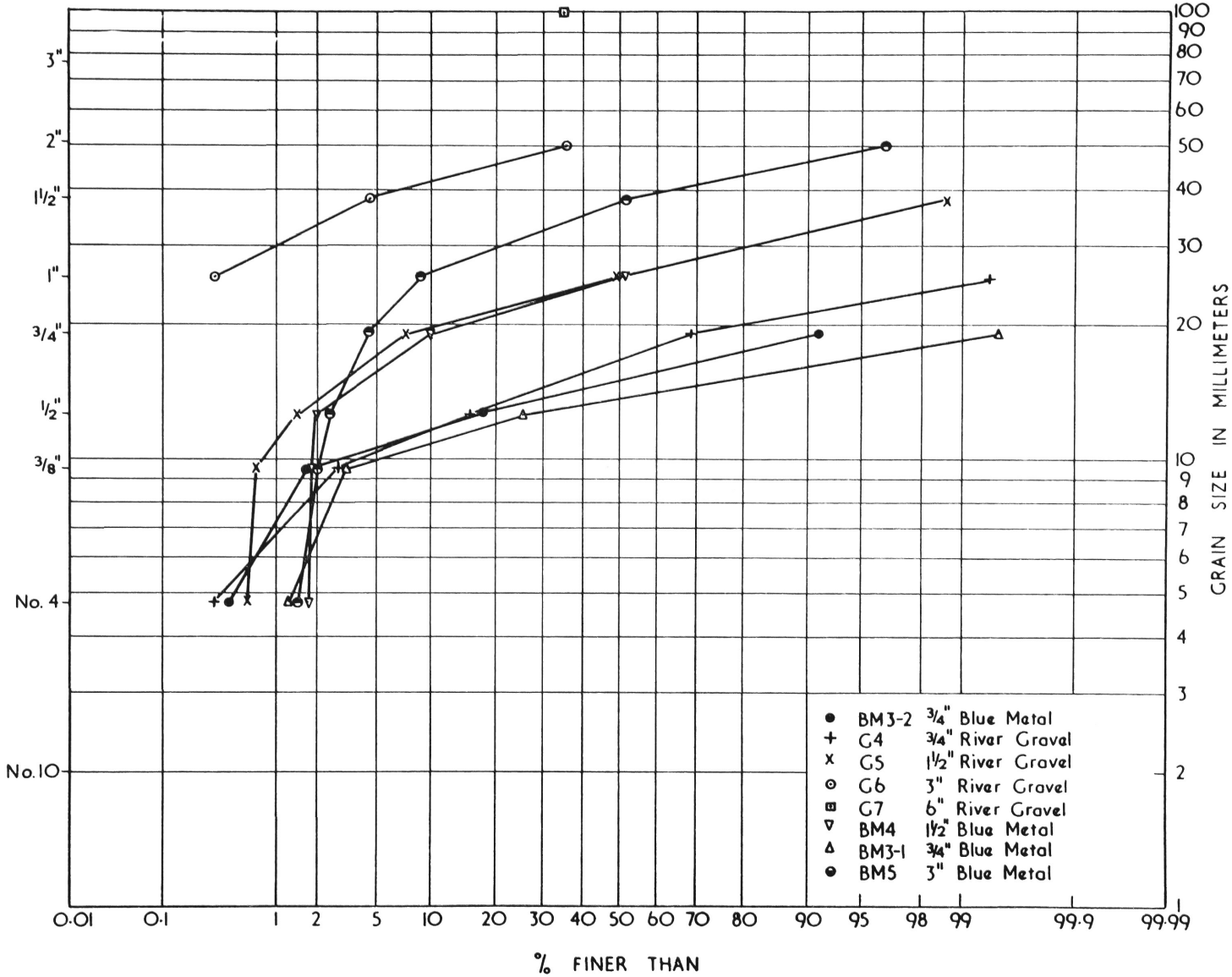

FIGURE 14

LOG PROBABILITY PLOT OF SIEVE ANALYSES — ¾" & COARSER MATERIALS

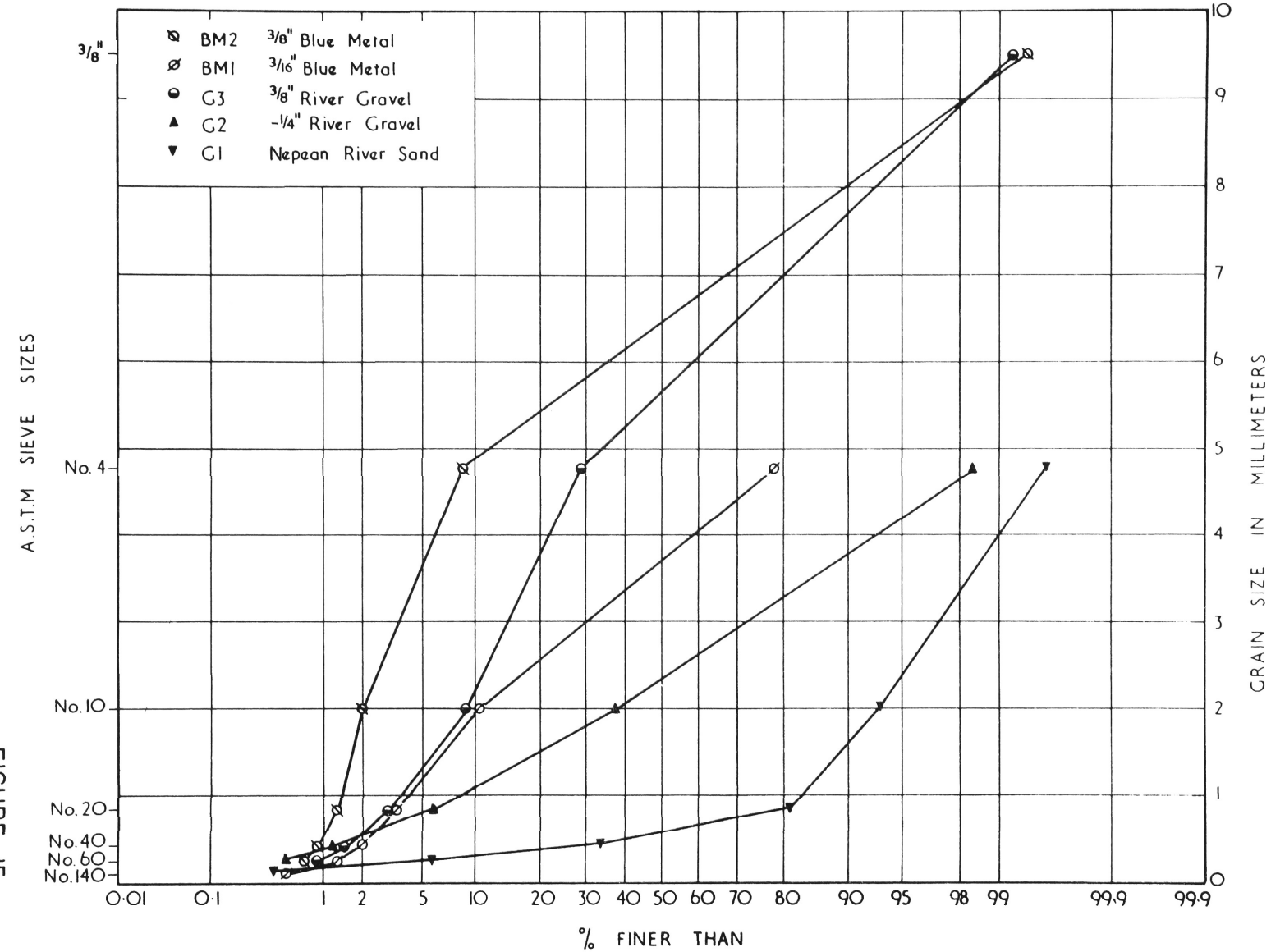

FIGURE 15

LINEAR PROBABILITY PLOT OF SIEVE ANALYSES — 3/8" & FINER MATERIALS

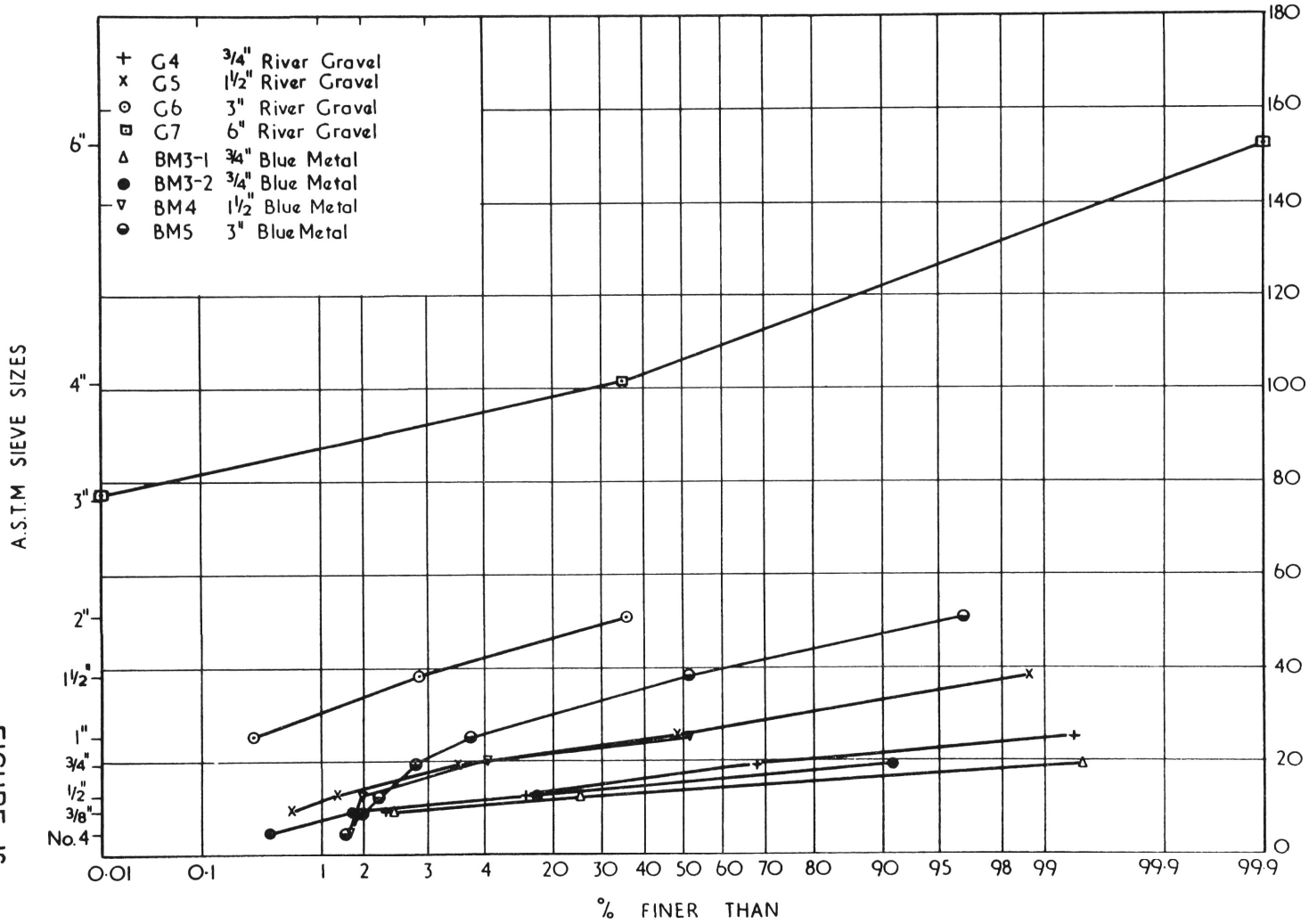

FIGURE 16

LINEAR PROBABILITY PLOT OF SIEVE ANALYSES — 3/4" & COARSER MATERIALS

an engineer must make approximate estimates of flow rates or hydraulic gradients without carrying out permeability tests.

The logarithmic probability plots of Figures 13 and 14 and the linear probability plots of Figures 15 and 16 identify those materials in which the particle sizes are approximately normally distributed and those in which the logarithms of particle size are normally distributed. Naturally occurring graded sands and gravels and artificial crushings tend to exhibit a log normal distribution and plot as straight lines on log probability paper. It will be seen from Figures 13 and 14 that the only material that showed this characteristic was the Nepean River sand. Most of the remaining materials would be better approximated by normal distributions since their gradings tend to plot as straight lines on linear probability paper in Figures 15 and 16. The $1\frac{1}{2}$ inch and 3 inch blue metal samples were exceptions in that their gradings do not approximate to straight lines on either type of plot.

The probability plots give a clearer qualitative picture of the grain size distributions of materials than do the conventional plots and allow their distributions to be classed as approximately normal, log normal or other. The use of a classification such as this, together with the median grain size and type of particle might be of assistance in the classification of permeability results, at least for

normally and log normally distributed materials. The use of a mean or median particle size and a standard deviation calculated from the sieve analysis results by a formula applicable to normal distributions, regardless of the actual distributions of the experimental results, is unsatisfactory as a measure of size and grading.

Marble sizes determined by measuring with calipers three mutually perpendicular diameters of 50 marbles of each size are as listed below.

Code	Nominal Diameter	Mean Diameter	Standard Deviation
M1	16 mm	16.0 mm	0.3 mm
M2	25 mm	24.9 mm	0.3 mm
M3	29 mm	29.0 mm	0.4 mm

The marble mixture, M123, consisted of 16, 25 and 29 mm marbles in the following proportions by weight:- 1.23: 1.05: 1.00. The marbles were only slightly eccentric in shape and since regular packings were not attempted they were treated as spherical particles.

(c) Fall Velocities

Fall velocities of particles were measured in an attempt to determine a factor which would characterise particle shape, size and grading. The median fall velocity of the particles of a granular medium is influenced by all three of these factors. The fall velocity is also a function of the particle specific gravity and the fluid properties, density and viscosity. These factors were kept constant

by carrying out all tests in water at a relatively constant temperature and adjusting results for the small particle specific gravity differences involved (see Appendix III). Since only coarse particles were involved it was considered that fall velocities would be high enough for drag coefficients to be independent of Reynolds number and median fall velocities to be a real measure of shape, size and grading.

A number of papers have been published dealing with correlations between physical characteristics of particles and their fall velocities in the turbulent range (e.g. Albertson (1952), Heywood (1962)); however, it was considered essential to make direct measurements of fall velocities in this case rather than to make physical size and shape measurements and to attempt to use the published correlations.

Initial tests on the consistency of timing falls by eye and stopwatch showed that approximately 100 particles should be timed separately for each material.

The results, summarized in Table 5 are plotted as frequency distributions on logarithmic probability paper in Figures 17 to 19 and on linear probability paper in Figures 20 to 22. Plotting was done in this form to determine whether the distributions were normal or log normal. Comparison of Figures 19, 21 and 22 shows that the only river gravel material for which the fall velocity distribution plotted as a straight line on linear probability paper was the -1/4

TABLE 5

Summary of Fall Velocity Test Results.

Material	Tank Cross Section	Timed Fall Distance (feet)	Number of Particles	Mean Fall Velocity (fps)	Median Velocity (fps)	Sample Standard Deviation (fps)	Coefficient of Variation
BM1 3/16" Bl. Metal	3ft. x 3ft.	3.5	100	0.63	0.61	0.18	0.29
BM1 3/16" Bl. Metal	6 in. dia.	2.5	100	0.70	0.69	0.20	0.29
BM2 3/8" Bl. Metal	3ft. x3ft.	3.5	105	0.89	0.88	0.21	0.24
BM2 3/8" Bl. Metal	6in. dia.	2.5	97	1.00	0.98	0.27	0.27
BM3-1 3/4" Bl. Metal	3ft. x3ft.	3.5	100	1.74	1.79	0.30	0.17
BM3-2 3/4" Bl. Metal	3ft. x3ft.	3.5	100	1.56	1.63	0.31	0.20
BM3-2 3/4" Bl. Metal	2ft. x1ft.	6.0	208	1.48	1.53	0.29	0.20
BM4 1½" Bl. Metal	3ft. x3ft.	3.5	100	2.03	2.12	0.38	0.19
BM5 3" Bl. Metal	3ft. x3ft.	3.5	100	2.36	2.43	0.50	0.21
G2 - 1/4" R. Gravel	6in. dia.	2.5	100	0.67	0.65	0.22	0.33
G3 3/8" R. Gravel	6in. dia.	2.5	96	1.06	1.06	0.21	0.20
G3 3/8" R. Gravel	3ft. x3ft.	3.5	100	0.91	0.93	0.25	0.28
G4 3/4" R. Gravel	3ft. x3ft.	3.5	99	1.80	1.82	0.28	0.15
G5 1½" R. Gravel	3ft. x3ft.	3.5	100	2.20	2.23	0.46	0.21
G6 3" R. Gravel	3ft. x3ft.	3.5	53	3.48	3.44	0.92	0.26
G7 6" R. Gravel	8ft. x8ft.	10.1	92	5.96	5.94	1.27	0.21
M1 16mm Marbles	3ft. x3ft.	3.5	50	2.64	2.74	0.18	0.068
M1 16mm Marbles	1.8ft. dia.	9.5	20	2.67	2.70	0.052	0.020
M2 25 mm Marbles	3ft. x3ft.	3.5	20	3.10	3.25	0.23	0.074
M2 25mm Marbles	1.8ft. dia.	9.5	20	3.20	3.26	0.10	0.031
M3 29mm Marbles	3ft. x3ft.	3.5	20	3.31	3.41	0.16	0.048
M3 29mm Marbles	1.8ft. dia.	9.5	20	3.41	3.48	0.08	0.023

TABLE 6

RESULTS OF SPECIFIC GRAVITY TESTS

(1) Material	(2) Weight Dry (gms)	(3) Weight Surface Wet (gms)	(4) Weight Surface Dry (gms)	(5) Weight Sub-merged in water (gms)	(6) Loss of weight (4)-(5) (gms)	(7) Specific Gravity
29 mm marbles	1,519		1,519	912	607	2.50
29mm marbles	1,352		1,352	810	542	2.49
16 mm marbles	1,235		1,235	741	494	2.50
16 mm marbles	933		933	560	373	2.50
3/4" river gravel	781	788	785	486	299	2.63
3/8"river gravel	674	689	681	419	262	2.63
3/4" blue metal (BM3-1)	658	662	660	429	231	2.86
3/4" blue metal (BM3-2)	830	834	832	540	292	2.85
3/8" blue metal	807	814	808	521	287	2.82
3/16" blue metal	908	929	906	584	322	2.81

TABLE 7

Fall Velocities adjusted for Specific Gravity Difference.

Material	Specific Gravity	Mean Fall Velocity ft/ sec.	Coefficient of Variation	Adjusted Mean Fall Velocity ft/ sec.
BM1 3/16" Bl. Metal	2.81	0.63	0.29	0.60
BM2 3/8" Bl. Metal	2.82	0.89	0.24	0.85
BM3-1 3/4" Bl. Metal	2.85	1.74	0.17	1.64
BM3-2 3/4" Bl. Metal	2.86	1.56	0.20	1.47
BM4 1½" Bl. Metal	2.85	2.03	0.19	1.92
BM5 3" Bl. Metal	2.85	2.36	0.21	2.23
G2. -1/ 4" River Gr.	2.63	0.67*	0.33	0.67
G3 3/8" River Gr.	2.63	0.91	0.28	0.92
G4 3/4" River Gr.	2.63	1.80	0.15	1.81
G5 1½" River Gravel	2.63	2.20	0.21	2.21
G6 3" River Gravel	2.63	3.48	0.26	3.50
G7 6" River Gravel	2.63	5.96+	0.21	6.00
M1 16 mm Marbles	2.50	2.64	0.068	2.77
M2 25 mm Marbles	2.50	3.10	0.074	3.25
M3 29 mm Marbles	2.50	3.31	0.048	3.47

N. B. All velocities from 3' x 3' tank except those marked

* In 6" dia. cylinder Probably 10 pc. lower in 3 ft. x 3 ft. tank

\+ In 8' x 8' tank.

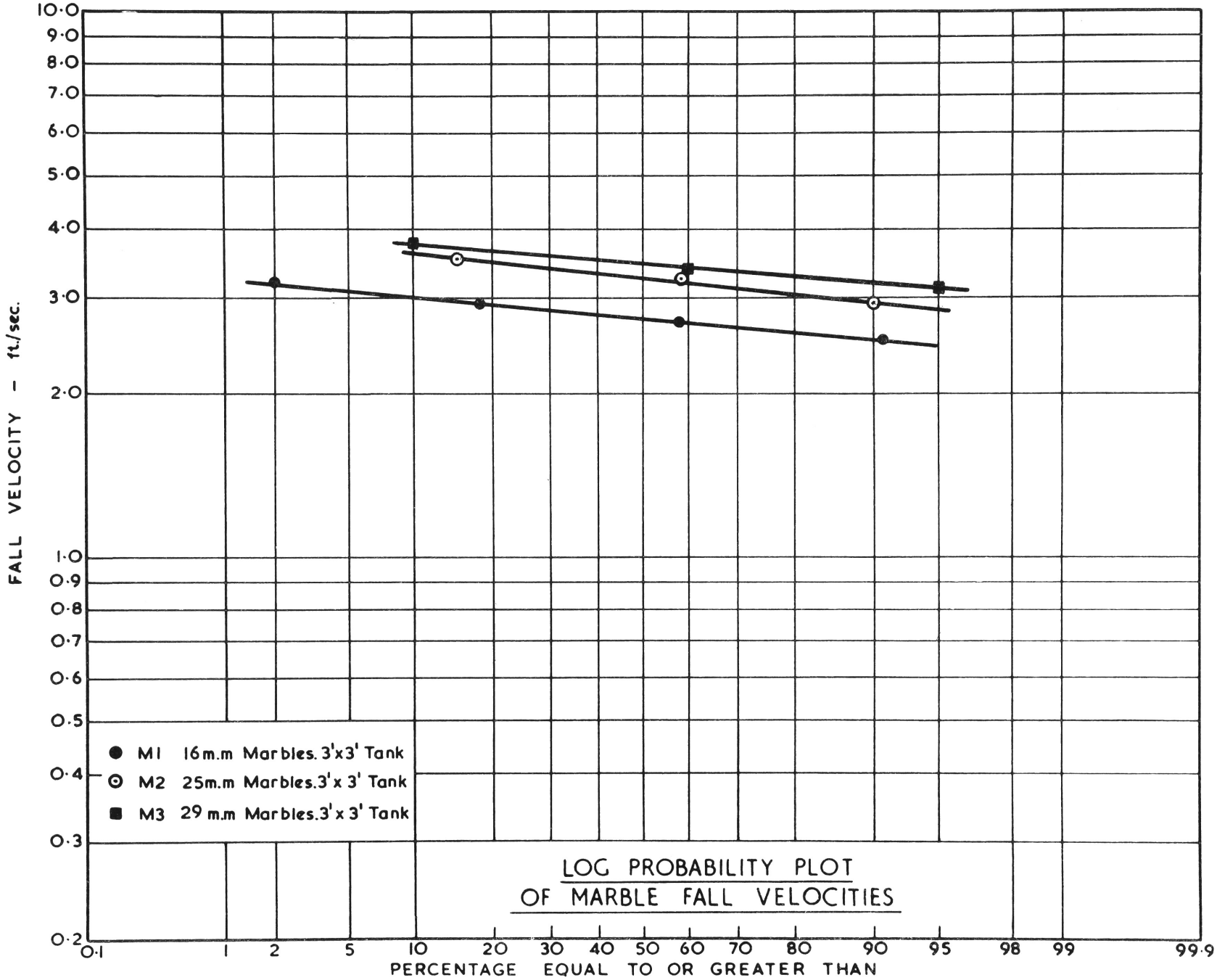
10·0
9·0
8·0
7·0
6·0
5·0
4·0
3·0
2·0
1·0
0·9
0·8
0·7
0·6
0·5
0·4
0·3
0·2
FALL VELOCITY - ft./sec.
M1 16m.m Marbles. 3'x3' Tank
M2 25m.m Marbles. 3'x 3' Tank
M3 29 m.m Marbles. 3'x 3' Tank
LOG PROBABILITY PLOT
OF MARBLE FALL VELOCITIES
0·1
1
2
5
10
20
30
40
50
60
70
80
90
95
98
99
99·9
PERCENTAGE EQUAL TO OR GREATER THAN

FIGURE 17

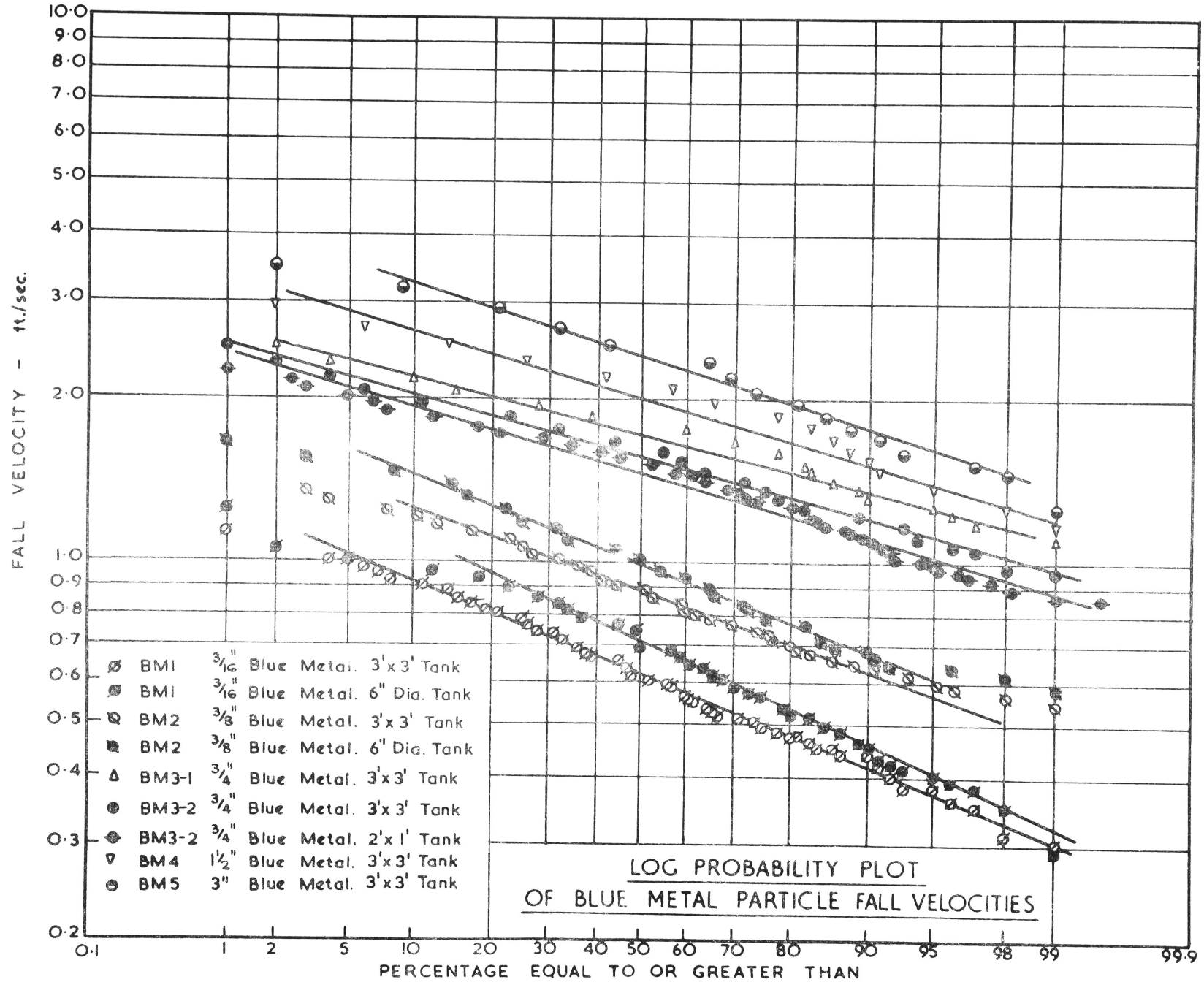
FALL VELOCITY - ft./sec.
10·0
9·0
8·0
7·0
6·0
5·0
4·0
3·0
2·0
1·0
0·9
0·8
0·7
0·6
0·5
0·4
0·3
0·2
0·1
1
2
5
10
20
30
40
50
60
70
80
90
95
98
99
99.9
PERCENTAGE EQUAL TO OR GREATER THAN
BM1 3/16" Blue Metal. 3'x3' Tank
BM1 3/16" Blue Metal. 6" Dia. Tank
BM2 3/8" Blue Metal. 3'x3' Tank
BM2 3/8" Blue Metal. 6" Dia. Tank
BM3-1 3/4" Blue Metal. 3'x3' Tank
BM3-2 3/4" Blue Metal. 3'x3' Tank
BM3-2 3/4" Blue Metal. 2'x1' Tank
BM4 1½" Blue Metal. 3'x3' Tank
BM5 3" Blue Metal. 3'x3' Tank
LOG PROBABILITY PLOT
OF BLUE METAL PARTICLE FALL VELOCITIES

FIGURE 18

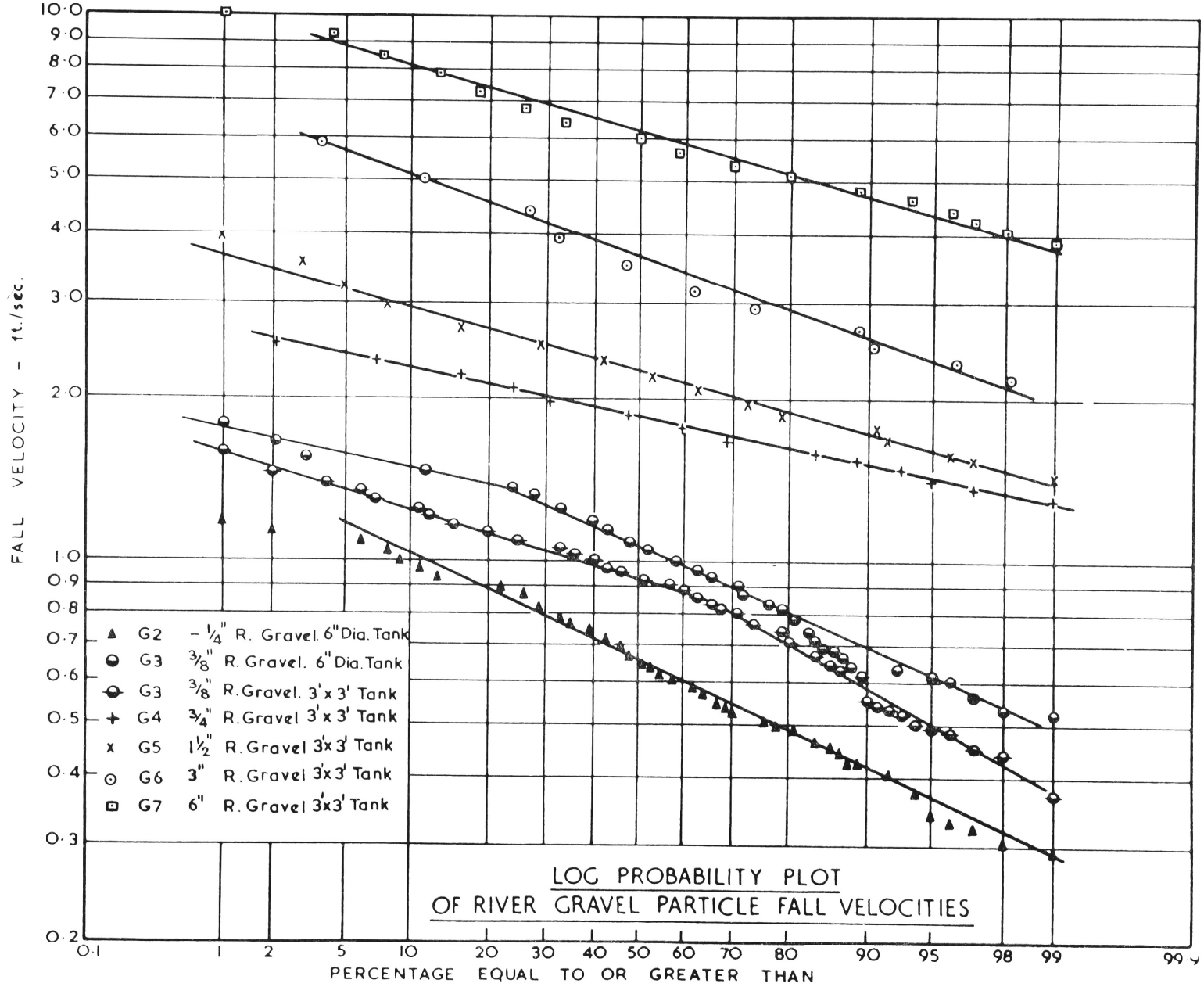
FALL VELOCITY - ft./sec.
10·0
9·0
8·0
7·0
6·0
5·0
4·0
3·0
2·0
1·0
0·9
0·8
0·7
0·6
0·5
0·4
0·3
0·2
G2 - 1/4" R. Gravel. 6" Dia. Tank
G3 3/8" R. Gravel. 6" Dia. Tank
G3 3/8" R. Gravel. 3' x 3' Tank
G4 3/4" R. Gravel 3' x 3' Tank
G5 1 1/2" R. Gravel 3' x 3' Tank
G6 3" R. Gravel 3' x 3' Tank
G7 6" R. Gravel 3' x 3' Tank
LOG PROBABILITY PLOT
OF RIVER GRAVEL PARTICLE FALL VELOCITIES
0·1
1
2
5
10
20
30
40
50
60
70
80
90
95
98
99
99·9
PERCENTAGE EQUAL TO OR GREATER THAN

FIGURE 19

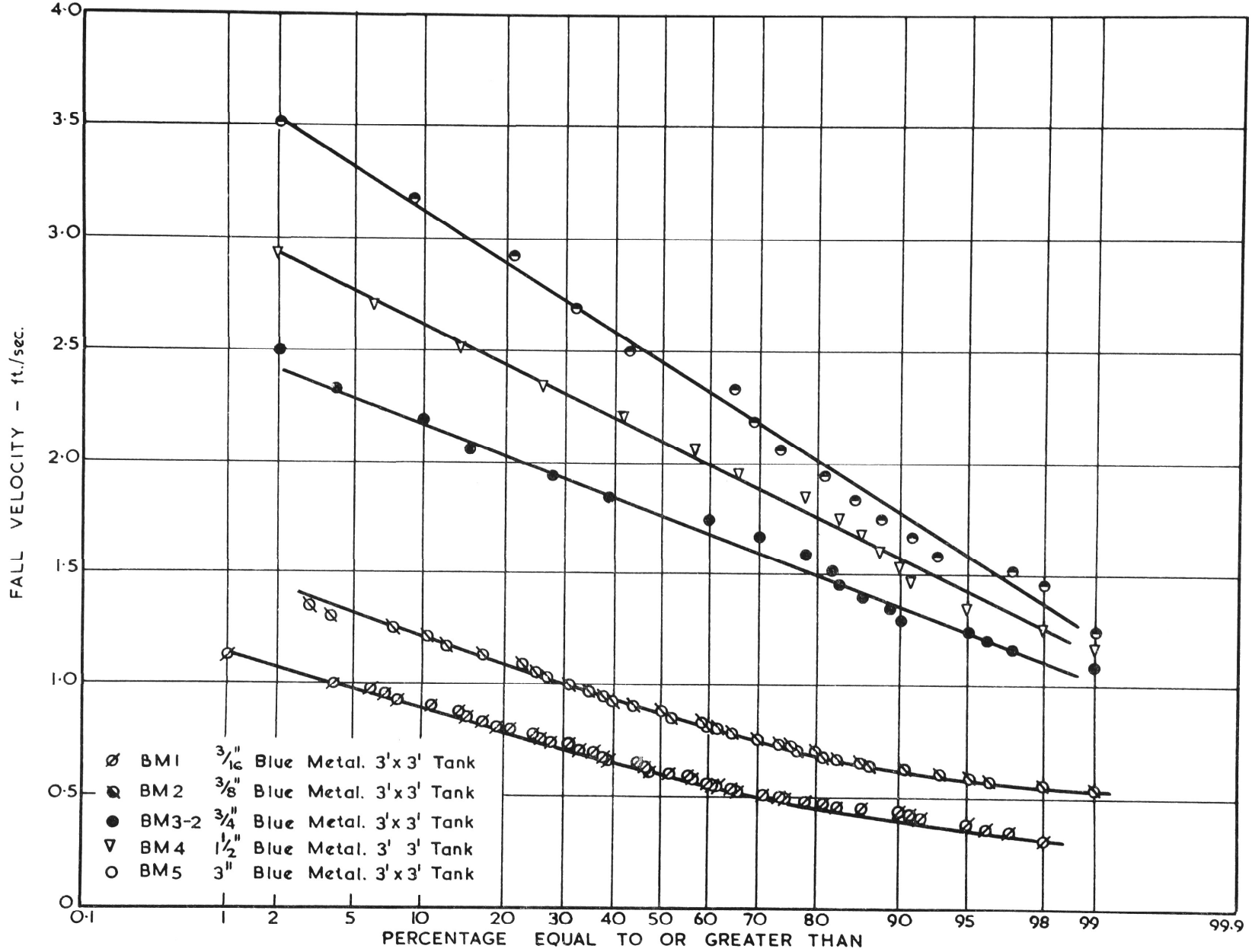

FIGURE 20

LINEAR PROBABILITY PLOT OF BLUE METAL PARTICLE FALL VELOCITIES

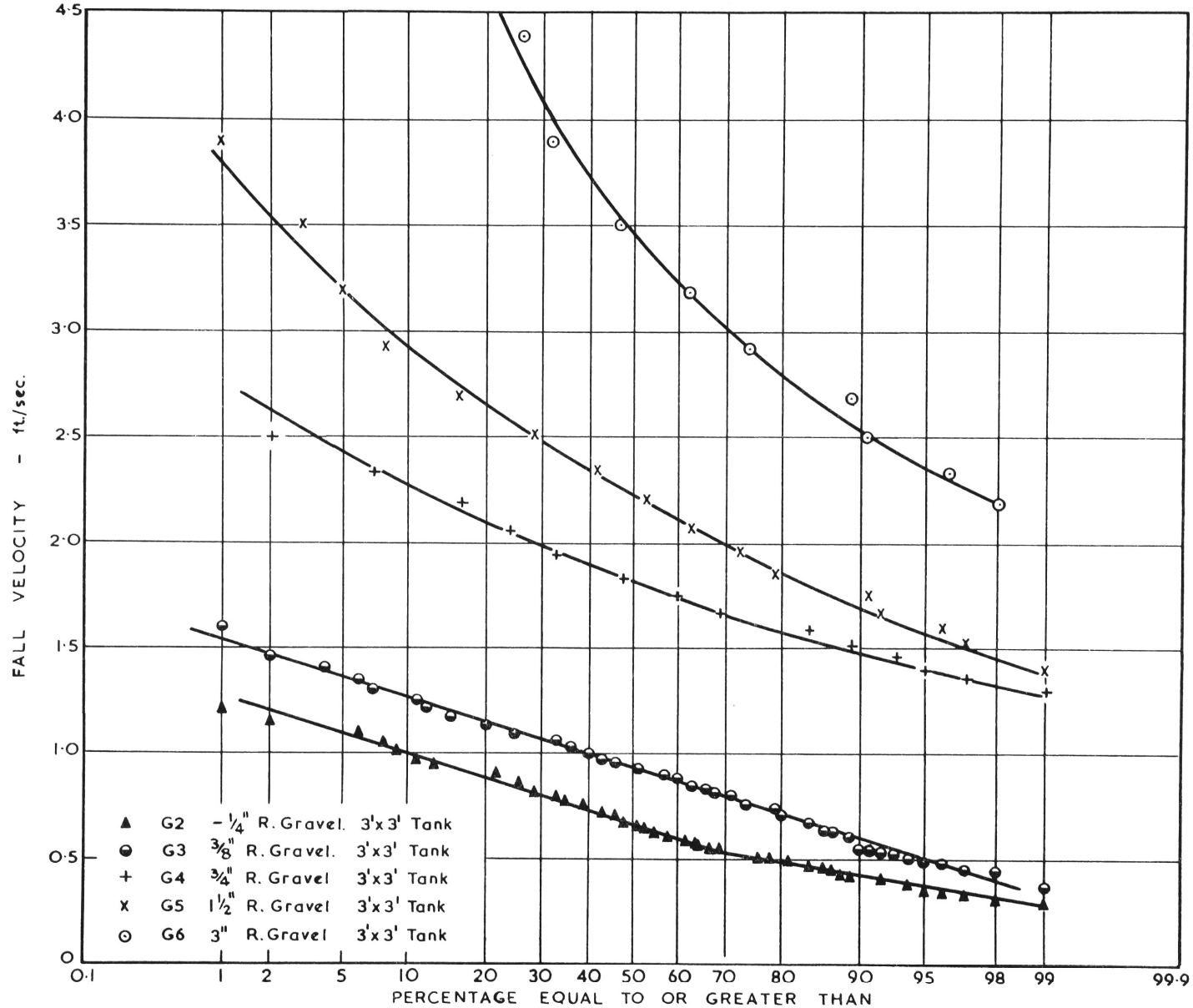

FIGURE 21

LINEAR PROBABILITY PLOT OF RIVER GRAVEL PARTICLE FALL VELOCITIES

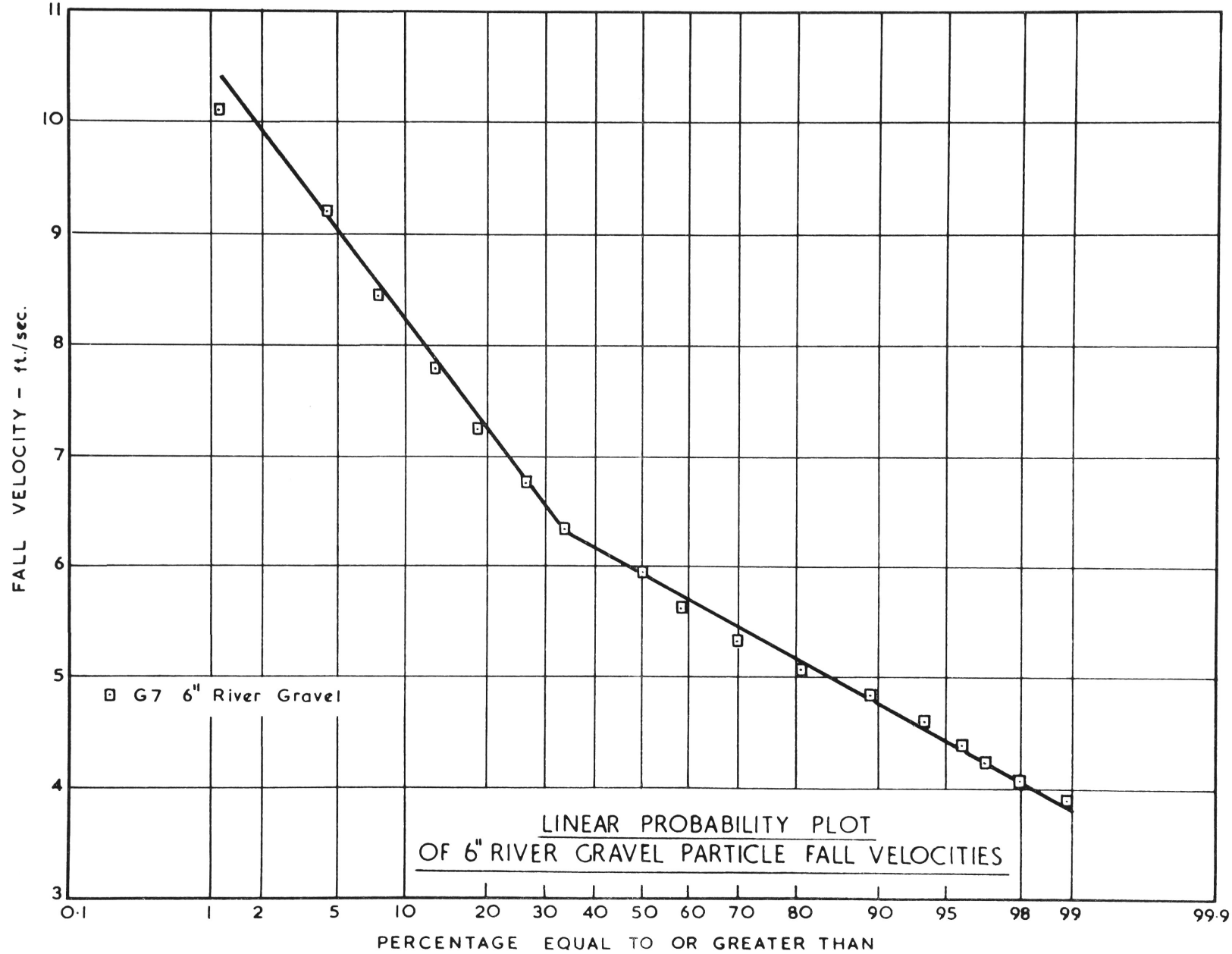
FALL VELOCITY - ft./sec.
11
10
9
8
7
6
5
4
3
G7 6" River Gravel
LINEAR PROBABILITY PLOT
OF 6" RIVER GRAVEL PARTICLE FALL VELOCITIES
0·1
1
2
5
10
20
30
40
50
60
70
80
90
95
98
99
99·9
PERCENTAGE EQUAL TO OR GREATER THAN

FIGURE 22

inch gravel, a material containing a large proportion of fine nearly spherical particles which fell at velocities not in the fully turbulent range. All other river gravels showed log normal distributions. Comparison of Figures 18 and 20 shows that all the blue metal particle fall velocity distributions could be considered as log normal. Although the 3/16 inch blue metal contained a large proportion of small particles these were very flaky and their fall did not appear to be influenced greatly by viscous effects.

The results indicate, therefore, that all particle fall velocity - frequency distributions except that for -1/4 inch river gravel can be treated as approximately log normal. The constancy of the type of distribution allows a meaningful comparison of median values to be made.

The use of fall velocities and median particle sizes in calculations of Reynolds numbers and friction factors and other pairs of dimensionless parameters is described in Section 8.3.

8.3 Generalization of Velocity - Hydraulic Gradient Relationship

(a) Use of Velocity - Hydraulic Gradient Plots

The failure of investigators in the past to obtain general Reynolds number-friction factor correlations applicable to a wide range of granular media has been discussed in Chapter 2. Those correlations which have been obtained have required permeameter tests to determine

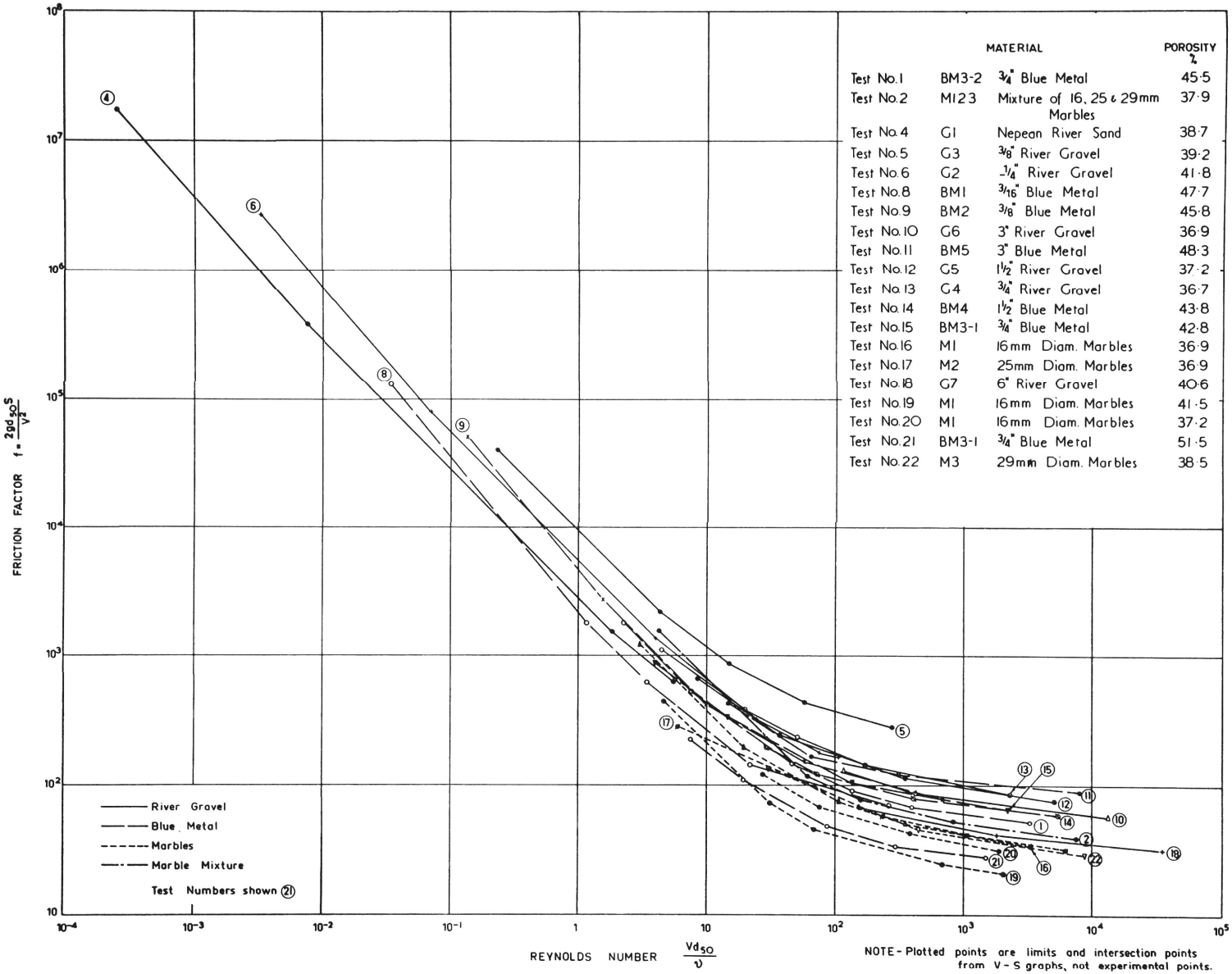

		MATERIAL	POROSITY %
Test No.1	BM3-2	3/4" Blue Metal	45·5
Test No.2	M123	Mixture of 16, 25 & 29mm Marbles	37·9
Test No.4	G1	Nepean River Sand	38·7
Test No.5	G3	3/8" River Gravel	39·2
Test No.6	G2	1/4" River Gravel	41·8
Test No.8	BM1	3/16" Blue Metal	47·7
Test No.9	BM2	3/8" Blue Metal	45·8
Test No.10	G6	3" River Gravel	36·9
Test No.11	BM5	3" Blue Metal	48·3
Test No.12	G5	1 1/2" River Gravel	37·2
Test No.13	G4	3/4" River Gravel	36·7
Test No.14	BM4	1 1/2" Blue Metal	43·8
Test No.15	BM3-1	3/4" Blue Metal	42·8
Test No.16	M1	16mm Diam. Marbles	36·9
Test No.17	M2	25mm Diam. Marbles	36·9
Test No.18	G7	6" River Gravel	40·6
Test No.19	M1	16mm Diam. Marbles	41·5
Test No.20	M1	16mm Diam. Marbles	37·2
Test No.21	BM3-1	3/4" Blue Metal	51·5
Test No.22	M3	29mm Diam. Marbles	38·5

FIGURE 23

FRICTION FACTOR VERSUS REYNOLDS NUMBER

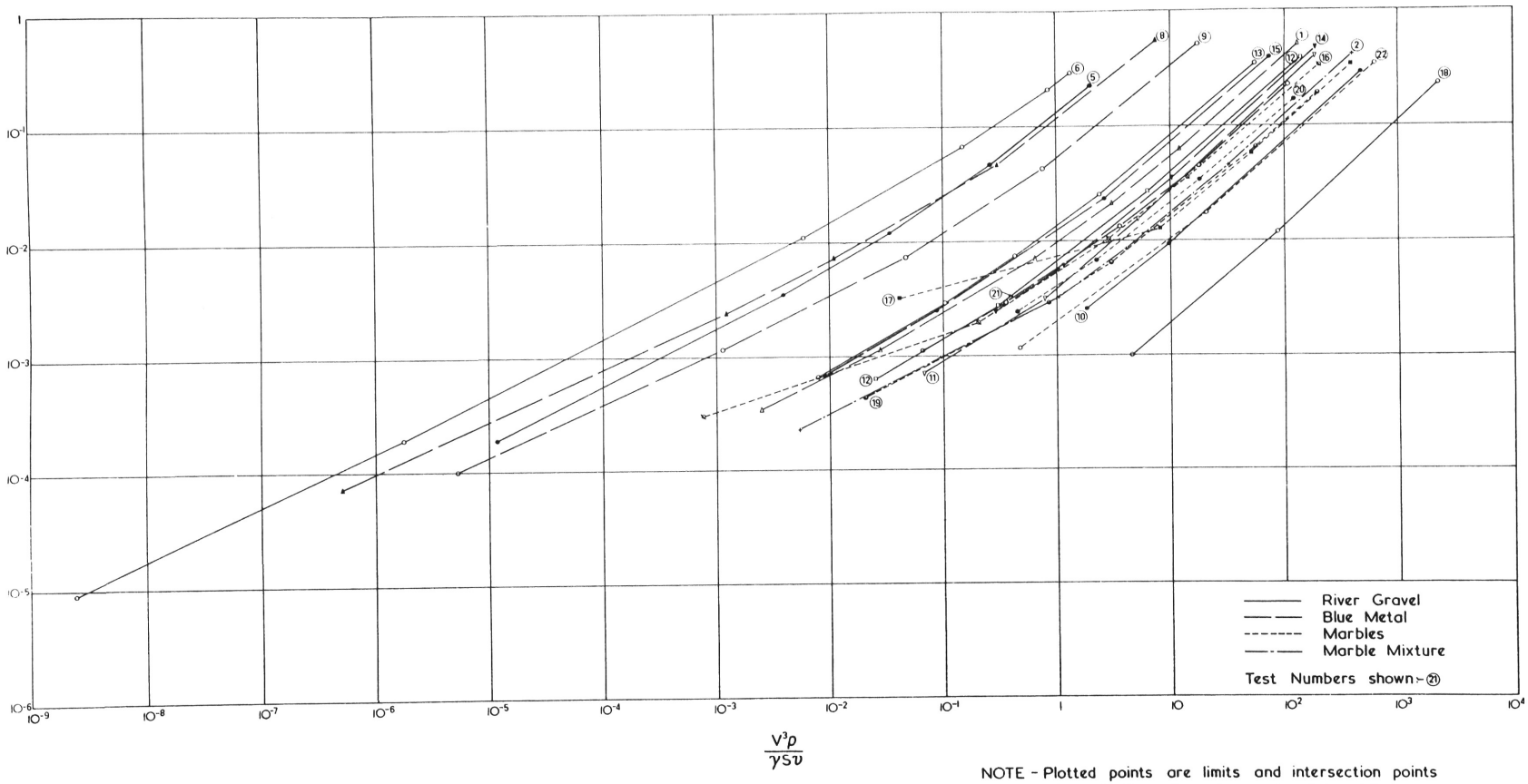

NOTE - Plotted points are limits and intersection points from V-S graphs, not experimental points.

FIGURE 24

$\frac{V}{V_f}$ VERSUS $\frac{V^3\rho}{\gamma s \upsilon}$

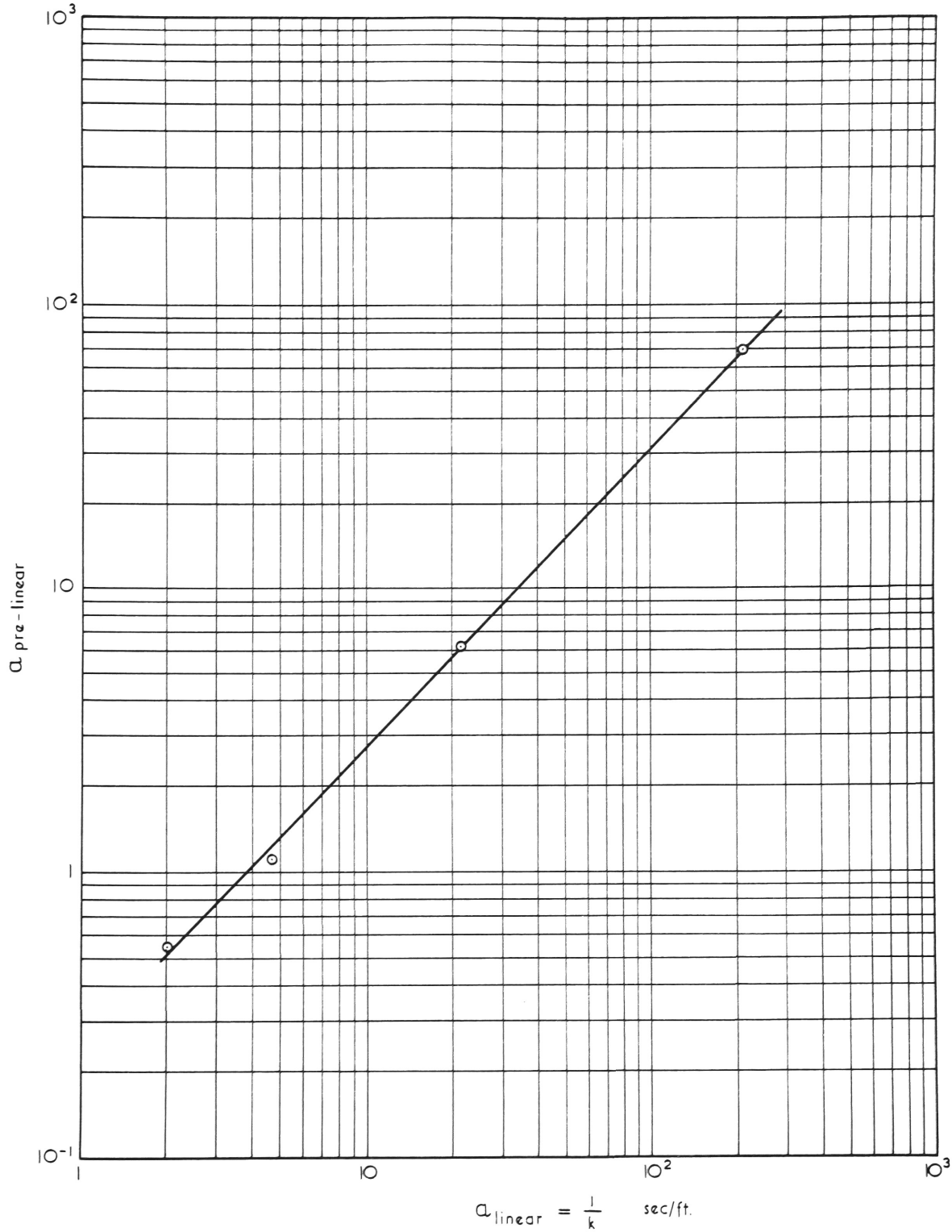

$a_{pre-linear}$ VERSUS a_{linear}

FIGURE 25

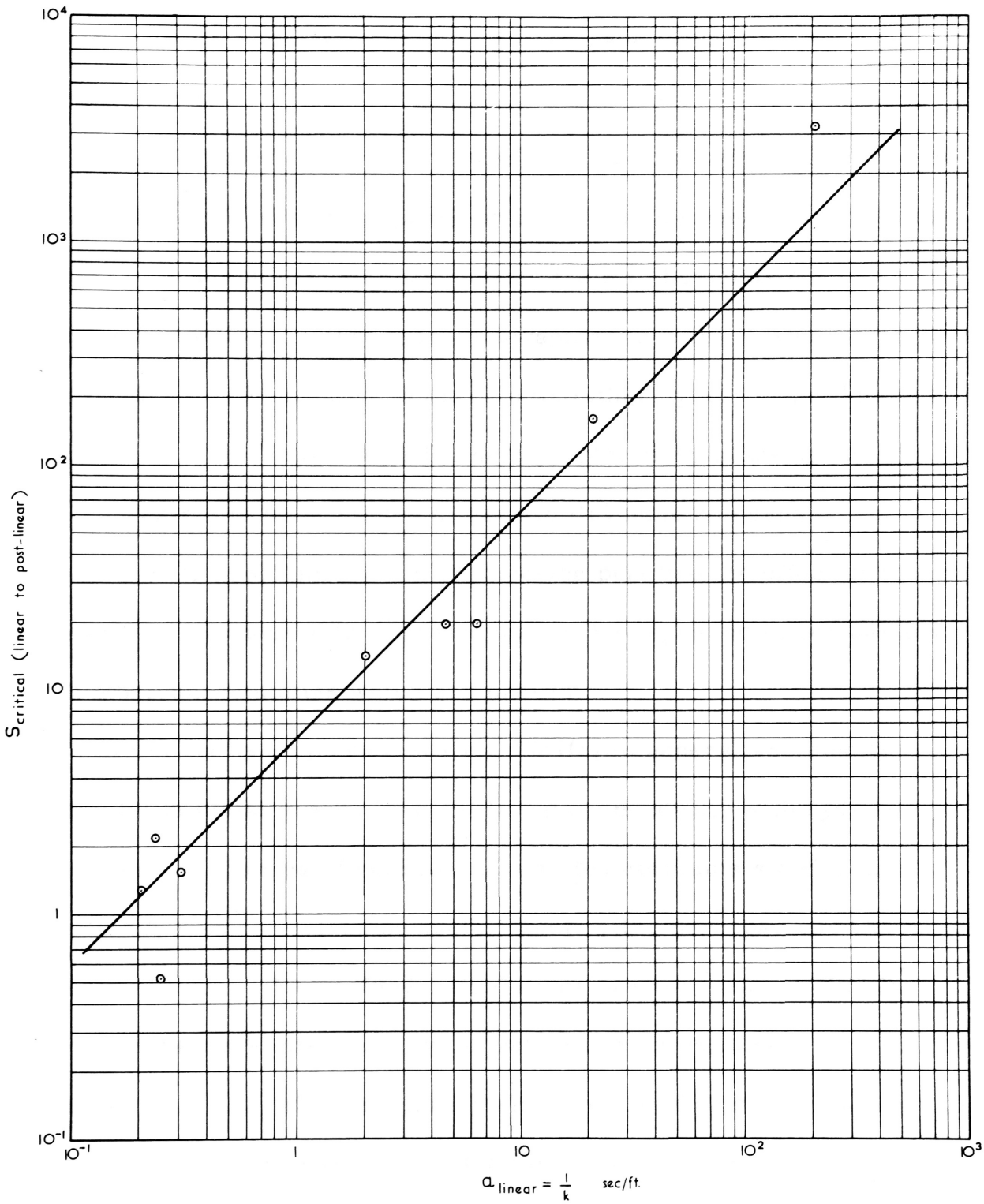

HYDRAULIC GRADIENT FOR UPPER LIMIT OF LINEAR REGIME ($S_{critical}$) VERSUS a_{linear}

FIGURE 26

characteristics such as permeability and shape factors before they could be used.

For purposes of use in engineering it seems logical at the present time to leave the results of permeability tests in terms of velocity and hydraulic gradient, rather than convert them to Reynolds number and friction factor form. There is no advantage in using Reynolds numbers unless they give generality to the results either by way of producing a common friction factor-Reynolds number plot or by allowing changes of flow regime to be predicted at certain Reynolds numbers. For most porous media problems met in engineering practice the effect of change of viscosity of water with temperature can be neglected in comparison with other uncertainties which are present.

Attempts by Slepička (1961(a), 1961(b))to generalise velocity - hydraulic gradient graphs by correlating permeability with hydraulic gradients for changes of regime and with the constants a and n in the equation $S = aV^n$ yielded no useful result with, perhaps, one exception discussed later. Most of the correlations are very poor. Similar correlations were attempted by the author for the results of this investigation. The following plots yielded no significant correlation:

(i) a for one regime versus a for adjacent regime

(ii) a for regime with $n \doteqdot 1.85$ versus a for linear regime

(iii) a for post-linear regime adjacent to linear regime versus a for linear regime

(iv) n about 1.85 versus a for n about 1.85

(v) hydraulic gradient for lower limit of linear regime versus a for linear regime.

Inspection of the results in Table 1 is sufficient to reveal the lack of correlation. Two correlations were, however, obtained. The first, between the value of a for the pre-linear regime and a for the linear regime, is shown in Figure 25. With only four points available for the graph it is possible that the correlation was only accidental.

The second, shown in Figure 26, between the hydraulic gradient for the upper limit of the linear (Darcy) regime and the value of a for this regime (i.e. between the hydraulic gradient for the upper limit of validity of Darcy's law and the reciprocal of the coefficient of permeability) is of practical significance. Differences between individual results and a mean curve are not greater than 150 pc., compared with a range 30 times as great as this for the corresponding Reynolds numbers determined from Figure 23. This range of Reynolds number would reduce to approximately 15 if the lines for the linear regimes were brought together by using K = permeability as the characteristic length in the computation of Reynolds numbers and friction factors.

It appears that the use of the correlation graph of Figure 26

would allow more accurate predictions of the upper limit of flow conditions for which Darcy's law is valid than predictions based on Reynolds number. However, more experimental results are needed for a wider range of material types and permeabilities before definite conclusions can be drawn. A similar correlation is reported by Slepička, but all of his results are for fine materials and his limiting hydraulic gradients cover a narrow range around the value 10. Two results by Izbas (see Slepička (1961(a)) for limiting values of hydraulic gradient approximately 5×10^{-3} are also plotted. A straight line is drawn on the log - log plot between the two sets of results but any number of curves could have been drawn to provide at least as good a fit. Predictions of limiting hydraulic gradient from Slepička's graph and Figure 26 differ by as much as 100 pc.

It is possible that both graphs are applicable only for the limited range of materials for which they were derived or that further experimental points would show that the shape of one or both of the graphs was incorrect.

An unfortunate feature of the use of the correlation between limiting hydraulic gradient and permeability is that the permeability must be determined by experiment if an accurate value is to be obtained. In many cases it would then be simpler to determine the limiting hydraulic gradient experimentally, rather than use a

correlation. However, in some cases it might be difficult with the available apparatus to reach the limiting gradient and a correlation would be useful.

(b) Friction Factor - Reynolds Number Plots

The conventional way of presenting permeability test results is on friction factor - Reynolds number graphs. Differences of presentation lie in the choice of velocity and particle characteristic length used to calculate the parameters and in the selection of either the Darcy or the Fanning friction factor.

The velocity most commonly used is the "filter" or "discharge" velocity, $V = \frac{\text{discharge}}{\text{gross area}}$.

Another hypothetical velocity, sometimes called the "voids velocity" is calculated by dividing the discharge by the "cross-sectional area of voids" i.e. "Voids velocity" = $V_V = \frac{V}{P}$. This velocity has no physical significance and there appears to be no justification for its use instead of the simpler term, V. Friction factor-Reynolds number plots on this basis (e.g. Parkin (1962)) or on the basis of more complicated adjustments of V (e.g. Bakhmeteff (and Feoderoff (1937)) show no more generality than plots made using V.

The friction factors and Reynolds numbers plotted in Figure 23 are calculated using the velocity, V.

A wide choice of particle characteristic lengths may be made.

Normally a "diameter" determined from the results of a sieve analysis is used. This may be a mean or median diameter or some other diameter such as D_{10}, the sieve opening through which 10 pc. of particles pass, chosen for general soil mechanics use on the basis of Hazen's tests on sand (see Terzaghi and Peck, Chapter 1 (1948)). An hydraulic radius based on particle volumes and estimated surface areas may also be used. For spherical particles, particularly uniform size materials which have been used extensively in tests, an actual diameter is the obvious choice.

The median diameters determined from sieve analyses have been used to calculate friction factors and Reynolds numbers plotted in Figure 23. Measured diameters were used for the marbles.

The lack of generality of friction factor - Reynolds number plots cannot be attributed solely to the coice of inappropriate length characteristics. Since the term "d" occurs to the first power in both Reynolds number and friction factor, a change of d in the processing of the results of tests on a particular material is equivalent to a displacement of the f-$\mathbb{R}$ curve, on a log log plot, at 45^{o} to both axes. The amount of the shift is given by $2 \log \frac{d}{d'}$ where d is the diameter originally used and d' is the new diameter. Once one f-$\mathbb{R}$ plot has been drawn, further f-$\mathbb{R}$ plots can be obtained simply by parallel shifts of the lines in appropriate directions at 45^{o} to the axes. It

is clear that f - IR lines will not reduce to a common line by adjustment of length characteristic unless they are parallel over their entire lengths. Comparison of the $\frac{d_{10}}{d_{50}}$ ratios listed in Table 2 and the linear regime sections of Figure 23 show that the use of the d_{10} value would not bring even these sections to a common line.

If it is desired to calculate the changes of d required to shift an f - IR line a certain amount it can be done by calculating

$$\log \frac{d + \Delta d}{d} = \frac{\beta}{\sqrt{2}}$$

where d is the "diameter" originally used in the calculations

Δd is the change in diameter required

β is the logarithmic scale distance measured at 45° to the axes and denoting the shift distance required.

It will be seen that the f - IR lines will not reduce to a common line by individual adjustment of the "diameters" used in the calculations, since they are far from parallel.

The lines may be drawn closer together by using $\sqrt{K}$ = $\sqrt{\text{Permeability}}$ as the characteristic length as Ward (1964) has done. This procedure has, however, only a mathematical and not a physical significance since $\sqrt{K}$ is a characteristic which has to be determined from the graphs themselves (or the V - S graphs from which they were determined) and is not a physical characteristic which can be

measured independently. Until some measurement which will correlate linearly with permeability can be found, no new light is thrown on the generalisation of the f - $\mathbb{R}$ plots by this procedure. If such a correlation could be found, the best that could be hoped for would be a common linear line with a number of post-linear lines for different geometrically similar media.

The use of $\sqrt{K}$ as the characteristic length also poses the problem of how to treat results of media for which a linear regime cannot be determined.

It will be noted that only those values of $\mathbb{R}$ and f corresponding to limits of data and intersection points on the V-S graphs are plotted. This is justified by the following argument which demonstrates that straight lines on the V-S plot will also plot straight on the f-$\mathbb{R}$ plot.

Combination of the equations $S = aV^n$

$$\text{and} \quad S = \frac{fV^2}{2gd}$$

$$\text{yields} \quad f = 2gd\, a\, V^{n-2}$$

$$= 2gd\, a \left(\frac{\mathbb{R}\nu}{d}\right)^{n-2}$$

For a given test series g and d are constant and ν is approximately constant (assumed so in plotting V-S lines)

$$\therefore \quad f = \text{constant} \times a\left(\frac{\mathbb{R}\,\nu}{d}\right)^{n-2}$$

$$\therefore \quad \log f = \log \text{constant} + \log a + (n-2)\log\left(\frac{\mathbb{R}\,\nu}{d}\right)$$

For a particular regime, n and a are constant. i.e. for each regime, log f = constant + (n - 2) log $\mathbb{R}$. Therefore each straight line on the V-S plots will plot as a straight line on the f-$\mathbb{R}$ plot.

The reason for curves with a large scatter of results joining the "laminar" and "turbulent" sections of most published f-$\mathbb{R}$ plots for a number of materials can be understood when the corresponding region of Figure 23 is inspected. If the individual test lines are not drawn, a random scatter of experimental points results.

The range of Reynolds numbers over which the upper limits of the linear regimes spread is from approximately 2 to 60. Thus a factor of 30 exists between the extreme values determined in these experiments. This factor could be reduced to approximately 15 by drawing the linear sections of the graphs together by replacing d by $\sqrt{K}$. It is evident that the commonly accepted critical Reynolds numbers 1 or 5, would be poor criteria for the limits of the linear regimes determined in these experiments.

The results also completely invalidate the calculation of critical velocities on the basis of analogy with flow in circular pipes for which critical Reynolds numbers of the order of 2,000 occur. Although post research has shown conclusively that such an analogy is completely invalid, calculations of critical velocities on this basis have appeared as recently as 1964 in a United States Geological Survey Professional Paper by Smith and Sayre (1964).

(c) Use of Fall Velocity as a Measure of Particle Size, Grading and Shape

The justification for using median particle fall velocities as a measure of the size, grading and shape of the particles of a granular medium is discussed in Section 8. 2 (c). Since the variation of the drag coefficient of a sphere caused by gradual movements of separation points cannot have a counterpart in the fall of angular particles, it was considered inappropriate to calculate the diameters of equivalent spheres with fall velocities equal to the median values determined. A justifiable comparison might be made with a "sphere" which had a drag coefficient independent of Reynolds number within the range of fall velocities encountered. An additional argument against attempting to use equivalent sphere diameters is the inability of alterations in d values to bring the f-$\mathbb{R}$ graphs of Figure 23 together. Equivalent diameters calculated from the fall velocity results could not therefore produce one general graph from all the experimental results. Examination of Figure 23 shows that some of the linear regime sections overlap post-linear sections of other lines and parallel shifts at an angle 45^{o} to the axes certainly would not bring about co-incidence.

Because no satisfactory comparison was possible if equivalent sphere diameters were used, it was decided to apply the fall velocities directly as an empirical measure of particle shape, size and grading. Using dimensional analysis, the variables

$$V,\ V_f,\ \rho,\ \mu,\ \frac{\Delta p}{\Delta x}$$

can be re-arranged into the dimensionless parameters $\frac{V}{V_f}$ and

$$\frac{V^3 \rho^2}{\frac{\Delta p}{\Delta x}\mu} = \frac{V^3 \rho}{\gamma S \nu}$$

Values of these parameters are listed in Table 2 and plotted on Figure 24. The plotted points represent the limits of data and intersections of the lines on the V-S plot. The justification for plotting only these points and drawing straight lines between is set out below.

Combining $S = aV^n$ and $\frac{V^3 \rho}{\gamma S \nu}$,

$$\frac{V^3 \rho}{\gamma S \nu} = \frac{V^{3-n} \rho}{\gamma a \nu}$$

$$= \frac{(\frac{V}{V_f})^{3-n} \rho\ V_f^{3-n}}{\gamma\ a\nu}$$

For each regime for each test series

V_f, ρ, n, γ , a, ν are constant (ν assumed constant in plotting V - S lines)

$$\therefore \frac{V^3 \rho}{\gamma S \nu} = (\frac{V}{V_f})^{3-n} \text{ x constant}$$

$$\therefore \log (\frac{V^3 \rho}{\gamma S \nu}) = \log \text{constant} + (3 - n) \log \frac{V}{V_f}$$

Thus, on a log log plot of $\frac{V^3 \rho}{\gamma S \nu}$ against $\frac{V}{V_f}$, V-S lines which plot straight on the V-S plot will plot as straight lines. It is, therefore,

only necessary to plot the intersection points and end points and draw straight lines between.

It is evident from the results that the use of fall velocities failed to generalise the permeability test results.

8. 4 Effect of Porosity on Permeability and Friction Factor

Several investigators have published empirical correlations between porosity and friction factor or permeability. A number of these are listed by Engelund (1953). Cohen de Lara (1955) plots several and shows that there are large discrepancies between the correlations except for porosities about 40 pc. Givan (1934) also shows that discrepancies exist.

The experiments of Gerber and Perrin (1962) and Yalin and Franke (1961) show that even for the same spherical particles in a permeameter at the same porosity the friction factor-Reynolds number graph may vary because of different arrangements of the spheres, particularly for small values of the ratio permeameter tube diameter to particle diameter. The inability to obtain one porosity - friction factor correlation may therefore be attributed to lack of geometrical similarity of porous media (i. e. of both particle shape and arrangement).

In the absence of correlations for specific types of granular media, there appears little justification in engineering practice to use the more complicated of the suggested correlations to predict the effect on friction

factor of change in porosity. The only exception to this would be if the media and flow conditions under consideration matched those for which the more complicated correlations were obtained.

An approximate estimate of the change might be made from the equation $f \propto \frac{1}{P^5}$ reported by Cohen de Lara (1955) and Mavis and Wilsey (1936). The latter reported exponents of P as low as 4 for some materials so estimates made on the assumption that $f \propto \frac{1}{P^5}$ may be greatly in error.

The only accurate way of determining the effect of porosity changes for a particular material appears to be to carry out a series of permeability tests for different porosities.

It has been suggested by the author that the only way in which friction-factor Reynolds number plots might be generalised is to determine a series of graphs for geometrically similar media. This might produce a plot similar to the pipe friction factor charts. In this case, testing a particular granular material at various porosities would be analogous to performing tests on a pipe whose diameter could be altered without altering the roughness projection heights. The tests would then be on geometrically dissimilar pipes. Friction factors and Reynolds numbers would plot on a curve cutting across the various $\frac{\text{roughness}}{\text{diameter}}$ lines. An explanation such as this with the possibility of a multitude of lines joining the results of tests on geometrically dissimilar

media caused by changes in porosity would explain the variety of porosity - friction factor correlations reported.

The permeability tests carried out in connection with this investigation on 16 mm diameter marbles, 3/4 inch blue metal and 3/4 inch river gravel were not intended to produce general correlations. They were intended to show whether the nature of the velocity - hydraulic gradient relationship changed with change in porosity and to allow spot checks to be made of published porosity - friction factor correlations. The results of these tests are plotted in Figures 7, 8 and 9. The results of three of the test series plotted in Figure 9 are the work of an undergraduate thesis student, A. Grove, working in conjunction with the author.

It is apparent from the Figures that although the nature of the V-S relationship does not change and correspondingly abrupt changes occur between straight line sections, the slopes of the lines, and thus values of the exponent, n, change with changes in porosity. In other words changes in porosity can cause changes in both a and n in the equation $S = aV^n$. This evidence supports the statement that permeability tests at various porosities are required if an accurate adjustment of friction factors for porosity changes is to be made.

Spot checks on the variation of friction factor with porosity for the 16 mm marbles and 3/4 inch blue metal at Reynolds numbers of

10^3, 10^2 and 10 yielded the following results:-

Material	Porosity change pc.		$\mathbb{R}=10^3$	$\mathbb{R}=10^2$	$\mathbb{R}\doteq 10$
3/4 inch blue metal	42.8 to 51.5	$\frac{1}{f}$ varies	$P^{4.8}$	$P^{5.3}$	$P^{4.9}$
16 mm marbles	36.9 to 41.5	as:	$P^{5.3}$	$P^{6.3}$	$P^{5.7}$

It is clear from this limited check that the use of the approximation $f \propto \frac{1}{P^5}$ may lead to large errors. Variations in the exponent of P for tests on a particular material result from the f - $\mathbb{R}$ graphs for different porosities not being parallel over their entire lengths. Only parallel lines will yield a constant exponent since $\log f_1 - \log f_2$ is constant for all $\mathbb{R}$ values, with parallel lines, and the ratio $\frac{f_1}{f_2}$ is therefore constant.

9. Conclusions

9.1 Form of Velocity - Hydraulic Gradient Relationship.

The results of this investigation show that the form of the velocity - hydraulic gradient relationship for the flow of water through coarse granular media consisting of spherical, rounded or angular particles is a discontinuous exponential one which may be expressed in the form

$$S = aV^n$$

A number of flow regimes occur, each with its own value of a and n. Abrupt changes of a and n separate the various regimes.

The regimes which may occur for flow through a particular porous medium may be classified into:

(i) A linear regime for which $n = 1$. In this regime Darcy's law is valid

$$\text{i.e. } S = aV$$
$$\text{or } V = kS$$

(ii) At least one pre-linear regime for which $n < 1$. In this regime non-Newtonian characteristics caused by interfacial tension effects are postulated for the permeating water.

(iii) Several post-linear regimes for which $n > 1$. At least a partial state of turbulence exists in these regimes. Values of n greater than 2 have been reported for very coarse materials.

9. 2 Turbulence Detection

The turbulence detector results gave a general indication of turbulence commencing near the upper limit of the linear regime. The results appeared to be influenced greatly by local flow conditions. Refinement of the detector circuitry and the insertion of probes at a number of points, perhaps in dummy particles, should give more accurate results.

9. 3 Wall Effects in Permeameters

Permeameter wall effects for tests on coarse materials showed up as an increase in average velocity of 5 to 10 pc. measured over the total cross sectional area of the permeameter compared with that measured across the inner section. This increase did not vary significantly with tube to particle diameter ratio down to approximately five.

9. 4 Generalisation of Velocity-Hydraulic Gradient Data

(a) No method of expressing velocity and hydraulic gradient results has yet been devised that will generalise the results of flow through a wide range of types of porous media. Limited correlations which have been published are useful only if applied to flow cases similar to those for which they were derived.

(b) Friction factor - Reynolds number plots can be expected to yield general relationships only for series of geometrically similar

porous media. Attempts to obtain a single general relationship for all media have not been successful.

(c) There is little justification at present for expressing velocity - hydraulic gradient data required for civil engineering use in friction factor - Reynolds number form since this form is more complicated and does not allow generalisations to be made.

(d) A correlation between coefficient of permeability, k ($k = \frac{1}{a_{linear}}$), and the hydraulic gradient corresponding to the upper limit of validity of Darcy's law gave a much better prediction of this limit than did a Reynolds number based on particle size. The application of this correlation involves additional information in that a measurement of permeability over at least a limited region of the linear regime is required.

(d) The value of a for the pre-linear regime appears to correlate with the value of a for the linear regime (or the coefficient of permeability, k). More information is required to confirm this.

(e) The use of measured fall velocities as a criterion of particle size, shape and grading does not unify the velocity-hydraulic gradient results for tests on similar or different types of material at approximately the same porosity.

9.5 Effect of Porosity Changes on Friction Factors

The experimental results showed that changes in a, n and the

hydraulic gradients for changes in regime accompanied porosity changes. No simple porosity - friction factor function applies to all porous media, or even to a particular porous medium independent of Reynolds number (for flow rate). Use under all conditions of the frequently quoted relationship $f \propto \frac{1}{P^5}$ can lead to large errors. The only accurate way of determining the effect of changes in porosity for a particular granular medium is to carry out permeability tests for various porosities.

9.6 Application of Results in Civil Engineering

(a) Accurate knowledge of the velocity - hydraulic gradient relationship for a particular coarse granular medium can only be obtained at present by undertaking permeability tests over the range of flow rates and hydraulic gradients pertinent to the problem being investigated.

(b) Small porosity changes result in large changes of velocity for a given hydraulic gradient. Control of porosity or careful evaluation of the effects of porosity changes for a particular porous medium must be achieved if predictions of flow rates and hydraulic gradients for flows through coarse granular beds are to be accurate.

(c) Velocities and hydraulic gradients are best plotted directly on log log paper for engineering use rather than a friction factor Reynolds number plots.

(d) Conventional flow nets and other analogies are applicable only

to flows in the linear regime and application of these to flows outside either the upper or lower limits of validity of the linear regime may lead to large errors.

(e) Accurate scaling up of model results on moderately coarse granular media to prototypes composed of very coarse granular particles can be achieved only if dynamic similarity with prototype conditions is attained in the model. This requires geometrically similar media and flow rates such that model and prototype flow regimes are the same.

(f) Permeameters for coarse granular materials should be designed to eliminate wall effects or an appropriate allowance should be made.

9.7 Further Research Required

(a) Investigation of flow regimes and values of n for very coarse granular media of the size used in prototype rock-fill structures is required to confirm model scaling techniques.

(b) Further investigation of velocities and hydraulic gradients for low flow rates is required before the reasons for the occurrence of pre-linear regimes can be confirmed.

(c) More accurate turbulence detection experiments are required to definitely establish at what point on the velocity-hydraulic gradient graph turbulence becomes established. Measurements of local

velocities, pressures and turbulent fluctuations are also needed to throw light on the causes of the abrupt changes in regime.

(d) Attempts to determine friction factor - Reynolds number correlations on the basis of geometrically similar series of media should be attempted. It is possible that in this way a general friction factor - Reynolds number chart could be built up.

(e) The application of statistical theory to define the requirements of "average" geometrical similarity in random packings of granular particles would be required before much progress could be made on generalising results for graded materials.

Acknowledgements

The author wishes to thank Professor C. H. Munro, Foundation Professor of Civil Engineering and Associate Professor H. R. Vallentine and the staff of the Water Research Laboratory for the assistance given in the conduct of this investigation.

10. References

Albertson, M. L. "Effect of Shape on the Fall Velocity of Gravel Particles" Proc. 5th Hydraulics Conference, Iowa, 243-261, 1952.

Anandakrishnan, M and Varadarajulu, G. H., "Laminar and Turbulent Flow of Water through Sand" A. S. C. E. Proc. 89, SM5, 1-15, 1963.

Bakhmeteff, B. A. and Feodoroff, N. V., "Flow through Granular Media" Jnl. Applied Mechanics 4A, 97-104, 1937.

Bikerman, J. J., "Surface Chemistry", New York, Academic Press, 2nd Edition. 1958.

Boreli, M. and Batinic, B. "Consideration sur la loi non-lineaire de filtration repartition des vitesses de filtration au voisinage du point de sortie". I. A. H. R. Proc. 9th Convention 506-515, 1961.

Cohen de Lara, G., "Coefficient de perte de charge en milieu poreux basé sur l'équilibre hydrodynamique d'un massif". La Houille Blanche, No. 2,167-176, 1955.

Collins, R. A. "Flow of Fluids through Porous Materials" N. York, Reinhold, 1961.

Engelund, F. "On the laminar and turbulent flows of ground water through homogeneous sand" Danish Acad. of Tech. Sciences, Trans. n. 3, 7-105, 1953 (English Translation).

Escande, L. "Experiments concerning the infiltration of water through a rock mass" Reprint from Proc. Minnesota International Hydraulics Convention, 1953.

Fishel, V. C. "Further Tests of Permeability with Low Hydraulic Gradients" A. G. U. Trans. 16th Ann. Meeting, 449-503, 1935

Gerber, S and Perrin, R. "Loss of Head in Flow through a Porous Medium of Identical Sheres" Compt. Rend. Acad. Sci. Paris, 225, 23, 3126-27, Dec. 1962.

Givan, C. V. "Flow of water through Granular Materials - Initial Experiments with Lead-Shot" A. G. U. Trans. 15, 572-579, 1934.

Hall, W. A. "An analytical derivation of the Darcy Equation" A. G. U. Trans., 37, 2, 185-188, 1956.

Harkins, W. D. "Physical Chemistry of Surface Films" New York, Reinhold, 1952.

Harleman, D. R. F., Melhorn, P. F., Rumer, R. R., Jr "Dispersion - Permeability Correlation in Porous Media", A. S. C. E. Jnl. 89, HY2, 67-85, March 1963.

Heywood, H. "Uniform and Non-Uniform Motion of Particles in Fluids" Proc. of the Symposium on the Interaction between Fluids and Particles, London, 1-8, 1962.

Hickox, G. H. "Flow through Granular Materials" A. G. U. Trans., 15, 567-571, 1934.

Hubbert, M. K. "The Theory of Ground-Water Motion" Journal of Geology, 48, 785-944, 1940.

Iberall, A. S. "Permeability of Glass Wool and other Highly Porous Media" J. Res. Nat. Bur. Stand. 45, 398, 1950.

Iffly, R. "Etude physique de l'écoulement des fluides dans les milieux poreux". Compte Rendu des Sixièmes Journées de L'Hydraulique, Société Hydrotechnique de France, 1, 17-23, 1960.

Jacob, C. E. "Engineering Hydraulics" (1950) (Ed. Rouse) Chapt. 5., N. York, Wiley.

Karadi, G and Nagy, I. V. "Investigations into the validity of the linear seepage law" I. A. H. R. Proc. 9th Convention, Dubrovnik, 556-566, 1961.

Madhav, M. R. and Subba Rao, K. S. "Flow of water through sands and permeability factor" Indian Institute of Science, Annual Report 1963.

Marshall, T. J. "Permeability Equations and their Models" Proc. of the Symposium on the Interaction between fluids and particles, London, 299-303, June 1962.

Mavis, F.T. and Wilsey, E.F. "A study of the permeability of sand" State Uni. of Iowa, Studies in Engineering, Bulletin 7, 1936.

Muskat, M. "The flow of homogeneous fluids through porous media" (1937) Michigan, Edwards, (2nd printing, 1946).

Nagy, I. "Au privire la valabilitatea legii lineare a infiltrației" (About the validity of the linear law of infiltration). Studii de Geotehnica, Fundații si Constructii Hidrotechnice, III 95-106. Institutul de Studii și Cercetări Hidrotehnice, Bucarest, 1961.

Parkin, A.K. "Rockfill dams with inbuilt spillways Part I - hydraulic characteristics" Dept. Civil Engineering, University of Melbourne, 1962.

Philip, J.R. "Fluid flow in porous media from the viewpoint of classical hydrodynamics" 2nd Aust. Conf. Soil Sci. 1957.

Rose, H.E. (1945 (a)) "An investigation into the laws of flow of fluids through beds of granular materials" Inst. Mech. Engrs. Proc. 153, 141-148, 1945.

Rose, H.E. (1945(b)) "The isothermal flow of gases through beds of granular materials" Inst. Mech. Engrs. Proc. 153, 148-153, 1945.

Rose, H.E. (1945) (c)) "On the resistance coefficient - Reynolds number relationship for fluid flow through a bed of granular material" Inst. Mech. Engrs. Proc., 153, 154-168, 1945.

Rose, H.E. and Rizk, A.M.A. "Further researches in fluid flow through beds of granular material" Inst. Mech. Engrs. Proc., 160, 493-511, 1949.

Rose, W.D. "Calculations based on Kozeny - Karman Theory" J. Geophys. Research, 64, 1, 103-110, 1959.

Saunders, O.A. and Ford, H. "Heat transfer in the flow of gas through a bed of solid particles" Iron and Steel Inst., Jour. 141, 291, 1940.

Scheidegger, A. E., "Statistical Hydrodynamics in porous media" Jour. Appl. Phys. 25, 8, 1954.

Scheidegger, A. E. "The physics of flow through porous media" Toronto, Uni. of Toronto Press, Revised Edn. 1960.

Schwartz, A. M. (et alia) Vol. I "Surface Activation", 1949
Vol. II "Surface Active Agents and Detergents, 1958, N. York, Interscience.

Slepička, F. (1961(a)) "Filtračnízákony" (The laws of filtration) Praha - Podbaba, 1961.

Slepička, F. (1961 (b)) "The laws of filtration and limits of their validity" I. A. H. R. Proc. 9th Convention, 383-394, 1961.

Smith W. O. and A. Nelson Sayre "Turbulence in ground-water flow" U. S. Geological Survey Professional Paper 402-E, 1964.

Swartzendruber, D. "Modifications of Darcy's law for the flow of water in soils" Soil Sci. 93, 22-29, 1962.

Tek, M. R. "Development of a generalized Darcy equation". Trans. Am. Inst. Mining, Metallurgical and Petroleum Engrs. 210, 45, 1957.

Terzaghi, K and Peck, R. "Soil Mechanics in Engineering Practice" Chapters 1 and 2 N. York, Wiley, 1948.

Van der Tuin, H. "La permeabilité et les applications pratiques des materiaux gros" Compte Rendu des Sixièmes Journées de L'Hydraulique, Société Hydrotechnique de France, 1, 17-23, 1960.

Verdeyen et Nuyens "Determination par formules et par essais en laboratoire du coefficient de permeabilité des sols" Proc. 5th Int. Conf. S. M. F. E., 1, 381, 1961.

Ward, J. C. "Turbulent flow in porous media" A. S. C. E. Jour., 90 HY5, 1964.

Watson, K. K. "The permeability of an idealised two-dimensional porous medium using the Navier-Stokes equations" Proc. 4th Aust. - N. Z. Conf. on Soil Mech. and Found. Eng. 37-40, 1963.

Wentz, C. A. and Thodos, G. "Total and form drag friction factors for the turbulent flow of air through packed and distended beds of spheres" A. I. Ch. E., Jour. 9, 3, 358-361, 1963.

Wilkins, J. K. "Flow of water through rock fill and its application to the design of dams" New Zealand Engineering 382-387, Nov. 15, 1955.

Yalin, S. and Franke, L. "Experimental investigation of the laws of filter flow" I. A. H. R. Proc. 9th Convention, 324-331, 1961.

Zenz, F. A. and Othmer, D. F. "Fluidization and fluid-particle systems" N. York, Reinhold, 1960.

APPENDIX I. Justification of Use of Piezometer Tapping Junction Boxes.

Let (i) the pressures at each of the four piezometer tappings at a certain level on the permeameter be p_1, p_2, p_3, p_4,

(ii) the pressure in the junction box be p

(iii) the equalising flows in the connecting tubes be q_1, q_2, q_3, q_4 and the corresponding velocities be v_1, v_2, v_3, v_4,

(iv) the lengths and diameters of all connecting tubes be l and δ respectively.

Assume the equalising flows are small enough to be laminar.

Then, calling q and v values towards the junction positive,

$$p_1 - p = \frac{32\mu l v_1}{\delta^2}$$

$$p_2 - p = \frac{32\mu l v_2}{\delta^2}$$

etc.

$$\therefore \quad p_1 = \frac{32\mu l v_1}{\delta^2} + p$$

$$p_2 = \frac{32\mu l v_2}{\delta^2} + p$$

etc.

$$\therefore \quad \frac{p_1+p_2+p_3+p_4}{4} = \frac{32\mu l}{4\delta^2}(v_1 + v_2 + v_3 + v_4) + p$$

$$= \frac{32\mu l}{\pi\delta^4}(q_1 + q_2 + q_3 + q_4) + p$$

$$\text{but } q_1 + q_2 + q_3 + q_4 = 0 \quad \text{(algebraically)}$$

$$\therefore \frac{p_1 + p_2 + p_3 + p_4}{4} = p$$

i. e. the pressure in the junction box is the arithmetic mean of the pressure at the four piezometer tappings provided

(i) connecting tube lengths are equal

(ii) tube diameters are equal

(iii) flow in the tubes is laminar.

Condition for Laminar Flow in Connecting Tubes

Actual tubes used were 1/4 inch I. D. plastic, 6 feet in length and not sharply curved.

Adopt critical Reynolds number of 2,000 and water at 60°F ($\nu = 1.2 \times 10^{-5}$ ft^2/ sec.)

Then upper limit of $v = \frac{2,000 \times 1.2 \times 10^{-5}}{0.02}$

$= 1.2$ ft/ sec.

$$\Delta p = 32 \frac{\mu}{\delta^2} l v$$

$$= \frac{32 \times 1.2 \times 10^{-5} \times 1.94 \times 6 \times 1.2}{(0.02)^2 \times 144} \text{ psi}$$

$= 0.093$ psi

$= 2\frac{1}{2}$ inches head of water

i. e. Maximum allowable head difference between an individual tapping and the junction box is $2\frac{1}{2}$ inches of water for laminar flow to occur.

APPENDIX II

TABLE 8

Permeability Test No. 1 on BM3-2 3/4" Blue Metal

Porosity (a) by draining voids 42.6 pc. (b) by weighing solids 45.5 pc.

Inner Flow Only			Total Flow		
Velocity(V) ft/sec.	Hydraulic Gradient(S)	Temp. °C.	Velocity(V) ft/sec.	Hydraulic Gradient(S)	Temp. °C.
0.461	3.50	15.5			
0.264	1.20	15.5			
0.106	0.217	15.5			
0.387	2.36	15.5			
0.368	2.34	15.5			
0.259	1.18	15.5			
0.155	0.455	15.5			
0.118	0.276	15.5			
7.35×10^{-2}	0.118	15.5			
5.15×10^{-2}	6.4×10^{-2}	15.5			
3.31×10^{-2}	2.96×10^{-2}	15.5			
1.59×10^{-2}	9.26×10^{-3}	15.5			
1.39×10^{-2}	7.05×10^{-3}	15.5			
6.25×10^{-3}	1.97×10^{-3}	15.5			
0.758	9.18	15.5			
0.707	7.65	15.5			
0.655	6.30	15.5			
0.762	9.27	15.5	0.858	9.11	15.5
			0.815	7.59	15.5
			0.725	5.91	15.5
			0.552	3.93	15.5
			0.330	1.45	15.5
			0.253	0.93	15.5
			0.245	0.85	15.5
			0.184	0.478	15.5
			0.148	0.33	15.5
			0.121	0.228	15.5
			7.97×10^{-2}	0.109	15.5
			5.01×10^{-2}	4.72×10^{-2}	15.5
			2.68×10^{-2}	1.65×10^{-2}	15.5
			1.79×10^{-2}	8.6×10^{-3}	15.5
			5.46×10^{-3}	1.5×10^{-3}	15.5

APPENDIX II TABLE 8 (cont'd.)

Permeability Test No. 1 on BM3-2 3/4" Blue Metal

Porosity (a) by draining voids 42.6 pc. (b) by weighing solids 45.5 pc.

Inner Flow Only			Total Flow		
Velocity(V) ft/sec.	Hydraulic Gradient(S)	Temp. °C.	Velocity(V) ft/sec.	Hydraulic Gradient(S)	Temp. °C.
1.26×10^{-2}	6.9×10^{-3}	15.5	1.44×10^{-2}	6.9×10^{-3}	15.5
5.48×10^{-3}	2.42×10^{-3}	15.5	6.28×10^{-3}	2.42×10^{-3}	15.5
1.51×10^{-3}	5.6×10^{-5}	15.5	1.70×10^{-3}	5.6×10^{-5}	15.5
2.57×10^{-2}	2.01×10^{-2}	15.4	2.94×10^{-2}	2.01×10^{-2}	15.4
2.03×10^{-2}	1.54×10^{-2}	15.4	2.37×10^{-2}	1.54×10^{-2}	15.4
1.17×10^{-2}	6.2×10^{-3}	15.4	1.35×10^{-2}	6.2×10^{-3}	15.4
6.0×10^{-4}	2.5×10^{-4}	15.4	1.3×10^{-3}	2.5×10^{-4}	15.4
2.2×10^{-3}	7.4×10^{-4}	15.4	2.8×10^{-3}	7.4×10^{-4}	15.4
4.8×10^{-3}	1.64×10^{-3}	15.4	5.6×10^{-3}	1.64×10^{-3}	15.4
8.3×10^{-3}	3.69×10^{-3}	15.4	9.7×10^{-3}	3.69×10^{-3}	15.4
1.25×10^{-2}	6.5×10^{-3}	15.4	1.46×10^{-2}	6.5×10^{-3}	15.4
2.04×10^{-2}	1.36×10^{-2}	15.4			
2.96×10^{-2}	2.49×10^{-2}	15.4			
4.60×10^{-2}	5.26×10^{-2}	15.4			
6.80×10^{-2}	0.104	15.4			
0.101	0.212	12			
0.101	0.211	13.8			
0.145	0.405	13.8			
0.198	0.720	14.1			
0.309	1.67	14.1			
0.390	2.63	14.2			
0.451	3.45	14.2			
0.520	4.49	14.3			
0.590	5.68	14.4			
0.687	7.50	14.4			
0.790	9.73	14.4			
0.598	5.75	14.3			
0.412	2.92	14.3			
0.296	1.53	14.3			
0.205	0.764	14.4			
0.140	0.382	14.4			
9.76×10^{-2}	0.194	14.4			
7.01×10^{-2}	0.108	13.2			
4.60×10^{-2}	5.11×10^{-2}	12.9			

APPENDIX II

TABLE 8 (cont'd.)

Permeability Test No. 1 on BM3-2 3/4" Blue Metal

Porosity (a) by draining voids 42.6 pc. (b) by weighing solids 45.5 pc.

Inner Flow Only			Total Flow		
Velocity(V) ft/sec.	Hydraulic Gradient(S)	Temp. ^{o}C.	Velocity(V) ft/sec.	Hydraulic Gradient(S)	Temp. ^{o}C.
2.72×10^{-2}	2.19×10^{-2}	12.8			
1.38×10^{-2}	7.46×10^{-3}	12.7			
8.26×10^{-3}	3.53×10^{-3}	12.7			
4.15×10^{-3}	1.39×10^{-3}	12.7			
1.91×10^{-3}	5.25×10^{-4}	12.7			
7.4×10^{-4}	1.3×10^{-4}	10.2			
6.4×10^{-4}	2.0×10^{-4}	10.3			
2.70×10^{-3}	9.2×10^{-4}	10.5			
4.10×10^{-3}	1.5×10^{-3}	10.5			
2.17×10^{-3}	6.7×10^{-4}	10.4			

APPENDIX II TABLE 9

Permeability Test No. 2 on: M123 Marble Mixture

Porosity (a) by draining voids 35.8 pc. (b) by weighing solids 37.9 pc.

Inner Flow Only			Total Flow		
Velocity(V) ft/sec.	Hydraulic Gradient(S)	Temp. °C	Velocity(V) ft/sec.	Hydraulic Gradient(S)	Temp. °C.
1.25	11.2	12.7			
1.24	11.2	12.7			
1.05	8.27	12.7			
0.888	6.14	12.7			
0.698	3.89	12.8			
0.526	2.30	12.8			
			1.21	10.2	12.9
			0.942	6.30	12.9
			0.772	4.29	12.9
			0.420	1.33	12.9
			0.272	0.591	12.9
1.83×10^{-3}	3.3×10^{-4}	12.0	1.81×10^{-3}	3.3×10^{-4}	12.1
4.25×10^{-3}	9×10^{-4}	11.9	3.77×10^{-3}	9×10^{-4}	11.9
6.00×10^{-3}	1.3×10^{-3}	11.9	5.52×10^{-3}	1.3×10^{-3}	11.9
7.87×10^{-3}	1.8×10^{-3}	12.1	7.62×10^{-3}	1.8×10^{-3}	12.1
9.77×10^{-3}	2.1×10^{-3}	12.0	8.94×10^{-3}	2.1×10^{-3}	12.0
1.21×10^{-2}	3.0×10^{-3}	11.5	1.17×10^{-2}	3.0×10^{-3}	11.5
1.57×10^{-2}	4.7×10^{-3}	11.6	1.51×10^{-2}	4.7×10^{-3}	11.6
1.72×10^{-2}	5.0×10^{-3}	11.7	1.64×10^{-2}	5.0×10^{-3}	11.7
2.27×10^{-2}	8.1×10^{-3}	12.2	2.22×10^{-2}	8.1×10^{-3}	12.7
3.41×10^{-2}	1.62×10^{-2}	13.1	3.41×10^{-2}	1.62×10^{-2}	13.8
5.15×10^{-2}	3.27×10^{-2}	14.7	5.18×10^{-2}	3.27×10^{-2}	14.7
7.78×10^{-2}	6.81×10^{-2}	14.4	7.93×10^{-2}	6.81×10^{-2}	13.9
0.117	0.142	13.2	0.119	0.142	13.1
0.180	0.305	12.9	0.184	0.305	12.8
1.52×10^{-3}	2.3×10^{-4}	13.7	9.6×10^{-4}	2.3×10^{-4}	13.8
9.22×10^{-4}	2.6×10^{-4}	13.7	7.09×10^{-4}	1.3×10^{-4}	13.7
1.67×10^{-3}	3.6×10^{-4}	13.8	1.62×10^{-3}	3.6×10^{-4}	13.8

APPENDIX II TABLE 10

Permeability Test No. 4 on G1 Nepean River Sand.

Porosity (a) by draining voids 27. 2 pc. (b) by weighing solids 38. 7 pc.

Inner Flow Only			Total Flow		
Velocity (V) ft/ sec.	Hydraulic Gradient(S)	Temp. °C.	Velocity (V) ft/ sec.	Hydraulic Gradient(S)	Temp. °C.
3.25×10^{-2}	7.75	11.0			
3.47×10^{-2}	8.06	11.0	3.45×10^{-2}	8.01	11.0
2.66×10^{-2}	6.15	10.9	2.69×10^{-2}	6.15	10.8
1.88×10^{-2}	4.24	10.8	1.89×10^{-2}	4.26	10.7
1.50×10^{-2}	3.13	10.7	1.40×10^{-2}	3.13	10.7
9.52×10^{-3}	1.96	10.7	8.76×10^{-3}	1.96	10.7
5.35×10^{-3}	1.12	10.6	4.97×10^{-3}	1.12	10.6
3.13×10^{-3}	0.659	10.5	2.91×10^{-3}	0.659	10.5
4.40×10^{-2}	11.02	9.3	4.29×10^{-2}	11.02	9.0
1.80×10^{-3}	0.400	8.9	1.63×10^{-3}	0.401	8.9
8.74×10^{-4}	0.198	8.9	7.99×10^{-4}	0.198	8.9
4.67×10^{-4}	0.103	9.0	4.27×10^{-4}	0.103	9.0
2.44×10^{-4}	5.48×10^{-2}	9.1	2.29×10^{-4}	5.48×10^{-2}	9.1
9.39×10^{-5}	1.92×10^{-2}	9.3	8.51×10^{-5}	2.09×10^{-2}	9.3
5.92×10^{-5}	1.15×10^{-2}	11.4	5.45×10^{-5}	1.27×10^{-2}	13.5
5.83×10^{-5}	1.27×10^{-2}	11.2			
4.08×10^{-4}	8.42×10^{-2}	11.2	3.60×10^{-4}	8.42×10^{-2}	11.2
1.88×10^{-3}	0.387	11.2	1.83×10^{-3}	0.387	11.2
1.76×10^{-5}	2.6×10^{-3}	11.2	1.29×10^{-5}	3.0×10^{-3}	11.2
3.28×10^{-5}	6.6×10^{-3}	11.2	2.66×10^{-5}	6.4×10^{-3}	11.3
4.52×10^{-2}	11.28	11.1	4.50×10^{-2}	11.28	11.1
2.1×10^{-6}	6.5×10^{-4}	11.3	2.39×10^{-6}	6.5×10^{-4}	11.3
9.45×10^{-6}	2.8×10^{-3}	11.3	8.65×10^{-6}	2.8×10^{-3}	

APPENDIX II

TABLE 11

Permeability Test No. 5 on G3 3/8" River Gravel.

Porosity (a) by draining voids 36.9 pc. (b) by weighing solids 39.2 pc.

Inner Flow Only			Total Flow		
Velocity(V) ft/sec.	Hydraulic Gradient(S)	Temp. °C.	Velocity(V) ft/ sec.	Hydraulic Gradient(S)	Temp. °C.
0.201	9.30	11.1			
0.203	9.40	11.1	0.220	9.41	11.1
0.142	5.13	11.0	0.155	5.10	11.0
8.66×10^{-2}	2.19	11.0	9.6×10^{-2}	2.19	10.9
6.02×10^{-2}	1.17	10.9	6.65×10^{-2}	1.18	10.9
4.04×10^{-2}	0.604	10.9	4.50×10^{-2}	0.615	10.9
2.74×10^{-2}	0.328	10.9	3.04×10^{-2}	0.328	10.9
2.03×10^{-2}	0.211	10.9	2.28×10^{-2}	0.212	10.9
1.31×10^{-2}	0.111	10.8	1.46×10^{-2}	0.111	10.9
7.42×10^{-3}	5.26×10^{-2}	10.9	8.701×10^{-3}	5.26×10^{-2}	10.5
1.74×10^{-4}	1.0×10^{-3}	10.5	2.09×10^{-4}	1.0×10^{-3}	10.5
2.74×10^{-4}	1.6×10^{-3}	10.5	4.15×10^{-4}	1.6×10^{-3}	10.5
3.41×10^{-4}	1.8×10^{-3}	10.3	4.40×10^{-4}	1.8×10^{-3}	10.3
6.95×10^{-4}	3.9×10^{-3}	10.3	9.55×10^{-4}	3.9×10^{-3}	10.3
8.52×10^{-4}	4.9×10^{-3}	10.5	1.13×10^{-3}	4.9×10^{-3}	10.5
1.74×10^{-3}	1.05×10^{-2}	10.4	2.56×10^{-3}	1.05×10^{-2}	10.4
3.26×10^{-3}	1.95×10^{-2}	10.4	4.43×10^{-3}	1.95×10^{-2}	10.5
5.00×10^{-3}	3.26×10^{-2}	10.5	7.04×10^{-3}	3.26×10^{-2}	10.5
			0.277	12.62	12.3

APPENDIX II TABLE 12

Permeability Test No. 6 on G2-1/ 4" River Gravel.

Porosity (a) by draining voids 37.1 pc. (b) by weighing solids 41.8 pc.

Inner Flow Only			Total Flow		
Velocity(V) ft/ sec.	Hydraulic Gradient(S)	Temp. °C.	Velocity(V) ft/ sec.	Hydraulic Gradient(S)	Temp. °C.
0.175	10.45	11.1	0.181	10.46	11.1
0.141	7.37	11.0	0.146	7.63	11.0
0.113	5.31	11.0	0.119	5.38	11.0
6.88×10^{-2}	2.55	11.0	7.25×10^{-2}	2.55	11.0
5.07×10^{-2}	1.68	10.9	5.38×10^{-2}	1.68	10.9
3.53×10^{-2}	1.03	10.9	3.75×10^{-2}	1.04	10.9
2.09×10^{-2}	0.532	10.9	2.23×10^{-2}	0.535	10.9
1.22×10^{-2}	0.283	10.9	1.32×10^{-2}	0.285	10.9
9.29×10^{-3}	0.208	10.9	1.00×10^{-2}	0.208	10.9
4.22×10^{-3}	9.01×10^{-2}	10.9	4.58×10^{-3}	9.02×10^{-2}	10.9
2.28×10^{-3}	4.81×10^{-2}	10.9	2.50×10^{-3}	4.82×10^{-2}	10.9
1.35×10^{-3}	2.89×10^{-2}	10.9	1.47×10^{-3}	2.89×10^{-2}	10.9
7.44×10^{-4}	1.54×10^{-2}	10.9	7.93×10^{-4}	1.54×10^{-2}	10.9
3.44×10^{-4}	7.7×10^{-3}	10.9	3.82×10^{-4}	7.5×10^{-3}	10.9
1.30×10^{-4}	2.8×10^{-3}	10.9	1.39×10^{-4}	2.6×10^{-3}	10.9
8.23×10^{-6}	1.6×10^{-4}	10.9	6.7×10^{-6}	1.6×10^{-4}	10.9
2.29×10^{-5}	6.6×10^{-4}	10.9	3.29×10^{-5}	6.6×10^{-4}	10.9
5.60×10^{-5}	1.3×10^{-3}	10.9	5.64×10^{-5}	1.3×10^{-3}	10.9
			0.203	12.72	10.5

APPENDIX II. TABLE 13.

Permeability Test No. 8 on: BM 1 3/16" Blue Metal

Porosity (a) by draining voids 45.9 pc. (b) by weighing solids 47.7 pc.

Inner Flow Only			Total Flow		
Velocity (V) ft/sec.	Hydraulic Gradient(S)	Temp. °C	Velocity (V) ft/sec.	Hydraulic Gradient(S)	Temp. °C
0.329	11.7	11.3	0.350	11.7	11.3
0.264	8.04	11.2	0.278	8.04	11.2
0.181	3.98	11.1	0.189	3.99	11.1
0.124	2.06	11.1	0.129	2.06	11.1
8.54×10^{-2}	1.10	11.1	8.94×10^{-2}	1.10	11.1
5.50×10^{-2}	0.537	11.0	5.78×10^{-2}	0.538	11.0
3.54×10^{-2}	0.273	11.0	3.76×10^{-2}	0.275	11.0
1.41×10^{-2}	7.53×10^{-2}	11.0	1.52×10^{-2}	7.53×10^{-2}	11.0
8.08×10^{-3}	3.80×10^{-2}	11.0	8.76×10^{-3}	3.81×10^{-2}	11.0
5.60×10^{-3}	2.50×10^{-2}	11.0	6.07×10^{-3}	2.50×10^{-2}	11.0
3.09×10^{-3}	1.31×10^{-2}	11.0	3.36×10^{-3}	1.31×10^{-2}	11.0
1.54×10^{-3}	6.45×10^{-3}	10.9	1.73×10^{-3}	6.55×10^{-3}	10.9
5.92×10^{-4}	3.03×10^{-3}	10.9	7.32×10^{-4}	3.03×10^{-3}	10.9
1.92×10^{-4}	1.3×10^{-3}	10.9	2.51×10^{-4}	7.4×10^{-4}	10.9
9.1×10^{-6}	8×10^{-5}	9.7	9.9×10^{-6}	8.10^{-5}	9.7
5.2×10^{-5}	4.1×10^{-4}	9.7	4.7×10^{-5}	3.3×10^{-4}	9.7
9.4×10^{-5}	7.4×10^{-4}	9.9	1.38×10^{-4}	7.4×10^{-4}	9.9
2.25×10^{-4}	1.4×10^{-3}	9.7	2.44×10^{-4}	1.4×10^{-3}	9.7

APPENDIX II. TABLE 14

Permeability Test No. 9 on BM2,3/ 8" Blue Metal.

Porosity (a) by draining voids 41.6 pc. (b) by weighing solids 45.8 pc.

Inner Flow Only			Total Flow		
Velocity (V) ft/ sec.	Hydraulic Gradient(S)	Temp. °C.	Velocity(V) ft/ sec.	Hydraulic Gradient(S)	Temp. °C.
0.463	12.42	11.6	0.500	12.35	11.3
0.386	9.37	10.9	0.433	9.28	11.1
0.294	5.89	10.5	0.331	5.88	10.5
0.242	4.10	10.6	0.269	4.10	10.6
0.165	2.04	10.6	0.185	2.04	10.5
0.114	1.06	10.6	0.128	1.06	10.5
7.69×10^{-2}	0.541	10.5	8.67×10^{-2}	0.542	10.5
5.05×10^{-2}	0.268	10.5	5.69×10^{-2}	0.268	10.5
3.38×10^{-2}	0.140	10.5	3.80×10^{-2}	0.140	10.5
2.11×10^{-2}	7.08×10^{-2}	10.5	2.42×10^{-2}	7.14×10^{-2}	10.5
1.28×10^{-2}	3.47×10^{-2}	10.4	1.46×10^{-2}	3.47×10^{-2}	10.4
7.71×10^{-3}	1.78×10^{-2}	10.4	8.82×10^{-3}	1.78×10^{-2}	10.4
3.66×10^{-3}	7.79×10^{-3}	10.4	4.27×10^{-3}	7.79×10^{-3}	10.4
1.20×10^{-3}	2.54×10^{-3}	10.4	1.39×10^{-3}	2.54×10^{-3}	10.4
3.38×10^{-4}	1.15×10^{-3}	10.3	5.24×10^{-4}	1.15×10^{-3}	10.3
1.12×10^{-4}	3.28×10^{-4}	10.3	9.48×10^{-5}	3.28×10^{-4}	10.3
2.28×10^{-4}	6.56×10^{-4}	10.3	3.58×10^{-4}	6.56×10^{-4}	10.3
3.04×10^{-4}	6.56×10^{-4}	10.3	3.93×10^{-4}	6.56×10^{-4}	10.3
2.31×10^{-3}	4.84×10^{-3}	10.3	2.71×10^{-3}	4.84×10^{-3}	10.3
2.36×10^{-3}	4.84×10^{-3}	10.3	2.69×10^{-3}	4.84×10^{-3}	10.3

APPENDIX II. TABLE 15

Permeability Test No. 10 on G6 3" River Gravel

Porosity (a) by draining voids 37.3 pc. (b) by weighing solids 36.9 pc.

Inner Flow Only			Total Flow		
Velocity(V) ft/ sec.	Hydraulic Gradient(S)	Temp. ^{o}C.	Velocity(V) ft/ sec.	Hydraulic Gradient(S)	Temp. ^{o}C.
1.02	5.04	11.5			
0.415	0.933	11.7	0.435	0.933	11.6
			1.08	5.10	11.2
0.294	0.483	11.1	0.318	0.485	11.1
0.835	3.47	10.9	0.885	3.47	11.0
0.602	1.70	10.9	0.620	1.70	10.9
0.217	0.273	10.9	0.233	0.275	10.9
0.150	0.135	10.9	0.160	0.135	10.9
0.104	6.80×10^{-2}	10.9	0.112	6.81×10^{-2}	10.8
7.08×10^{-2}	3.38×10^{-2}	10.8	7.63×10^{-2}	3.39×10^{-2}	10.8
1.44×10^{-2}	2.1×10^{-3}	11.0	1.51×10^{-2}	2.1×10^{-3}	11.1
8.23×10^{-3}	9×10^{-4}	11.4	8.72×10^{-3}	9×10^{-4}	11.4
4.66×10^{-2}	1.55×10^{-2}	12.0	4.91×10^{-2}	1.56×10^{-2}	12.6
3.27×10^{-2}	8.0×10^{-3}	13.0	3.37×10^{-2}	8.0×10^{-3}	13.4
1.95×10^{-2}	3.2×10^{-3}	13.4	2.09×10^{-2}	3.2×10^{-3}	13.4
1.54×10^{-3}	2×10^{-5}	13.3	1.58×10^{-3}	2×10^{-5}	13.3
9.46×10^{-3}	9×10^{-4}	13.3	9.46×10^{-3}	9×10^{-4}	13.3

APPENDIX II. TABLE 16

Permeability Test No. 11 on BM5. 3" Blue Metal.

Porosity (a) by draining voids 46.3 pc. (b) by weighing solids 48.3 pc.

Inner Flow Only			Total Flow		
Velocity(V) ft/ sec.	Hydraulic Gradient(S)	Temp. °C.	Velocity(V) ft/ sec.	Hydraulic Gradient(S)	Temp. °C.
0.870	9.18	10.7	1.01	9.38	10.9
0.636	4.85	10.7	0.723	4.85	10.7
0.460	2.62	10.5	0.530	2.64	10.6
0.364	1.72	9.8	0.419	1.73	10.2
0.279	0.999	10.5	0.319	1.00	10.5
0.196	0.505	10.6	0.223	0.505	10.6
0.125	0.213	10.7	0.144	0.211	10.7
1.85×10^{-3}	1.7×10^{-4}	10.8	1.68×10^{-3}	1.7×10^{-4}	10.8
1.27×10^{-2}	3.3×10^{-4}	10.8	1.44×10^{-2}	3.3×10^{-3}	10.8
6.67×10^{-3}	1.0×10^{-3}	10.9	7.30×10^{-3}	1.0×10^{-3}	10.9
5.34×10^{-3}	8×10^{-4}	10.9	6.17×10^{-3}	8x10-4	10.9
8.67×10^{-2}	0.105	11.9	9.93×10^{-2}	0.106	12.0
5.90×10^{-2}	0.511	12.4	6.73×10^{-2}	0.512	12.6
3.94×10^{-2}	2.41×10^{-2}	12.8	4.52×10^{-2}	2.4×10^{-2}	12.9
2.89×10^{-2}	1.36×10^{-2}	12.8	3.29×10^{-2}	1.35×10^{-2}	12.9
2.01×10^{-2}	6.8×10^{-3}	12.8	2.32×10^{-2}	7.0×10^{-3}	12.7

APPENDIX II. TABLE 17.

Permeability Test No. 12 on G5 $1\frac{1}{2}$" River Gravel.

Porosity (a) by draining voids 34.9 pc. (b) by weighing solids 37.2 pc.

Inner Flow Only			Total Flow		
Velocity(V) ft/ sec.	Hydraulic Gradient(S)	Temp $^{o}C.$	Velocity(V) ft/ sec.	Hydraulic Gradient(S)	Temp $^{o}C.$
0.796	9.05	11.0	0.833	9.06	11.0
0.394	2.43	11.0	0.413	2.43	11.0
0.616	5.57	11.0	0.648	5.51	11.0
0.272	1.20	11.0	0.288	1.21	11.0
0.190	0.612	11.0	0.199	0.612	11.0
0.135	0.321	11.0			
9.00×10^{-2}	0.154	11.0			
5.90×10^{-2}	7.17×10^{-2}	10.9			
3.79×10^{-2}	3.33×10^{-2}	10.9	3.98×10^{-2}	3.31×10^{-2}	10.9
2.59×10^{-2}	1.74×10^{-2}	10.9	2.71×10^{-2}	1.72×10^{-2}	10.9
1.45×10^{-2}	6.6×10^{-3}	10.9	1.49×10^{-2}	6.6×10^{-3}	10.9
9.15×10^{-3}	3.12×10^{-3}	10.9	9.55×10^{-3}	3.12×10^{-3}	10.9
6.12×10^{-3}	1.64×10^{-3}	11.0	6.42×10^{-3}	1.64×10^{-3}	11.0
3.30×10^{-3}	6.5×10^{-4}	11.0	3.29×10^{-3}	6.5×10^{-4}	11.0
1.45×10^{-3}	2.5×10^{-4}	11.0	1.51×10^{-3}	2.5×10^{-4}	11.0

APPENDIX II. TABLE 18.

Permeability Test No. 13 on G4 3/ 4" River Gravel.

Porosity (a) by draining voids 33. 9 pc. (b) by weighing solids 36. 7 pc.

Inner Flow Only			Total Flow		
Velocity (V) ft/ sec.	Hydraulic Gradient(S)	Temp. °C.	Velocity(V) ft/ sec.	Hydraulic Gradient(S)	Temp. °C.
0.619	9.87	11.3	0.667	9.90	11.4
0.540	7.45	10.8	0.565	7.43	10.8
0.362	3.75	10.9	0.386	3.75	10.9
0.257	1.94	10.9	0.273	1.92	10.9
0.178	0.995	11.0	0.190	1.00	11.0
0.124	0.523	11.0	0.133	0.519	11.0
8.13×10^{-2}	0.246	11.1	8.73×10^{-2}	0.244	11.2
5.72×10^{-2}	0.132	11.2			
3.68×10^{-2}	6.34×10^{-2}	11.2	3.99×10^{-2}	6.33×10^{-2}	11.2
2.33×10^{-2}	3.03×10^{-2}	11.2			
1.36×10^{-2}	1.30×10^{-2}	11.3	1.47×10^{-2}	1.30×10^{-2}	11.3
8.38×10^{-3}	6.3×10^{-3}	11.3	9.11×10^{-3}	6.3×10^{-3}	11.3
5.36×10^{-3}	3.3×10^{-3}	11.3	5.68×10^{-3}	3.3×10^{-3}	11.3
3.07×10^{-3}	1.64×10^{-3}	11.3	3.31×10^{-3}	1.64×10^{-3}	11.3
1.65×10^{-3}	7×10^{-4}	11.4	1.60×10^{-3}	7×10^{-4}	11.4
4.54×10^{-4}	3.5×10^{-4}	11.4	6.2×10^{-4}	3.5×10^{-4}	11.4

APPENDIX II.

TABLE 19

Permeability Test No. 14 on BM4 $1\frac{1}{2}$" Blue Metal

Porosity (a) by draining voids 41.8 pc. (b) by weighing solids 43.8 pc.

Inner Flow Only			Total Flow		
Velocity(V) ft/ sec.	Hydraulic Gradient(S)	Temp. $^{o}C.$	Velocity(V) ft/ sec.	Hydraulic Gradient(S)	Temp. $^{o}C.$
0.880	8.66	11.2	0.955	8.51	11.3
0.747	6.25	11.2	0.813	6.21	11.2
0.538	3.19	11.2			
0.385	1.85	10.9	0.420	1.85	10.9
0.277	0.965	11.0	0.267	0.916	11.0
0.197	0.512	11.0	0.213	0.505	11.0
0.136	0.255	11.0			
9.37×10^{-2}	0.127	11.1	0.103	0.127	11.1
6.48×10^{-2}	6.55×10^{-2}	11.2			
4.45×10^{-2}	3.32×10^{-2}	11.2	4.91×10^{-2}	3.35×10^{-2}	11.3
3.02×10^{-2}	1.70×10^{-2}	10.3			
2.03×10^{-2}	8.7×10^{-3}	11.3			
1.34×10^{-2}	4.1×10^{-3}	11.3	1.47×10^{-2}	4.1×10^{-3}	11.3
8.85×10^{-3}	2.1×10^{-3}	11.3			
6.06×10^{-3}	1.2×10^{-3}	11.4			
4.89×10^{-3}	1.0×10^{-3}	11.4	5.30×10^{-3}	1.0×10^{-3}	11.4
1.75×10^{-3}	1.6×10^{-4}	11.4			

APPENDIX II. TABLE 20.

Permeability Test No. 15 on BM3-1. 3/ 4" Blue Metal.

Porosity (a) by draining voids 39. 5 pc. (b) by weighing solids 42. 8 pc.

Inner Flow Only			Total Flow		
Velocity(V) ft/ sec.	Hydraulic Gradient(S)	Temp. ^{o}C.	Velocity(V) ft/ sec.	Hydraulic Gradient(S)	Temp ^{o}C.
0. 659	9. 55	11. 6	0. 738	9. 55	11. 6
0. 482	5. 15	11. 7	0. 533	5. 13	11. 7
0. 352	2. 97	11. 8			
0. 247	1. 51	11. 9	0. 273	1. 52	11. 9
0. 173	0. 782	12. 0			
0. 119	0. 394	12. 1	0. 133	0. 394	12. 1
8.27×10^{-2}	0. 206	11. 8	9.37×10^{-2}	0. 208	11. 9
5.47×10^{-2}	9.95×10^{-2}	12. 0			
3.66×10^{-2}	5.02×10^{-2}	12. 0			
2.42×10^{-2}	2.56×10^{-2}	11. 9	2.74×10^{-2}	2.56×10^{-2}	11. 8
1.35×10^{-3}	5.0×10^{-4}	10. 6	1.45×10^{-3}	5×10^{-4}	10. 6
1.24×10^{-2}	9.8×10^{-3}	10. 7	1.40×10^{-2}	9.8×10^{-3}	10. 7
9.62×10^{-3}	6.6×10^{-3}	10. 8	1.11×10^{-2}	6.6×10^{-3}	10. 8
6.38×10^{-3}	3.7×10^{-3}	10. 8	7.35×10^{-3}	3.7×10^{-3}	10. 8
3.59×10^{-3}	1.6×10^{-3}	10. 9			
2.86×10^{-3}	1.2×10^{-3}	10. 9			
1.74×10^{-2}	1.61×10^{-2}	11. 0			

APPENDIX II. TABLE 21.

Permeability Test No. 16 on M1 16 mm. Dia. Marbles.

Porosity (a) by draining voids 36.9 pc. (b) by weighing solids 36.9 pc.

Inner Flow Only			Total Flow		
Velocity(V) ft/sec.	Hydraulic Gradient(S)	Temp. ^{o}C.	Velocity(V) ft/sec.	Hydraulic Gradient(S)	Temp. ^{o}C.
0.89	7.84	11.5	0.95	7.90	11.6
0.781	5.96	11.6	0.812	5.92	11.6
0.617	4.04	12.0	0.676	4.06	12.0
0.399	1.86	12.0	0.414	1.86	12.0
0.288	1.01	12.1			
0.202	0.526	12.1	0.214	0.521	12.1
0.137	0.259	12.2			
9.23×10^{-2}	0.127	12.2			
6.34×10^{-2}	6.65×10^{-2}	12.3	6.87×10^{-2}	6.85×10^{-2}	12.3
6.71×10^{-4}	2.5×10^{-4}	11.3	9.05×10^{-4}	2.5×10^{-4}	11.3
1.20×10^{-3}	3.3×10^{-4}	11.3	1.45×10^{-3}	3.3×10^{-4}	11.3
2.25×10^{-3}	6.6×10^{-4}	11.3	2.48×10^{-3}	6.6×10^{-4}	11.3
4.64×10^{-3}	1.36×10^{-3}	11.4	5.12×10^{-3}	1.36×10^{-3}	11.4
7.98×10^{-3}	2.82×10^{-3}	11.3	8.73×10^{-3}	2.82×10^{-3}	11.3
1.34×10^{-2}	5.82×10^{-3}	11.4	1.48×10^{-2}	5.82×10^{-3}	11.4
2.17×10^{-2}	1.18×10^{-2}	11.2			
3.33×10^{-2}	2.32×10^{-2}	11.0	3.58×10^{-2}	2.32×10^{-2}	11.0
5.22×10^{-2}	4.91×10^{-2}	11.3			
7.77×10^{-2}	9.78×10^{-2}	11.3			
0.119	0.203	12.0			

APPENDIX II. TABLE 22

Permeability Test No. 17 on: M2 25 mm marbles

Porosity (a) by draining voids 38.0 pc. (b) by weighing solids 36.9 pc.

Inner Flow Only			Total Flow		
Velocity(V) ft/ sec.	Hydraulic Gradient(S)	Temp. ^{o}C	Velocity(V) ft/ sec.	Hydraulic Gradient(S)	Temp. ^{o}C
		11.9	7.73×10^{-4}	2.3×10^{-4}	11.9
1.59×10^{-3}	7×10^{-5}	12.0	1.05×10^{-3}	7×10^{-5}	12.0
2.06×10^{-3}	1.6×10^{-4}	12.1	1.73×10^{-3}	1.6×10^{-4}	12.1
4.00×10^{-3}	4.1×10^{-4}	12.1	3.94×10^{-3}	4.1×10^{-4}	12.1
5.33×10^{-3}	7.4×10^{-4}	12.0	5.99×10^{-3}	7.4×10^{-4}	12.0
8.1×10^{-3}	1.4×10^{-3}	12.2	9.17×10^{-3}	1.4×10^{-3}	12.2
1.24×10^{-2}	2.5×10^{-3}	12.5	1.40×10^{-2}	2.5×10^{-3}	12.5
1.42×10^{-2}	3.36×10^{-3}	12.3			
2.17×10^{-2}	6.5×10^{-3}	12.2			
3.36×10^{-2}	1.33×10^{-2}	12.1	3.86×10^{-2}	1.33×10^{-2}	12.0
5.04×10^{-2}	2.66×10^{-2}	12.3			
7.58×10^{-2}	5.45×10^{-2}	12.6	8.72×10^{-2}	5.45×10^{-2}	12.7
0.118	0.120	12.4	0.135	0.120	11.9
0.180	0.254	11.5			
0.257	0.500	11.2	0.298	0.507	11.1
0.381	1.03	11.1	0.633	2.04	11.0
0.567	2.04	11.0			
0.808	4.15	11.0			
1.06	6.93	11.0	1.19	7.02	11.0

APPENDIX II. TABLE 23.

Permeability Test No. 18 on G7 6" River Gravel.

Porosity (a) by draining voids 40. 4 pc. (b) by weighing solids 40. 6 pc.

Inner Flow Only			Total Flow		
Velocity(V) ft/ sec.	Hydraulic Gradient(S)	Temp. °C.	Velocity(V) ft/ sec.	Hydraulic Gradient(S)	Temp. °C.
1.98×10^{-3}	1×10^{-5}	12.0	1.74×10^{-3}	1×10^{-5}	12.0
6.51×10^{-3}	1×10^{-4}	12.0	6.39×10^{-3}	1×10^{-4}	12.0
1.35×10^{-2}	4.4×10^{-4}	12.0	1.46×10^{-2}	4.4×10^{-4}	12.0
3.12×10^{-2}	2.05×10^{-3}	11.9	3.35×10^{-2}	2.05×10^{-3}	11.8
2.39×10^{-2}	1.25×10^{-3}	11.8	2.56×10^{-2}	1.25×10^{-3}	11.8
4.91×10^{-2}	4.42×10^{-3}	11.7			
7.02×10^{-2}	9.07×10^{-3}	11.6	7.77×10^{-2}	9.07×10^{-3}	11.5
0.111	2.12×10^{-2}	11.2			
0.164	4.46×10^{-2}	11.2	0.183	4.46×10^{-2}	11.2
0.241	9.26×10^{-2}	11.3			
0.400	0.246	11.3			
0.325	0.164	11.3	0.357	0.164	11.3
1.34	2.52	13.5	1.45	2.44	11.4
1.22	2.01	13.4			
0.902	1.03	13.4			
0.596	0.490	13.4	0.652	0.493	13.5
			0.930	1.01	13.5
			1.32	2.01	13.5
0.827	0.974	13.4			
1.01×10^{-2}	2.7×10^{-4}	11.7	1.12×10^{-2}	2.7×10^{-4}	11.7
1.99×10^{-2}	9.1×10^{-4}	11.5			

APPENDIX II. TABLE 24

Permeability Test No. 19 on M1 16 mm. Dia. Marbles

Porosity (a) by draining voids 41.3 pc. (b) by weighing solids 41.5 pc.

Inner Flow Only			Total Flow		
Velocity(V) ft/sec.	Hydraulic Gradient(S)	Temp. °C.	Velocity(V) ft/sec.	Hydraulic Gradient(S)	Temp. °C.
0.406	1.06	14.6	0.433	1.06	14.6
0.272	0.499	14.5	0.290	0.499	14.5
0.190	0.260	14.5	0.204	0.260	14.4
1.15×10^{-3}	1.8×10^{-4}	14	1.38×10^{-3}	1.8×10^{-4}	14
6.16×10^{-3}	1.02×10^{-3}	12	6.71×10^{-3}	1.02×10^{-3}	12
1.41×10^{-2}	3.1×10^{-3}	12	1.47×10^{-2}	3.1×10^{-3}	12
2.54×10^{-2}	7.9×10^{-3}	12			
0.105	9.46×10^{-2}	15	0.112	9.46×10^{-2}	15
7.25×10^{-2}	4.87×10^{-2}	15.1			
4.38×10^{-2}	2.05×10^{-2}	15.2	4.62×10^{-2}	2.05×10^{-2}	15.3
2.38×10^{-3}	3.3×10^{-4}	15.5	2.05×10^{-3}	3.3×10^{-4}	15.5
5.5×10^{-3}	6.6×10^{-4}	15.5	4.89×10^{-3}	6.6×10^{-4}	15.5

APPENDIX II. TABLE 25

Permeability Test No. 20 on M1 16 mm Dia. Marbles

Porosity (a) by draining voids 37.8 pc. (b) by weighing solids 37.2 pc.

Inner Flow Only			Total Flow		
Velocity(V) ft/ sec.	Hydraulic Gradient(S)	Temp. $^{o}C.$	Velocity(V) ft/ sec.	Hydraulic Gradient(S)	Temp. $^{o}C.$
0.412	1.62	15.0	0.424	1.62	15.0
0.265	0.726	15.3			
0.174	0.337	15.3	0.184	0.337	15.3
9.05×10^{-2}	0.104	15.2			
2.52×10^{-2}	1.16×10^{-2}	15.2			
6.55×10^{-3}	1.53×10^{-3}	15.3	6.65×10^{-3}	1.53×10^{-3}	15.3

APPENDIX II. TABLE 26

Permeability Test No. 21 on BM3-1 3/ 4" Blue Metal (loosely packed)

Porosity (a) by draining voids 48. 5 pc. (b) by weighing solids 51. 5 pc.

Inner Flow Only			Total Flow		
Velocity(V) ft/ sec.	Hydraulic Gradient(S)	Temp. °C	Velocity(V) ft/ sec.	Hydraulic Gradient(S)	Temp. °C
0. 389	1. 39	15. 8	0. 420	1. 39	15. 8
0. 233	0. 511	15. 6	0. 250	0. 511	15. 7
0. 389	1. 40	15. 7	0. 423	1. 40	15. 7
0. 231	0. 513	15. 7	0. 250	0. 513	15. 7
0. 159	0. 259	15. 6			
0. 109	0. 130	15. 6	0. 119	0. 130	15. 5
7.12×10^{-2}	6.0×10^{-2}	15. 5			
2.30×10^{-2}	8.6×10^{-3}	15. 5			
5.19×10^{-2}	3.5×10^{-2}	15. 6	5.67×10^{-2}	3.5×10^{-2}	15. 6
3.77×10^{-2}	2.0×10^{-2}	15. 7			
2.13×10^{-3}	3.3×10^{-4}	15. 7	2.35×10^{-3}	2.5×10^{-4}	15. 7
2.96×10^{-3}	4.9×10^{-4}	15. 7			
5.09×10^{-3}	9.8×10^{-4}	15. 7	5.8×10^{-3}	9.8×10^{-4}	15. 7
5.22×10^{-3}	9.8×10^{-4}	15. 8			
8.60×10^{-3}	2.05×10^{-3}	15. 9	9.26×10^{-3}	1.97×10^{-3}	15. 9
1.59×10^{-2}	5.0×10^{-3}	15. 9			

APPENDIX II. TABLE 27

Permeability Test No. 22 on M3 29 mm. Dia. Marbles.

Porosity (a) by draining voids 38.0 pc. (b) by weighing solids 38.5 pc.

Inner Flow Only			Total Flow		
Velocity(V) ft/sec.	Hydraulic Gradient(S)	Temp. ^{o}C.	Velocity(V) ft/sec.	Hydraulic Gradient(S)	Temp. ^{o}C.
1.11	5.86	16.0			
0.821	3.25	15.4			
0.688	2.28	17.0			
			1.19	5.61	17.0
			0.69	1.88	17.0
0.391	0.824	16.8			
0.256	0.369	16.8			
0.174	0.182	16.7	0.168	0.181	16.2
1.59×10^{-3}	2.5×10^{-4}	17.3	1.55×10^{-3}	2.5×10^{-4}	17.3
3.91×10^{-3}	3.3×10^{-4}	17.3	4.04×10^{-3}	3.3×10^{-4}	17.3
6.07×10^{-3}	7.4×10^{-4}	17.3	6.81×10^{-3}	7.4×10^{-4}	17.3
1.08×10^{-2}	1.64×10^{-3}	17.3			
2.25×10^{-2}	5.4×10^{-3}	17.2			
1.49×10^{-2}	2.8×10^{-3}	17.2			
3.82×10^{-2}	1.19×10^{-2}	17.4			
5.97×10^{-2}	2.59×10^{-2}	17.4			
8.55×10^{-2}	4.90×10^{-2}	17.0	9.40×10^{-2}	4.90×10^{-2}	17.0
0.125	9.89×10^{-2}	17.0			
0.181	0.196	17.0			
0.259	0.383	17.0			
0.388	0.822	17.0			
8.65×10^{-2}	5.08×10^{-2}	17.2			
0.145	0.130	17.0			

APPENDIX III.

Method of Adjustment of Fall Velocities for Specific Gravity Differences.

Consider two particles 1 and 2 of the same size and shape, but different specific gravities SG_1 and SG_2 falling through the same fluid at terminal velocities V_{f_1} and V_{f_2}.

For particle 1, Volume x $(SG_1 - 1.00) \times \gamma_w = C_{D_1} A \frac{1}{2} \rho V_{f_1}^2$.

For particle 2, Volume x $(SG_2 - 1.00) \times \gamma_w = C_{D_2} A \frac{1}{2} \rho V_{f_2}^2$

where γ_w = specific weight of water

A = particle cross-sectional area normal to the fall.

Provided the terminal velocities are such that the drag coefficients, C_{D_1} and C_{D_2} fall on the flat part of the C_D - $\mathbb{R}$ curve and provided the specific gravity difference $SG_1 - SG_2$ is not great enough to cause the terminal velocities and corresponding Reynolds numbers to differ greatly, $C_{D_1} \doteq C_{D_2}$

$$\therefore \frac{V_{f_1}^2}{V_{f_2}^2} = \frac{SG_1 - 1.00}{SG_2 - 1.00}$$

The effect on Reynolds number of the variation of temperature over the range of the experiments is negligible.

If the specific gravities caused the Reynolds numbers to differ by a factor of 2, the coefficients of drag for spherical particles would differ by 5 pc. for Reynolds numbers between 5×10^2 and 2×10^5. This would

result in an error of $2\frac{1}{2}$ pc. in the value of the adjusted fall velocity. For non-spherical particles the error would be less because of the flatter drag coefficient graphs.

Trial and error calculations show that for spherical particles and specific gravities between 2.9 and 2.6 this accuracy is met if the fall velocities are adjusted to a common S.G. value of 2.65 (that of quartz) and Reynolds numbers corresponding to fall velocities are not less than 10^2. A check of the fall velocities and diameters listed in Table 2 shows that these requirements are met except for -1/4" river gravel.